#331 SPECIAL ISSUE SEPTEMBER 2016

ICES CIEM

ICES REPORT ON OCEAN CLIMATE 2015

Prepared by the Working Group on Oceanic Hydrography

ICES COOPERATIVE RESEARCH REPORT

RAPPORT DES RECHERCHES COLLECTIVES

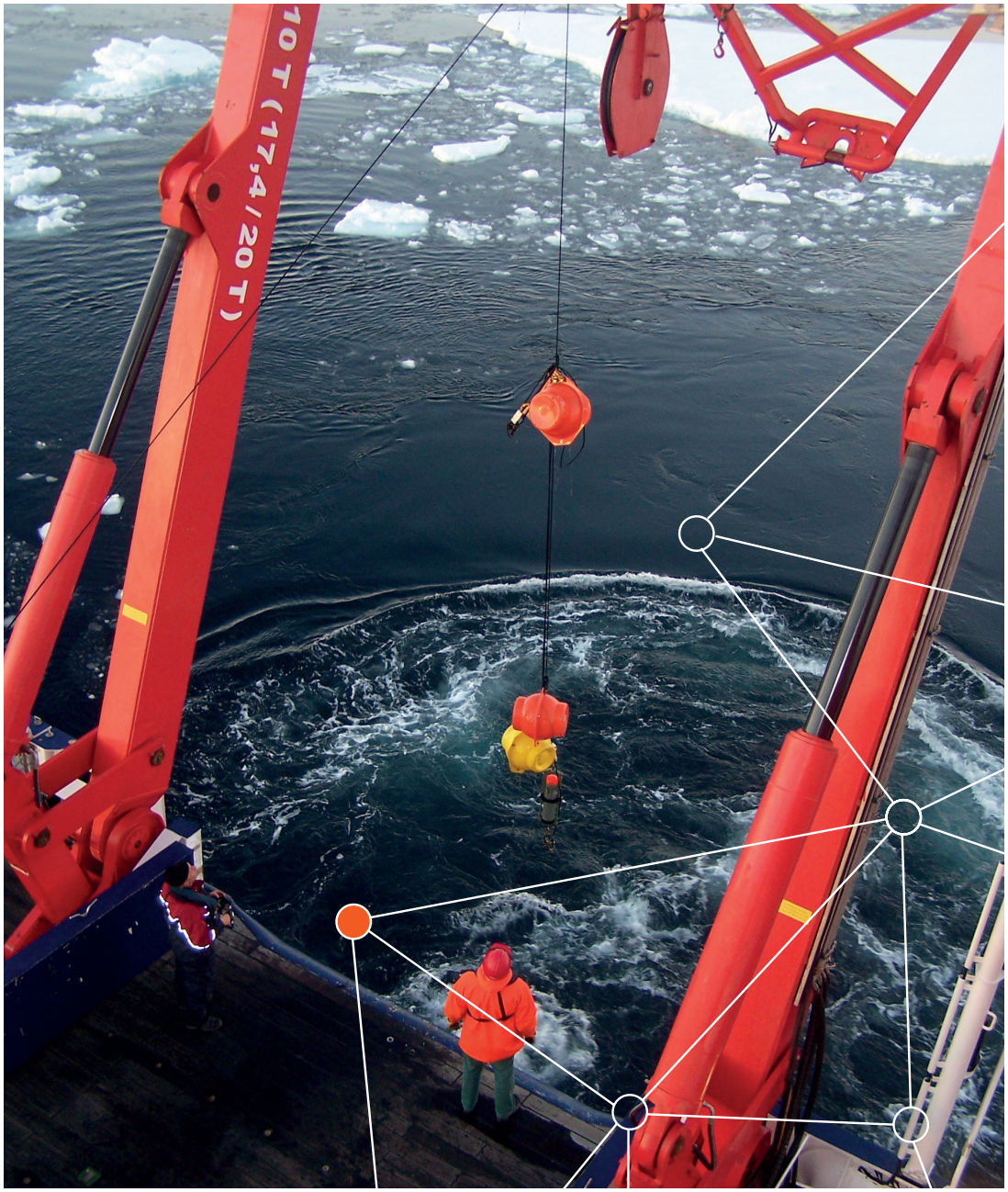

ICES INTERNATIONAL COUNCIL FOR THE EXPLORATION OF THE SEA
CIEM CONSEIL INTERNATIONAL POUR L'EXPLORATION DE LA MER

Cover image and photo above:
Agnieszka Beszczynska-Möller,
AWI, Germany.

International Council for the Exploration of the Sea
Conseil International pour l'Exploration de la Mer

H. C. Andersens Boulevard 44–46
DK-1553 Copenhagen V
Denmark
T (+45) 33 38 67 00
F (+45) 33 93 42 15
www.ices.dk

Recommended format for purposes of citation:
Larsen, K. M. H., Gonzalez-Pola, C., Fratantoni, P., Beszczynska-Möller, A., and Hughes, S. L. (Eds). 2016. ICES Report on Ocean Climate 2015. ICES Cooperative Research Report No. 331. 79 pp.

Series Editor: Emory D. Anderson

Editors: Karin M. H. Larsen, Cesar Gonzalez-Pola, Paula Fratantoni, Agnieszka Beszczynska-Möller, and Sarah L. Hughes

ISBN: 978-87-7482-188-5
ISSN: 1017-6195

CONTENTS

1. INTRODUCTION

Long time-series of ocean properties are rare for the surface ocean and even rarer for the deep ocean. The North Atlantic region is unusual in having a relatively large number of locations at which oceanographic data have been collected repeatedly for many years or decades; the longest records go back more than a century.

The collation of these valuable data in the *ICES Report on Ocean Climate* (IROC) provides the very latest information from the ICES Area of the North Atlantic and the Nordic seas. This report describes the status of sea temperature and salinity in 2015 at locations where the ocean is regularly measured, including observed trends over the past decade – and longer where possible.

The first section of the report contains information from the longest time-series, offering the best possible overview of changes in the ICES area. Although the focus of the report is on temperature and salinity measurements, additional complementary datasets are provided throughout the report on topics such as sea level pressure, air temperature, and ice cover.

The main focus of this report is the observed variability in the upper ocean (the upper 1000 m). The introductory section includes gridded fields, constructed by optimal analysis of the Argo float data and distributed by the Coriolis data centre in France. Later in the report, a short section summarizes the variability of the intermediate and deep waters of the North Atlantic. In this section, additional time-series from the Western Iberian Margin (IROC 2014; Larsen *et al.*, 2016) and the Canary Basin (new) have been included.

The data presented here represent an accumulation of knowledge collected by many individuals and institutions through decades of observations. While it would be impossible to list them all, a list of contacts for each dataset is provided at the end of the report, including e-mail addresses for the individuals who provided the information and the data centres at which the full archives of data are held. Many of the data included in this report are available to download via a web tool at http://ocean.ices.dk/iroc.

For those interested in a more detailed overview of a particular region, a full description of the datasets used to develop the time-series presented in this report can be found in the annual meeting reports of the ICES Working Group on Oceanic Hydrography (WGOH) at http://www.ices.dk/community/groups/Pages/WGOH.aspx.

1.1 HIGHLIGHTS OF THE NORTH ATLANTIC FOR 2015

Lower-than-normal air temperatures were observed throughout the year across the Subpolar Gyre region. Air temperatures over the Northwest Atlantic were particularly cold in the first half of the year.

By the end of the year, higher-than-normal air temperatures were observed over the European continent, from the Iberian Coast to Svalbard.

Sea surface temperatures in the North Sea, along the Norwegian coast, and in the Baltic Sea remained higher than normal, except in summer.

The substantial cold anomaly centred near 50°N in the central North Atlantic persisted through 2015, expanding to influence areas covered by the *in situ* time-series. Lower-than-normal temperatures were observed south of Iceland and in the southern part of the Nordic seas. Temperatures observed in the Iceland Basin were the lowest since 1996.

Despite colder-than-normal winter air temperatures over the North American continent, ocean temperatures remained above normal on the Northeast US continental shelf.

Following a period of high salinities observed between 2009 and 2011, freshening has been observed in the upper layers of the Irminger Sea, the Iceland Basin, Hatton–Rockall, and into the Nordic seas.

The freshening that was first observed in the upper central waters of the Bay of Biscay region during 2014 continued and strengthened.

The maximum ice extent in the Baltic Sea was a record low, with an early peak. In the Barents Sea, the peak was reached in February, two months earlier than normal.

1.2 HIGHLIGHTS OF THE NORTH ATLANTIC ATMOSPHERE IN WINTER 2014/2015

The winter North Atlantic Oscillation (NAO) index was at its most positive (+3.56) since 1995 and the fourth strongest in the last 110 years. The Azores High was strong, but limited in its zonal extension, carrying stronger-than-normal winds between Scotland and the Labrador Sea, but weaker winds west of the Iberian Coast. The wind direction over the Iberian Coast was the reverse of prevailing wind conditions.

Winter air temperatures were higher than normal over the Nordic seas, Scandinavia, and central and eastern Europe, but were particularly low across the Northeast American continent, Labrador, West Greenland, and the Subpolar Gyre.

1.3 INITIAL ASSESSMENT OF THE NORTH ATLANTIC ATMOSPHERE IN WINTER 2015/2016

An initial assessment of the North Atlantic atmosphere at the end of the IROC year is included. Atmospheric conditions during winter are a determining factor of oceanic conditions for the following year; therefore, this outlook offers some predictive capability for spring–autumn 2016.

The sea level pressure pattern for December 2015–March 2016 indicates that it was a positive, but weaker, NAO index than experienced in the preceding two winters. Average windspeeds from south of Iceland to the Barents Sea were weak, while winds were stronger than normal from the central North Atlantic towards the Bay of Biscay and into the English Channel.

Air temperatures were cold over the Subpolar Gyre, including over the Irminger Sea and Iceland Basin. Warmer-than-average conditions were evident over all the continental land masses as well as the Mid-Atlantic Bight, Baltic Sea, North Sea, Barents Sea, and the Nordic seas.

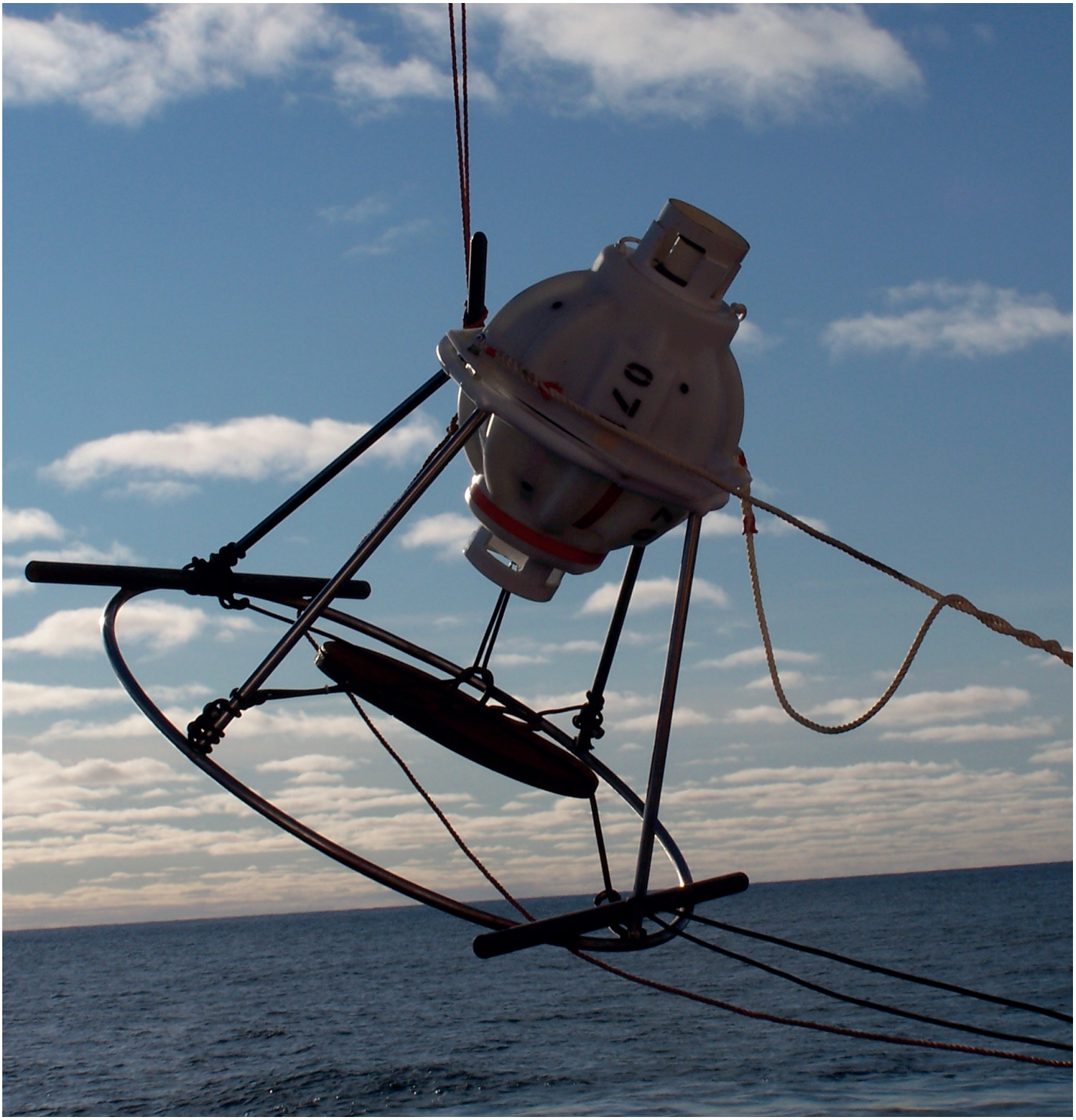

Photo: Agnieska Beszczynska-Möller, AWI, Germany.

NORTH ATLANTIC UPPER OCEAN TEMPERATURE: OVERVIEW

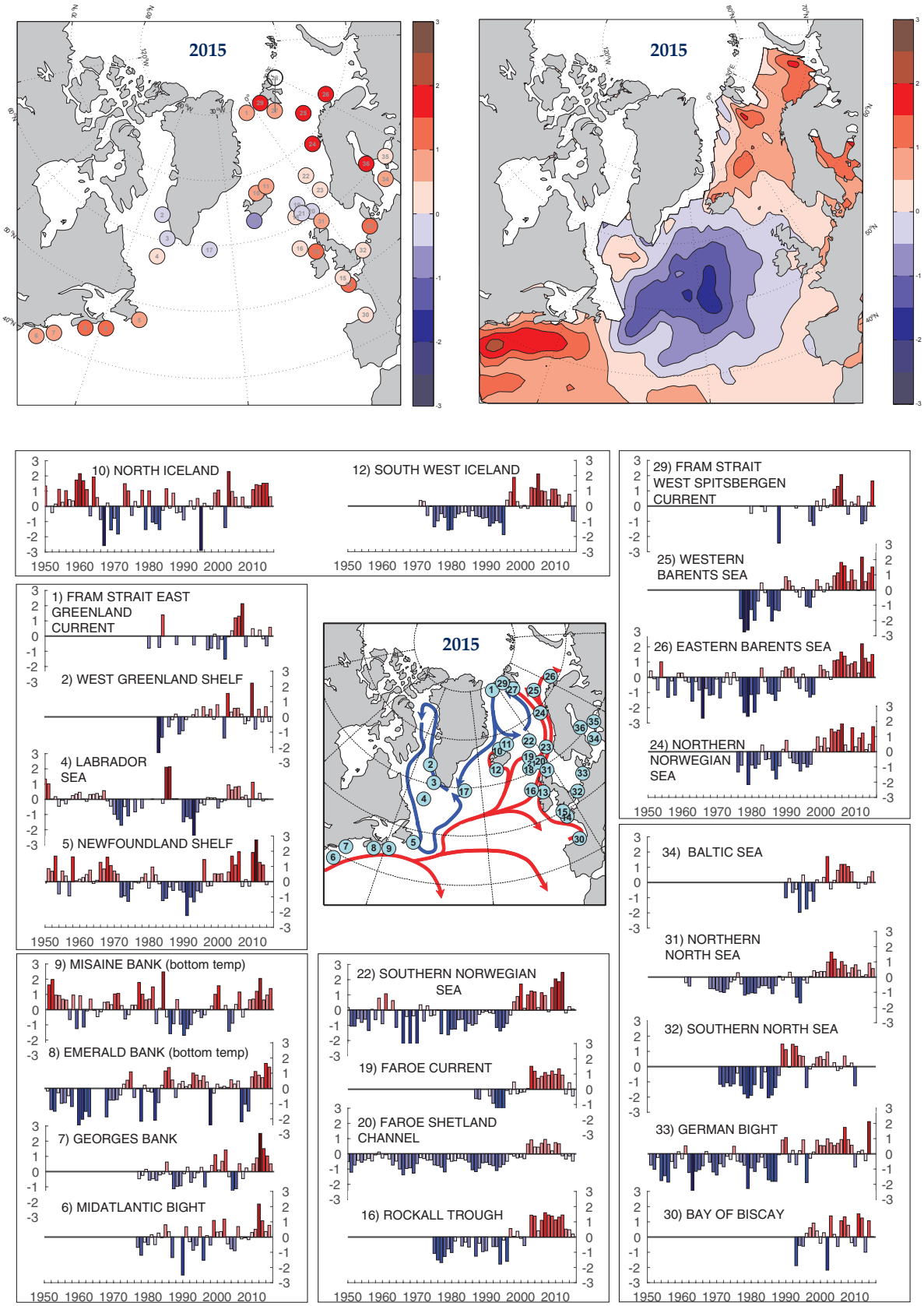

Figure 1.

Upper ocean temperature anomalies at selected locations across the North Atlantic. The anomalies are normalized with respect to the standard deviation (s.d.; e.g. a value of +2 indicates 2 s.d. above normal). Upper panels: maps of conditions in 2015; (left) data from in situ *observations; (right) 2015 anomalies relative to the 1981–2010 base period, calculated from OISST.v2 data (see Figure 3). Lower panels: time-series of normalized anomalies at each of the selected stations. Colour intervals 0.5 s.d.; red = positive/warm; blue = negative/cool. See Figure 13 for a map supplying more details about the locations in this figure.*

NORTH ATLANTIC UPPER OCEAN SALINITY: OVERVIEW

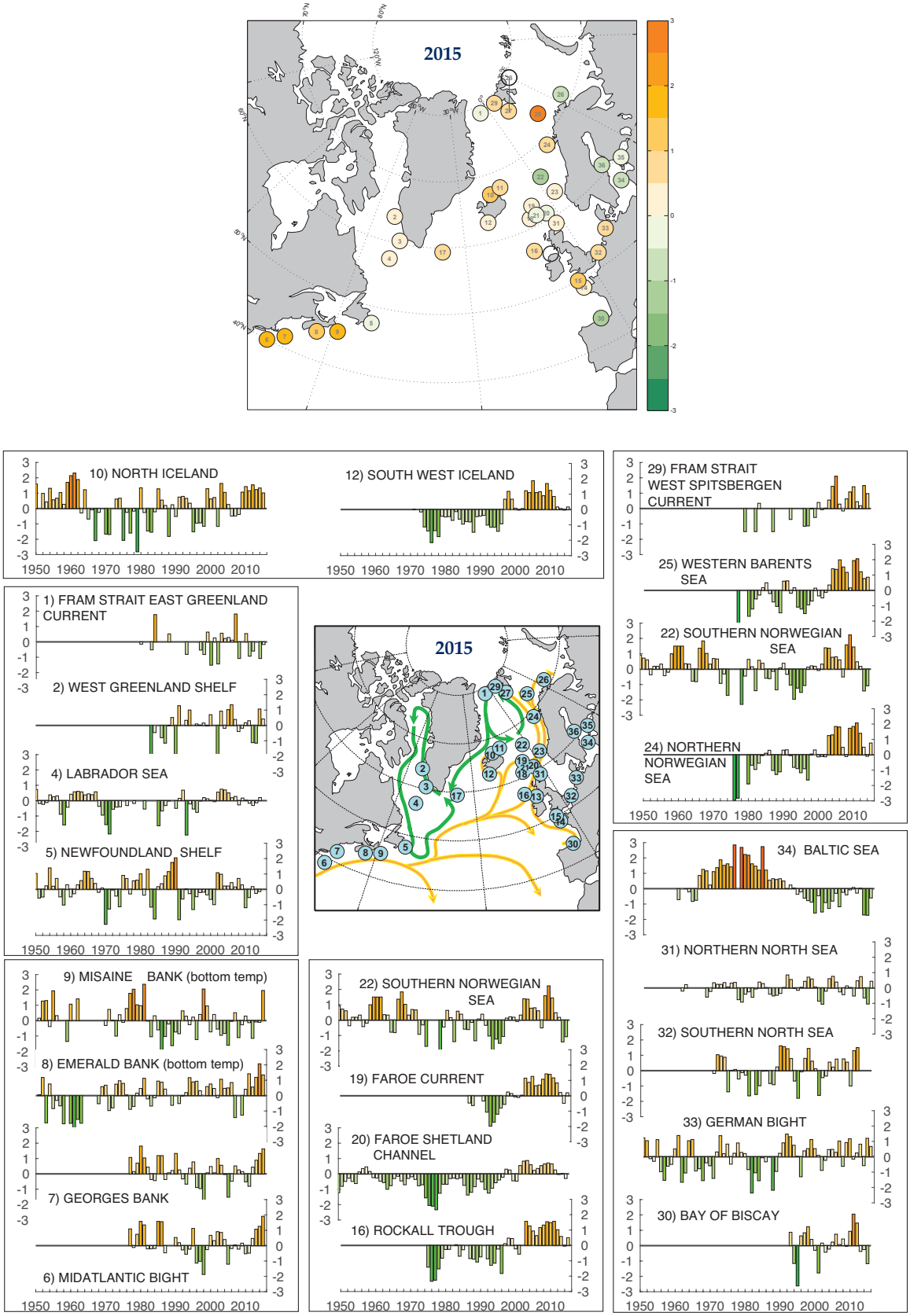

Figure 2.

Upper ocean salinity anomalies at selected locations across the North Atlantic. The anomalies are calculated relative to a long-term mean and normalized with respect to the s.d. (e.g. a value of +2 indicates 2 s.d. above normal). Upper panel: map of conditions in 2015. Lower panels: time-series of normalized anomalies at each of the selected stations. Colour intervals 0.5 s.d.; orange = positive/saline; green = negative/fresh. See Figure 13 for a map supplying more details about the locations in this figure.

2. SUMMARY OF UPPER OCEAN CONDITIONS IN 2015

In this section, conditions in the upper layers of the North Atlantic during 2015 are summarized using data from (i) a selected set of sustained observations, (ii) gridded sea surface temperature (SST) data, and (iii) gridded vertical profiles of temperature and salinity from Argo floats.

2.1 *In situ* stations and sections

Where *in situ* section and station data are presented in the summary tables and figures, normalized anomalies have been provided to allow better comparison of trends in the data from different regions (figures 1–3; tables 1 and 2). Anomalies have been normalized by dividing the values by the s.d. of the data during 1981–2010 (or the closest time period available). A value of +2 thus represents data (temperature or salinity) at 2 s.d. higher than normal.

"Sustained observations" or "time-series" are regular measurements of ocean temperature and salinity made over a long period (10–100 years). Most measurements are made between one and four times a year, but some are made more frequently.

"Anomalies" are the mathematical differences between each individual measurement and the average values of temperature, salinity, or other variables at each location. Positive anomalies in temperature and salinity mean warm or saline conditions; negative anomalies mean cool or fresh conditions.

"Seasonal cycle" describes the short-term changes at the ocean surface brought about by the passing of the seasons; the ocean surface is cold in winter and warms through spring and summer. Temperature and salinity changes caused by the seasonal cycle are usually much greater than the prolonged year-to-year changes described here.

Photo: Penny Holliday, NOC, UK.

	2006	2007	2008	2009	2010	2011	2012	2013	2014	2015
1 (12)	1.31	2.13	-0.69		0.49	0.01	0.40	-0.18	-0.64	0.58
2 (1)	0.57	0.18	-0.46	-0.25	2.22	-0.81	0.50	-0.33	0.67	-0.30
3 (1)	-0.29	1.04	0.06	0.70	1.15	0.57	1.28	0.18	0.83	-0.47
4 (2b)	0.84	0.14	0.26	-0.49	1.12	0.01	0.39	-0.10	-0.01	
5 (2)	1.96	-0.32	0.14	-0.30	1.91	2.74	1.27	1.09	-0.20	0.69
6 (2c)	0.69	-0.12	-0.05	-0.17	0.30	0.51	2.17	1.07	0.36	0.77
7 (2c)	0.52	-0.46	0.24		0.51	0.90	2.51	1.51	1.03	0.51
8 (2)	0.49	-2.20	-1.04	-1.50	0.76	1.12	0.87	0.71	1.64	1.40
9 (2)	1.16	-0.49	0.06	0.65	0.69	1.20	2.05	0.64	0.96	1.39
10 (3)	-0.02	0.61	-0.09	-0.10	1.10	1.43	1.38	1.52	1.52	0.63
11 (3)	0.25	-0.65	0.64	0.46	0.30	1.03	0.64	0.79	1.89	0.89
12 (3)	1.01	0.96	0.40	1.12	1.11	0.73	-0.07	0.25	0.77	-0.98
13 (4b)	1.24			1.37	0.56	1.07	0.74	0.65	1.68	1.02
14 (4b)	-1.22	1.88	0.20	-0.65	-2.04	0.20	0.54			
15 (4b)	-1.86	1.01	0.40	-0.66	0.02	0.05	0.59	-0.26	0.70	0.26
16 (5)	1.10	1.60	1.45	1.38	1.13	1.31	1.45	0.52	0.48	0.20
17 (5b)	0.36	1.17	-0.56	-0.73	0.55	0.69	-0.29		-0.01	-0.43
18 (6)	1.00	1.10	1.30	1.41	0.73	1.28	-0.03	0.04	0.55	0.13
19 (6)	0.85	1.10	0.92	1.20	0.98	1.34	0.93	-0.32	0.43	-0.45
20 (7)	0.70	0.95	0.63	0.20	0.74	0.66	-0.13	-0.34	-0.14	-0.48
21 (7)	0.58	0.71	0.75	0.92	1.35	0.91	0.34	0.45	0.60	-0.09
22 (10)	1.14	0.96	-0.11	1.48	2.05	1.87	2.47	-0.19	0.23	
23 (10)	1.28	1.89	0.19	1.71	0.86	1.12	0.44	0.55	0.33	0.40
24 (10)	2.08	0.45	0.03	1.58	0.33	0.91	1.23	0.14	0.49	1.65
25 (11)	1.82	1.59	0.55	1.33	0.65	-0.03	2.17	0.56	1.12	1.52
26 (11)	1.66	1.39	0.81	0.90	1.02	0.28	2.20	1.25	1.00	1.50
27 (12)	2.17	1.08	-0.18	0.57	0.42	1.01	0.90	0.06	1.10	0.92
28 (10)	1.57	0.65	0.22	0.53	-0.01		0.60	-0.23	1.17	
29 (12)	2.12	1.58	1.28	1.53	1.49	1.66	1.07	1.14	1.53	1.98
30 (4)	1.07	1.33	0.77	-0.37	-0.60	1.53	1.25	-1.00	1.07	0.02
31 (8&9)	1.02	0.79	0.28	0.61	0.81	0.45	0.04	0.15	0.92	0.56
32 (8&9)	0.38	1.23	-0.07	0.28	-2.08	-0.12	-0.79	-1.49	2.35	0.26
33 (8&9)	0.94	1.74	0.94	0.57	-0.87	0.15	0.24	-0.45	2.12	1.11
34 (9b)	1.19	1.19	1.05	0.70	0.05	-0.38		-0.11	0.37	0.72
35 (9b)	1.14	0.68	1.17	1.36	0.42	-1.06	0.52	0.84	0.01	
36 (9b)	-0.02	1.00	1.26	1.33	-0.53	-0.97	-0.16	0.02	1.43	

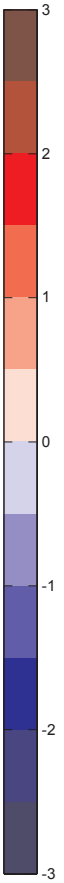

	2006	2007	2008	2009	2010	2011	2012	2013	2014	2015
1 (12)	0.11	1.81	-1.08		0.54	-0.93	-0.60	-1.38	-1.08	-0.17
2 (1)	1.35	0.39	-0.40	-0.18	0.17	0.31	-1.12	-1.15	1.07	0.42
3 (1)	-0.34	0.29	0.11	1.24	0.07	1.20	-0.14	0.80	-0.47	0.15
4 (2b)	0.19	0.27	-0.28	0.17	0.03	-0.17	-0.31	-0.14	0.20	
5 (2)	0.44	0.16	0.71	0.29	-1.20	-0.54	0.18	-0.27	-0.15	-0.21
6 (2c)	-0.19	0.05	-0.23	0.16	-0.53	-0.49	0.47	1.07	1.26	1.91
7 (2c)	-0.48	0.52	0.26	0.15	-0.52	-0.81	0.44	0.89	1.33	1.63
8 (2)	0.85	-1.43		-1.28	0.42	1.42	0.56	1.19	2.07	1.35
9 (2)	-0.05	0.51	-1.11	-0.27	0.29	-0.13	-1.16	-0.09	-0.11	1.96
10 (3)	-0.49	-0.48	-0.39	1.07	1.43	1.16	1.54	1.24	1.34	1.01
11 (3)	0.96	0.95	1.07	0.66	0.99	1.13	1.55	1.22	-0.04	0.90
12 (3)	1.10	1.16	0.90	1.69	1.24	0.85	0.17	0.06	-0.04	0.17
13 (4b)										
14 (4b)	0.54	1.19		-0.02	-0.18	0.85	1.42			
15 (4b)	0.86	1.09	0.39	0.75	0.46	1.31	0.76	0.79	0.46	1.38
16 (5)	0.64	1.16	1.33	1.54	1.49	1.57	1.02	0.58	-0.05	0.50
17 (5b)	0.77	0.98	0.00	0.13	1.39	0.85	0.46		0.35	0.71
18 (6)	0.49	0.51	1.22	1.61	1.53	1.41	0.31	0.46	-0.08	0.32
19 (6)	0.66	0.70	1.08	1.43	1.39	1.17	0.83	0.22	-0.49	0.20
20 (7)	0.23	0.35	0.54	0.65	0.71	0.65	0.26	-0.04	0.02	-0.30
21 (7)	0.44	0.26	0.58	1.08	1.18	0.75	0.65	0.17	-0.35	-0.27
22 (10)	0.81	0.61	-0.51	1.59	2.23	1.45	0.48	0.18	-1.42	
23 (10)	0.70	0.97	0.51	2.01	1.82	1.53	0.69	0.30	-0.63	0.09
24 (10)	1.81	0.48	-0.12	1.73	1.85	2.07	1.40	0.49	-0.10	0.77
25 (11)	1.99	1.53	1.18	0.16	1.95	2.06	1.22	0.77	0.86	4.66
26 (11)	0.88	1.42	0.16	0.52	0.88	1.60	0.34	-0.02	0.16	-0.74
27 (12)	1.61	1.26	0.39	0.65	0.91	1.70	1.68	0.98	1.59	0.70
28 (10)	1.89	1.45	0.92	0.71	0.82		1.45	1.00	1.74	
29 (12)	2.11	0.29	-0.16	0.63	1.08	1.42	0.45	0.18	1.50	0.97
30 (4)	0.75	0.07	0.43	-0.04	0.93	2.05	1.47	-0.38	-0.26	-1.18
31 (8&9)	-0.26	-0.44	0.14	0.03	-0.53	0.47	0.74	-0.65	-1.05	0.44
32 (8&9)	0.76	0.01	0.77	0.56	-1.00	1.30	1.50			
33 (8&9)	1.02	-0.63	0.93	1.17	-0.15	0.25	0.82	-0.58	1.21	0.67
34 (9b)	-1.18	-0.24	-0.40	-0.08	0.08	-0.29	0.03	-1.71	-1.74	-0.61
35 (9b)	1.92	0.20	0.12	0.63	0.85	0.06	-1.00	0.85	0.11	
36 (9b)	0.57	0.99	0.32	0.62	2.13	1.92	1.01	0.39	1.00	

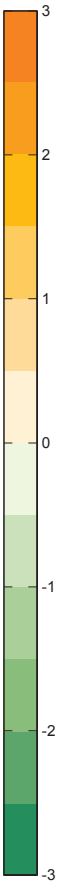

Tables 1 and 2.

Changes in temperature (Table 1, top) and salinity (Table 2, bottom) at selected stations in the North Atlantic region during the past decade, 2006–2015. The index numbers on the left can be used to cross-reference each point with information in figures 1 and 2 and Table 3. The numbers in brackets refer to the sections in Chapter 4. Unless specified, these are upper-layer anomalies. The anomalies are normalized with respect to the s.d. (e.g. a value of +2 indicates that the data—temperature or salinity—for that year were 2 s.d. above normal). Blank boxes indicate that data were unavailable for a particular year at the time of publication. Note that no salinity data are available for station 13. Colour intervals 0.5 s.d.; red = warm; blue = cold; orange = saline; green = fresh.

Index	Description	Section	Measurement depth	Reference period	Lat	Lon	Mean *T*, ^0C	S.d. *T*, ^0C	Mean S	S.d.S
1	Fram Strait – East Greenland Current	4.20	50–500 m	1983–2010	78.83	−6.00	0.69	0.57	34.650	0.135
2	Fylla section – Station 4 – Greenland Shelf	4.02	0–50 m	1983–2010	63.88	−53.37	2.64	1.10	33.162	0.392
3	Cape Desolation section – Station 3 – Greenland Shelf	4.02	75–200 m	1983–2010	60.47	−50.00	5.72	0.66	34.923	0.062
4	Central Labrador Sea	4.03	15–50 m	1981–2010	57.07	−50.92	4.68	0.69	34.635	0.176
5	Station 27 – Newfoundland Shelf temperature – Canada	4.04	0–175 m	1981–2010	47.55	−52.59	0.33	0.39	31.946	0.166
6	NE US Continental Shelf – Northern Mid-Atlantic Bight	4.06	1–30 m	1981–2010	40.00	−71.00	11.36	0.94	32.710	0.430
7	NE US Continental Shelf – Northwest Georges Bank	4.06	1–30 m	1981–2010	41.50	−68.30	10.00	0.79	32.580	0.270
8	Emerald Basin – Central Scotian Shelf – Canada	4.05	250 m (near bottom)	1981–2010	44.00	−63.00		0.83		0.151
9	Misaine Bank – Northeast Scotian Shelf – Canada	4.05	100 m (near bottom)	1981–2010	45.00	−59.00		0.63		0.134
10	Siglunes Station 2–4 – North Iceland – North Icelandic Irminger Current – Spring	4.07	50–150 m	1981–2010	67.00	−18.00	3.41	0.98	34.859	0.108
11	Langanes Station 2–6 – Northeast Iceland – East Icelandic Current – Spring	4.07	0–50 m	1981–2010	67.50	−13.50	1.22	0.61	34.729	0.067
12	Selvogsbanki Station 5 – Southwest Iceland – Irminger Current – Spring	4.07	0–200 m	1981–2010	63.00	−21.47	7.88	0.47	35.187	0.049
13	Point 33 – Astan	4.09	5 m	1998–2010	48.78	−3.94	12.79	0.34	35.206	0.112
14	Western Channel Observatory(WCO) – E1 – UK	4.09	0–40 m	1981–2010	50.03	−4.37	12.43	0.93	35.200	0.100
15	Malin Head Weather Station	4.10	Surface	1981–2010	55.37	−7.34	10.25	0.57		
16	Ellett Line – Rockall Trough – UK (section average)	4.11	30–800 m	1981–2010	56.75	−11.00	9.35	0.28	35.351	0.036
17	Central Irminger Sea subpolar-mode water	4.14	200–400 m	1991–2010	59.40	−36.80	4.35	0.53	34.900	0.031
18	Faroe Bank Channel – West Faroe Islands	4.15	Upper layer high salinity core	1988–2010	61.40	−8.30	8.80	0.36	35.302	0.043
19	Faroe Current – North Faroe Islands (modified North Atlantic water)	4.15	Upper layer high salinity core	1987–2010	63.00	−6.00	8.11	0.39	35.249	0.043
20	Faroe Shetland Channel – Shetland Shelf (North Atlantic water)	4.15	Upper layer high salinity core	1981–2010	61.00	−3.00	9.95	0.47	35.398	0.051
21	Faroe Shetland Channel – Faroe Shelf (modified North Atlantic water)	4.15	Upper layer high salinity core	1981–2010	61.50	−6.00	8.32	0.54	35.259	0.055
22	Ocean Weather Station Mike	4.18	50 m	1981–2010	66.00	2.00	7.71	0.44	35.176	0.036
23	Southern Norwegian Sea – Svinøy section – Atlantic water	4.18	50–200 m	1981–2010	63.00	3.00	8.04	0.39	35.234	0.039
24	Central Norwegian Sea – Gimsøy section – Atlantic water	4.18	50–200 m	1981–2010	69.00	12.00	6.89	0.34	35.154	0.031
25	Fugløya – Bear Island section – Western Barents Sea – Atlantic inflow	4.19	50–200 m	1981–2010	73.00	20.00	5.55	0.46	35.078	0.035
26	Kola section – Eastern Barents Sea	4.19	0–200 m	1981–2010	71.50	33.50	4.22	0.52	34.771	0.056
27	Greenland Sea section – West of Spitsbergen 76.5°N	4.20	200 m	1996–2010	76.50	10.05	3.19	0.61	35.058	0.043
28	Northern Norwegian Sea – Sørkapp section – Atlantic water	4.18	50–200 m	1981–2010	76.33	10.00	4.08	0.60	35.073	0.038
29	Fram Strait – West Spitsbergen Current	4.20	50–20 m	1983–2010	78.83	7.00	3.11	0.69	35.027	0.038
30	Santander Station 6 (Shelf Break) – Bay of Biscay – Spain	4.08	0–30 m	1993–2010	43.71	−3.78	15.74	0.32	35.460	0.160
31	Fair Isle Current water (waters entering the North Sea from the Atlantic)	4.16	0–100 m	1981–2010	59.00	−2.00	9.93	0.61	34.874	0.132
32	Section average – Felixstowe – Rotterdam – 52°N	4.1	Surface	1981–2010	52.00	3.00		0.72		0.212
33	North Sea – Helgoland Road	4.16	Surface	1981–2010	54.18	7.90	10.26	0.75	32.096	0.568
34	Baltic Proper – East of Gotland – Baltic Sea	4.17 4.17	Surface T Surface S	1990–2010 1981–2010	57.50	19.50	9.27	1.03	7.172	0.196
35	Baltic – LL7 – Baltic Sea	4.17	70 m	1991–2010	59.51	24.50	3.97	0.73	7.961	0.666
36	Baltic – SR5 – Baltic Sea	4.17	110 m	1991–2010	61.05	19.35	3.27	0.58	6.428	0.141

Table 3.

Details of the datasets included in figures 1 and 2 and tables 1 and 2. Blank boxes indicate that no information was available for the area at the time of publication. T = temperature, S = salinity. Some data are calculated from an average of more than one station; in such cases, the latitudes and longitudes presented here represent a nominal midpoint along that section.

2.2 SEA SURFACE TEMPERATURE

Sea surface temperatures across the entire North Atlantic have also been obtained from a combined satellite and *in situ* gridded dataset. Figure 3 shows the seasonal SST anomalies for 2015 (relative to 1981–2010) extracted from the Optimum Interpolation SST dataset (OISST.v2) provided by the NOAA–CIRES Climate Diagnostics Center, USA. The 1981–2010 climatology was prepared from a combination of the Extended Reconstructed Sea Surface Temperature (ERSST) and OISST data[1]. At high latitudes, where *in situ* data are sparse and satellite data are hindered by cloud cover, the data may be less reliable. Regions with ice cover for >50% of the averaging period appear blank.

[1]http://www.cpc.ncep.noaa.gov/products/people/yxue/sstclim/Note_SST_Climatology_1981-2010.doc.

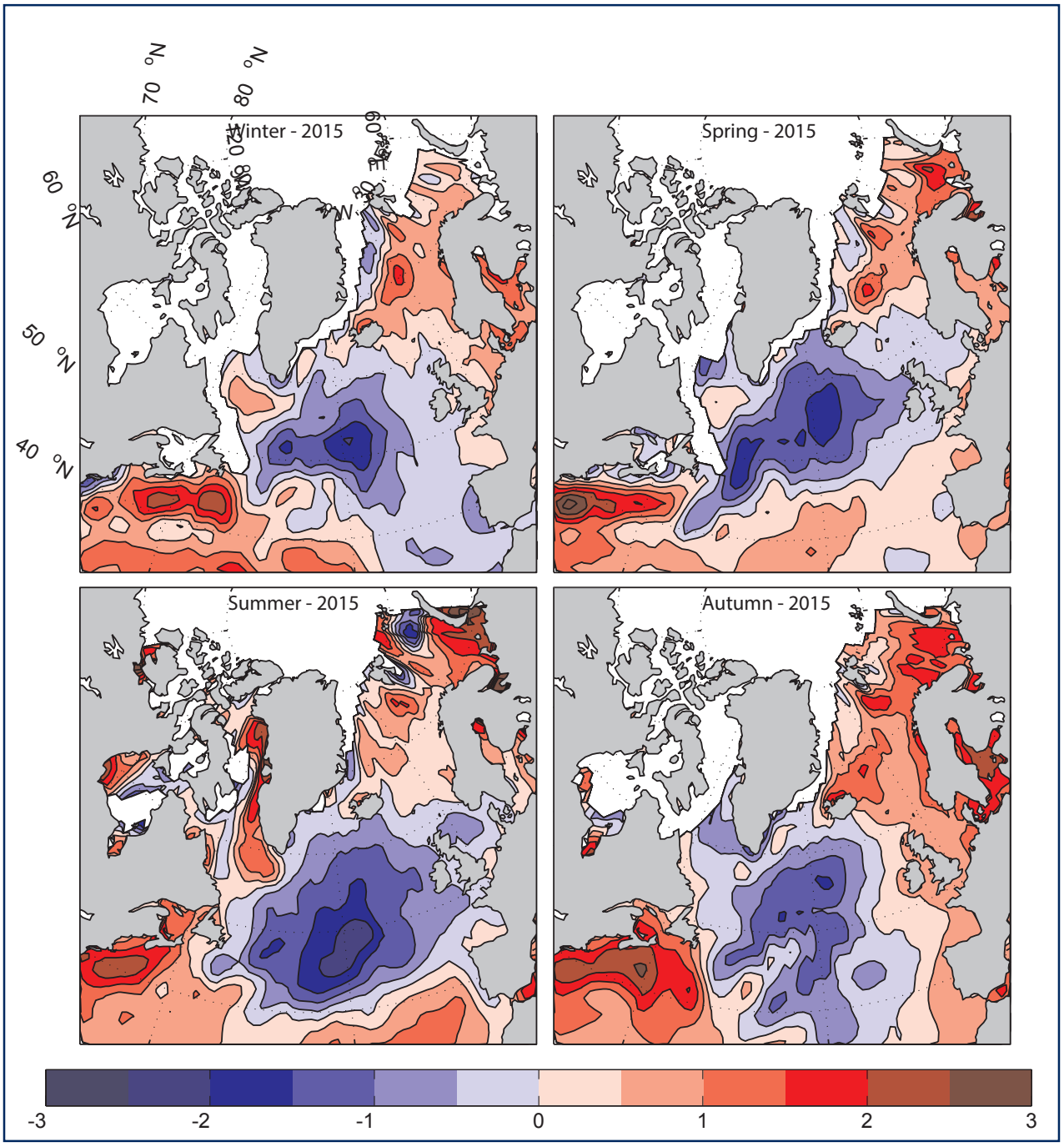

Figure 3.
Maps of seasonal sea surface temperature anomalies (°C) over the North Atlantic for 2015 from the NOAA Optimum Interpolation SST.v2 dataset provided by the NOAA–CIRES Climate Diagnostics Center, USA. The colour-coded temperature scale is the same in all panels. In this case, the anomaly is calculated with respect to normal conditions for 1981–2010. The data are produced on a 1° grid from a combination of satellite and in situ *temperature data. Regions with ice cover for >50% of the averaging period are left blank.*

2.3 GRIDDED TEMPERATURE AND SALINITY FIELDS

"Argo and the *in situ* analysis system"

The Argo[2] network of profiling floats has been set up to monitor large-scale global ocean variability. Argo data are transmitted in real-time and quickly made available by the two Global Data Assembly Centres (the Argo-GDAC ftp servers US GODAE/FNMOC/USA in Monterrey and Coriolis at Ifremer Brest in France). Delayed-mode data are also available; these datasets have undergone more detailed quality control and calibration. Depending on the timing of the analysis process, the most recent 1–2 years of data presented in this report may come from a near real-time dataset, and older data will come from the higher-quality, delayed-mode datasets.

The dataset presented here was prepared at the Coriolis data centre[3]. Although the ARGO dataset remains the main contribution in the open ocean, Coriolis assembles many types of data transmitted in real-time, merging the ARGO dataset with data collected by the Global Telecommunications System (GTS) relating to mooring, marine animals, gliders, and conductivity, temperature and depth profilers (CTDs). As the ISAS analysis was designed to produce monthly synthesis over the global ocean, the time- and space-scales have been adjusted to the most general data availability. Overall, this dataset is less skilled at describing conditions in the shallower marginal seas.

In the North Atlantic, the ARGO dataset has adequately described temperature and salinity conditions of the upper 2000 m since 2002. This dataset is thus suitable for an overview of the oceanographic conditions in the deeper and more central regions of the North Atlantic basin and complements the data from the IROC repeat stations and sections which are collected mainly at the periphery of the basin.

Figures 4 and 5 illustrate the 2015 seasonal mean fields of temperature and salinity at 10 m as anomalies from a reference climatology in the World Ocean Atlas (WOA-05 – Antonov *et al.*, 2006; Locarnini *et al.*, 2006). Annual mean anomalies of temperature and salinity for recent years at two selected depths, 10 and 1000 m, are presented in figures 6 and 7. Finally, in Figure 8, the winter (February) mixed-layer depth is shown. Note that the mixed-layer depth (z) is defined as the depth where the temperature has decreased by 0.5°C from the temperature measured at 10 m [T(z) < T(10 m) – 0.5]. This criterion is not suitable for areas where effects of salinity are important (ice melting) or where the basic stratification is weak. Therefore, results in the Labrador Sea, around Greenland, and in the Gulf of Lion are not significant.

Temperature and salinity fields are estimated on a regular half-degree (Mercator scale) grid using the Coriolis *In Situ* Analysis System (ISAS). For data between 2002 and 2012, the results presented here were produced with delayed-mode data from version 6 of ISAS (Gaillard, 2015). For the years 2013–2015, delayed-mode data are not yet available; therefore, near-real-time data (NRTISAS, with near-real-time processing done by Coriolis) are presented. Temperature and salinity anomalies are calculated relative to monthly climatological averages prepared from the World Ocean Atlas (WOA-05 – Antonov *et al.*, 2006; Locarnini *et al.*, 2006).

The ISAS gridded fields are based entirely on *in situ* products, whereas OISST is a combination of *in situ* and satellite sea surface temperatures. Comparison of figures 3 and 4 demonstrates that the patterns of surface anomalies match reasonably well. The main differences are in the region east of Newfoundland, which may be due to the undersampling of the high variability in this region in the ARGO dataset. One great advantage of the ISAS dataset is the inclusion of both temperature and salinity fields as well as subsurface data. These data also offer valuable information on conditions in the central North Atlantic, where *in situ* sampling from hydrographic surveys is sparse and infrequent.

During winter 2015 (figures 4 and 5), near-surface waters were cold and fresh in a large portion of the northern North Atlantic, centred on ca. 50°N. This feature, which was also observed in 2014 (Figure 6), persisted throughout the year in 2015, spreading in extent during summer and autumn and extending southward of 40°N in autumn 2015. In 2015, however, the cool fresh anomaly covered a larger region than observed in 2014 and also began spreading to the ocean margins where it is more likely to be observed in the *in situ* datasets (figures 3 and 4).

Annual mean anomalies for the ocean interior at a depth of 1000 m are shown in Figure 7. The Greenland, Labrador, and Irminger seas continue to be warmer than normal, a pattern that has persisted since at least 2009. In contrast, conditions have been cooler and fresher than normal east of 30°W in the Iceland Basin and Rockall Trough over the same time period.

Variations in the February mixed-layer depth (defined as the depth where temperature differs by more than 0.5°C from the 10 m value) are shown in Figure 8. The extremely deep (600 m) mixed layer seen in the 2014 map obtained from near-real-time temperature fields in the temperate eastern North Atlantic looks unrealistic. Such values are not present in the 2015 maps when mixed layer depths returned to 200–300 m, similar to that observed in the period 2009–2013. An error in the dataset or issues with the threshold algorithm cannot be excluded. The ISAS15 reanalysis presently in preparation will replace the 2013–2015 period in the next IROC report.

[2]http://www.argo.ucsd.edu/.

[3]http://www.coriolis.eu.org.

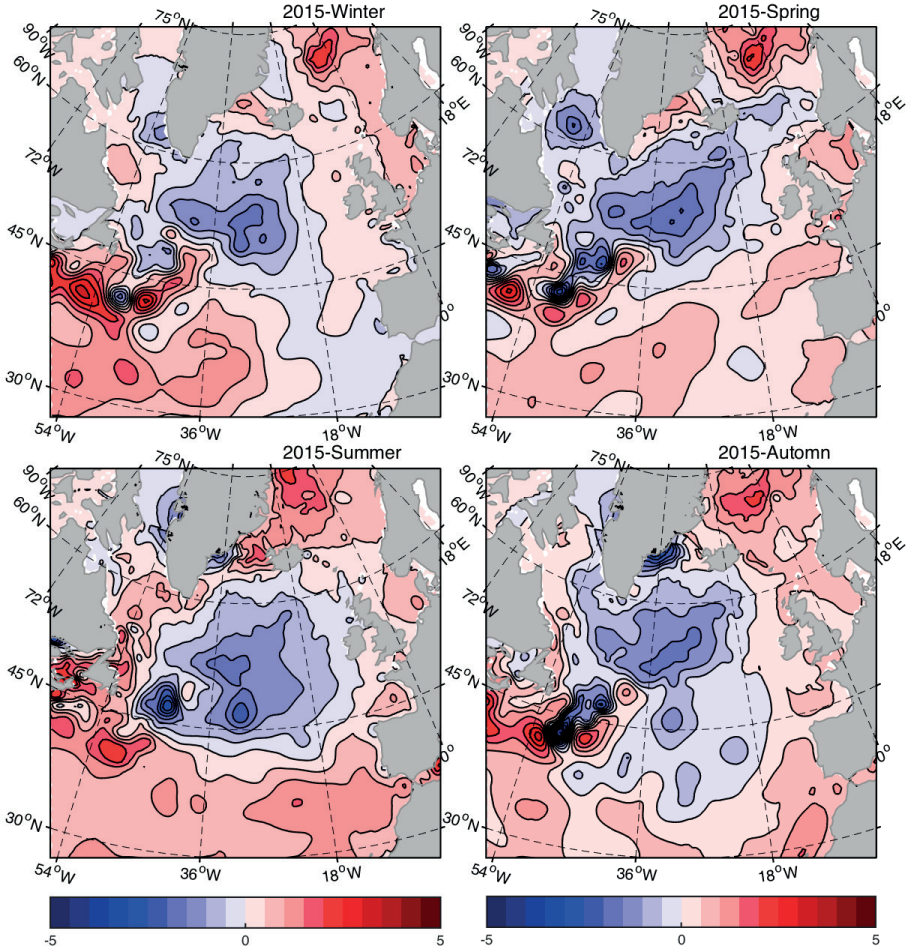

Figure 4.
Maps of 2015 seasonal temperature anomalies at 10 m depth in the North Atlantic. Anomalies are the differences between the ISAS monthly mean values and the reference climatology, WOA-05. The colour-coded temperature scale is the same in all panels. From the ISAS monthly analysis of Argo data.

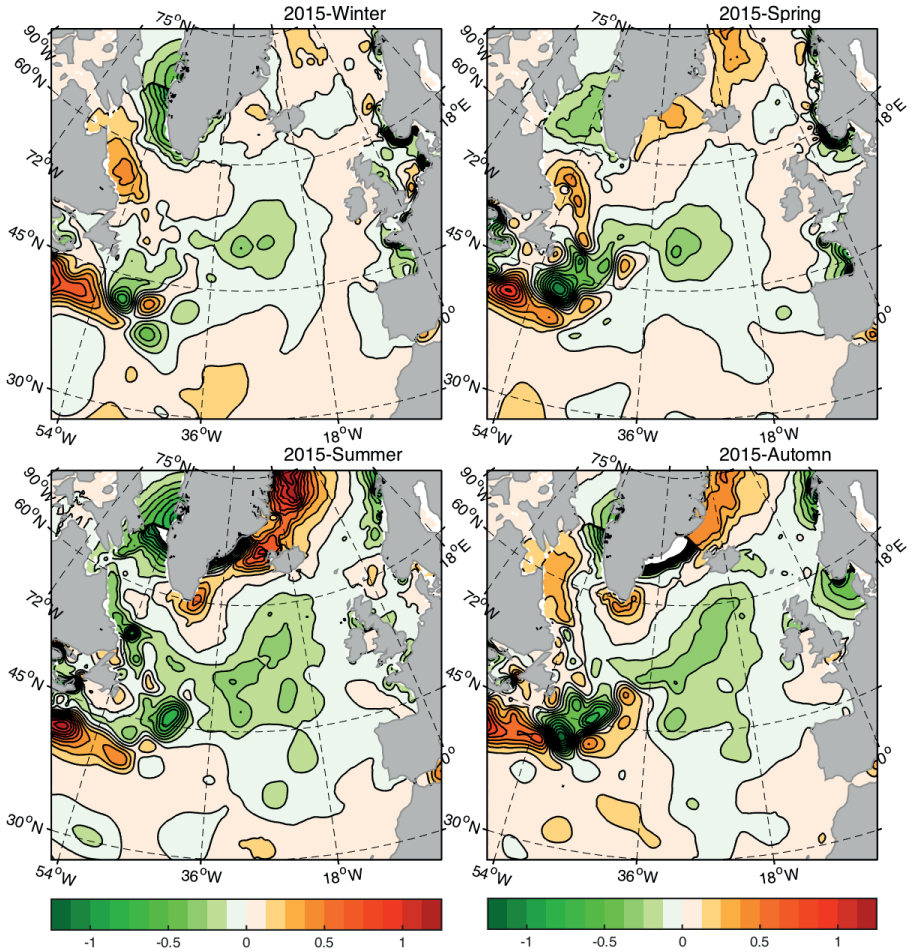

Figure 5.
Maps of 2015 seasonal salinity anomalies at 10 m depth in the North Atlantic. Anomalies are the differences between the ISAS monthly mean values and the reference climatology, WOA-05. The colour-coded salinity scale is the same in all panels. From the ISAS monthly analysis of Argo data.

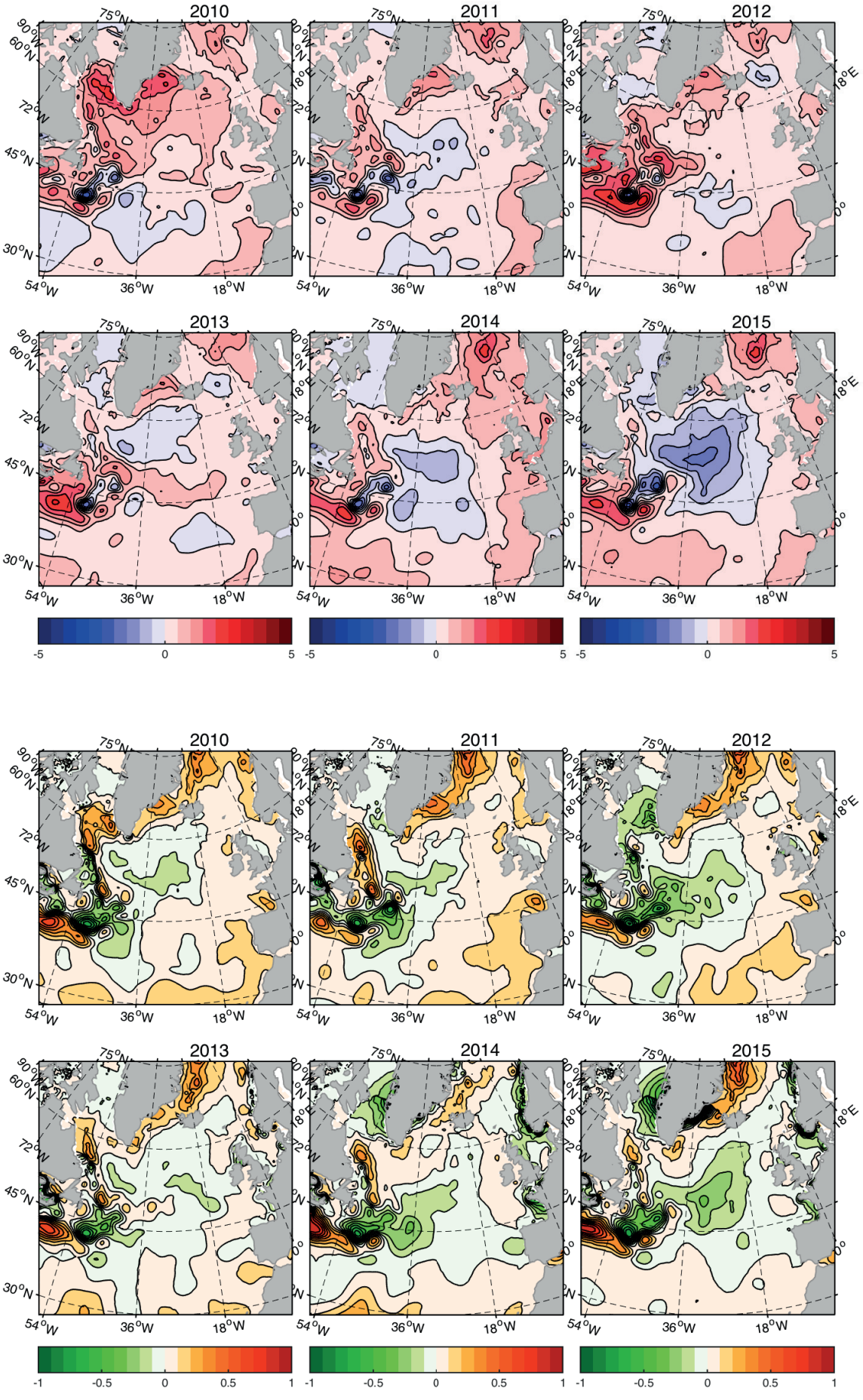

Figure 6.

Maps of annual temperature (upper) and salinity (lower) anomalies at 10 m for 2010–2015. From the ISAS monthly analysis of Argo data.

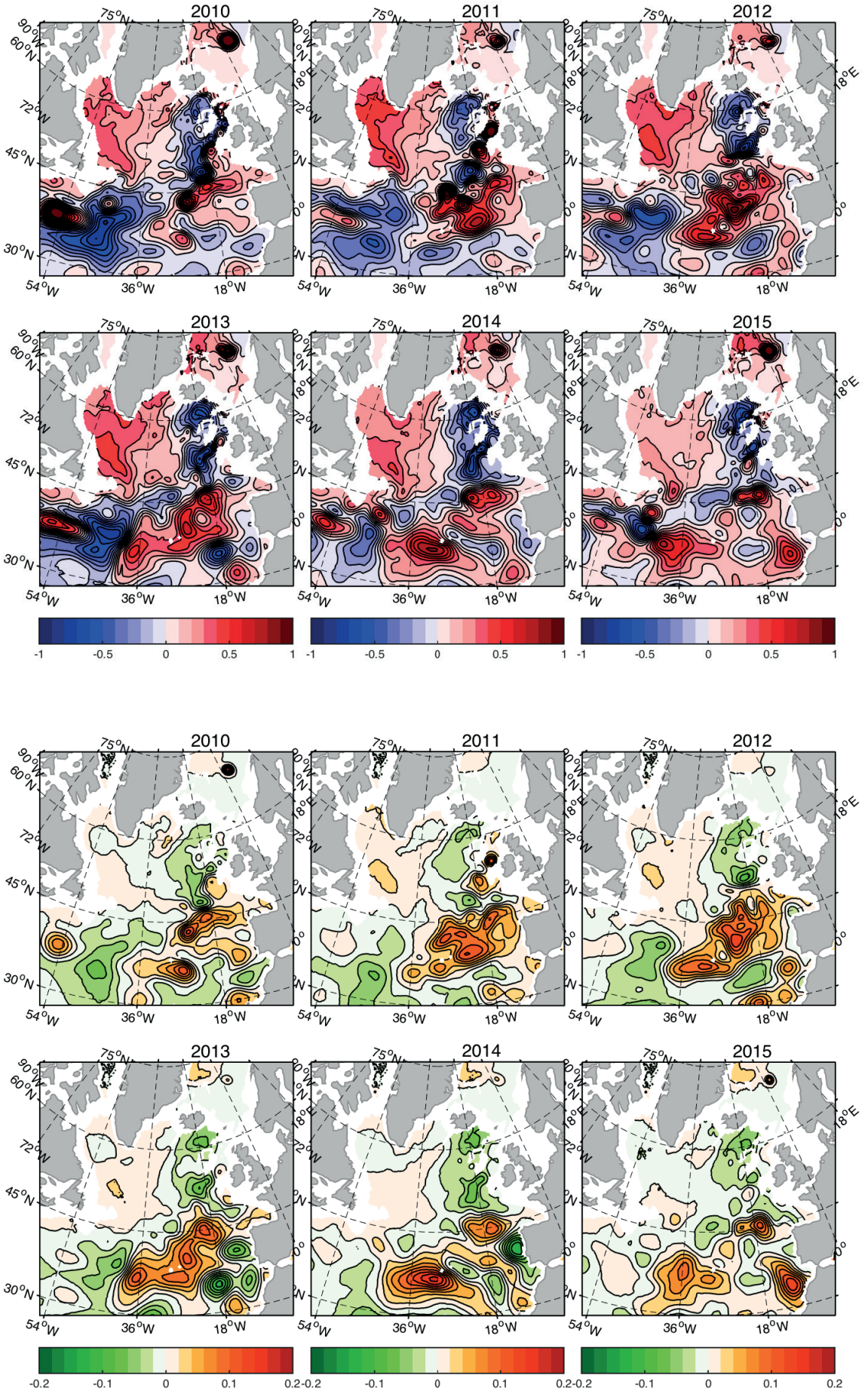

Figure 7.

Maps of annual temperature (upper) and salinity (lower) anomalies at 1000 m for 2010–2015. From the ISAS monthly analysis of Argo data.

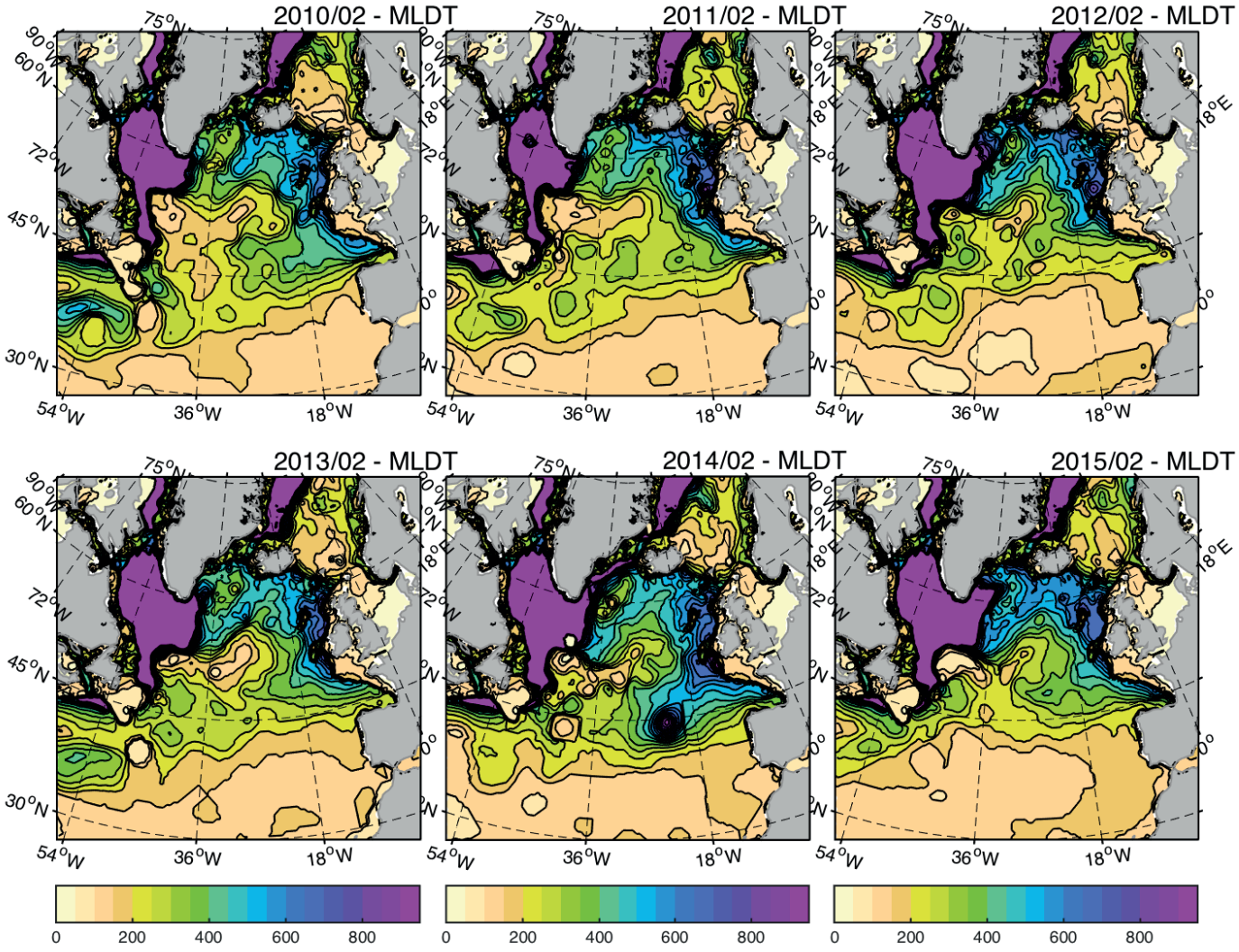

Figure 8.

Maps of North Atlantic winter (February) mixed-layer depths for 2010–2015. From the ISAS monthly analysis of Argo data. Note that the mixed-layer depth is defined as the depth at which the temperature has decreased by more than 0.5°C from the temperature at 10 m. This criterion is not suitable for areas where effects of salinity are important (ice melting) or where the basic stratification is weak. Therefore, results in the Labrador Sea, around Greenland, and in the Gulf of Lion are not significant.

Photo: Jannica Haldin, ICES.

3. THE NORTH ATLANTIC ATMOSPHERE

3.1 Sea level pressure and windspeed

The North Atlantic Oscillation (NAO) is a pattern of atmospheric variability that has a significant impact on oceanic conditions. It affects windspeed, precipitation, evaporation, and the exchange of heat between ocean and atmosphere, and its effects are most strongly felt in winter. The NAO index is a simple device used to describe the state of the NAO. It is a measure of the strength of the sea-level air pressure gradient between Iceland and Lisbon, Portugal. When the NAO index is positive, there is a strengthening of the Icelandic low-pressure system and the Azores high-pressure system. This produces stronger mid-latitude westerly winds, with colder and drier conditions over the western North Atlantic and warmer and wetter conditions in the eastern North Atlantic. When the NAO index is negative, there is a reduced pressure gradient and the effects tend to be reversed.

When the NAO is weak, two additional dominant atmospheric regimes have been recognized as useful descriptors: (i) the Atlantic Ridge mode, when a strong anticyclonic ridge develops off western Europe (similar to the East Atlantic pattern); and (ii) the blocking regime, when the anticyclonic ridge develops over Scandinavia. The four regimes (positive NAO, negative NAO, Atlantic Ridge, and blocking) have all been occurring at around the same frequency (20–30% of all winter days) since 1950. These modes of variability are revealed through cluster analyses of sea-level pressure (SLP) rather than examining point-to-point SLP gradients.

There are several slightly different versions of the NAO index calculated by climate scientists. The Hurrell winter (December/January/February/March, or DJFM) NAO index (Hurrell *et al.*, 2003) is most commonly used and is particularly relevant to the eastern North Atlantic. Note that although winter may be thought of as coming at the end of the year, here the "winter season" spans an annual boundary and precedes the year of interest. Therefore, the winter of December 2014–March 2015 determines conditions for summer 2015.

Following a long period of increase, from an extreme and persistent negative phase in the 1960s to a most extreme and persistent positive phase during the late 1980s and early 1990s, the Hurrell NAO index underwent a large and rapid decrease during winter 1995/1996. In many of the years between 1996 and 2009, the Hurrell winter NAO index was both fairly weak and a less useful descriptor of atmospheric conditions, mainly because of the sea-level pressure following patterns not typical of the NAO.

In winter 2010, the index was strongly negative (Figure 9), and its anomaly pattern exerted a dominant influence on atmospheric conditions. This was the strongest negative anomaly since 1969 and the second strongest negative value for the Hurrell winter NAO index on record (starting in 1864). In winter 2014/2015, the Hurrell winter NAO index was strongly positive (+3.56) for a second year, representing the strongest NAO index since 1995 and the fourth most positive NAO index in the last 110 years (Hurrell *et al.*, 2016).

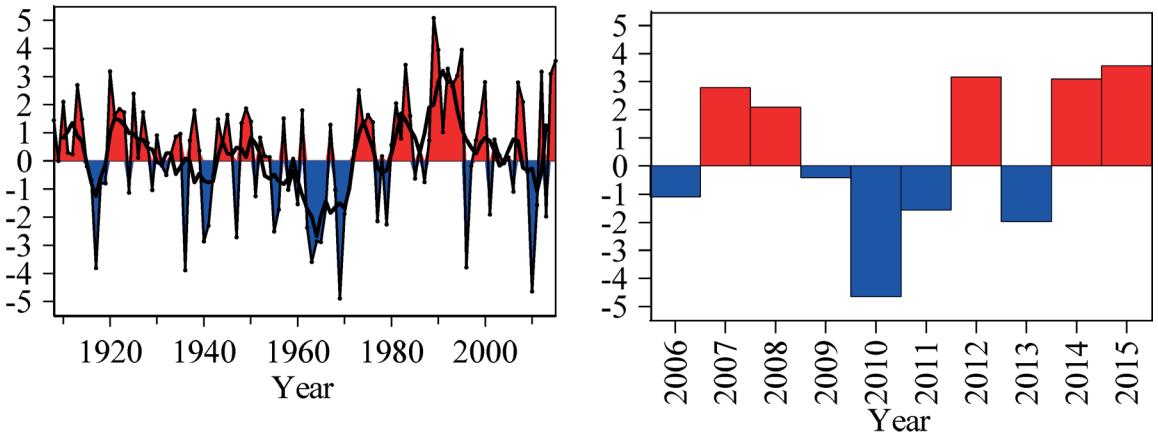

Figure 9.

The Hurrell winter (DJFM) NAO index for the past 100 years, with a two-year running mean applied (left panel), and for the current decade (right panel). Data source: NAO Index Data provided by the Climate Analysis Section, NCAR, Boulder, CO, USA (Hurrell et al.*, 2016). Updated regularly. Accessed 3 April 2016. https://climatedataguide.ucar.edu/climate-data/hurrell-north-atlantic-oscillation-nao-index-station-based.*

The atmospheric conditions indicated by the NAO index are more clearly understandable when the anomaly fields are mapped. Ocean properties are particularly dominated by winter conditions, hence the inclusion of maps of sea-level pressure for the winter period (Figure 10).

The top panel of Figure 10 shows the winter SLP averaged over 30 years (1981–2010). The dominant features ("action centres") are the Iceland Low, situated southwest of Iceland, and the Azores High, west of Gibraltar. The middle panel of Figure 10 shows the mean SLP for winter 2015 (December 2014, January–March 2015), and the bottom panel shows the 2015 winter SLP anomaly (i.e. the difference between the top and middle panels). In winter 2015, both the Iceland Low and the Azores High were strong, with the main difference being that the Iceland Low was stronger and extended farther south than normal, while the Azores High was stronger and also farther west than usual. The resultant sea-level pressure anomaly exhibited a strong positive centre over the Azores with limited extension zonally.

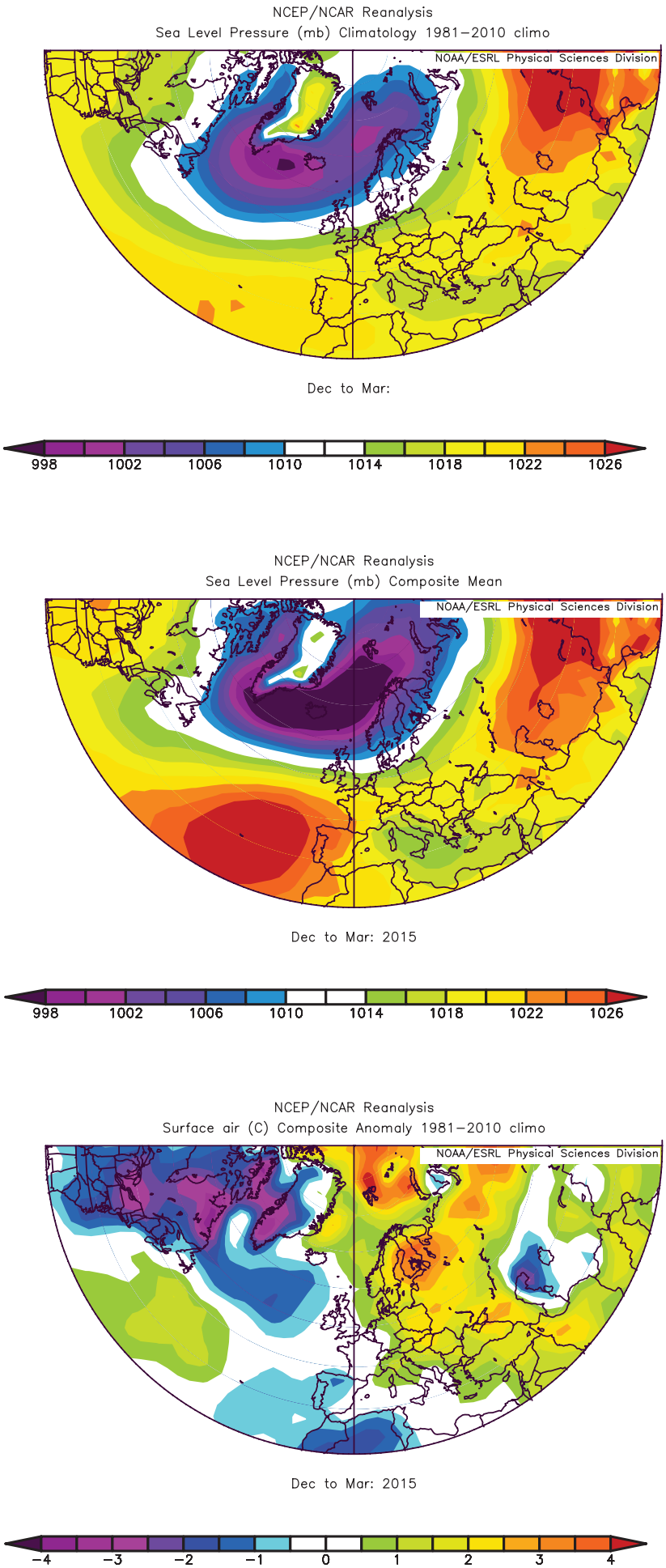

Figure 10.
Winter (DJFM) sea-level pressure (SLP) fields. Top panel: SLP averaged over 30 years (1981–2010). Middle panel: mean SLP in winter 2015 (December 2014, January–March 2015). Bottom panel: winter 2015 SLP anomaly—the difference between the top and middle panels. Images provided by the NOAA/ESRL Physical Sciences Division, Boulder, CO, USA (available online at http://www.cdc.noaa.gov/).

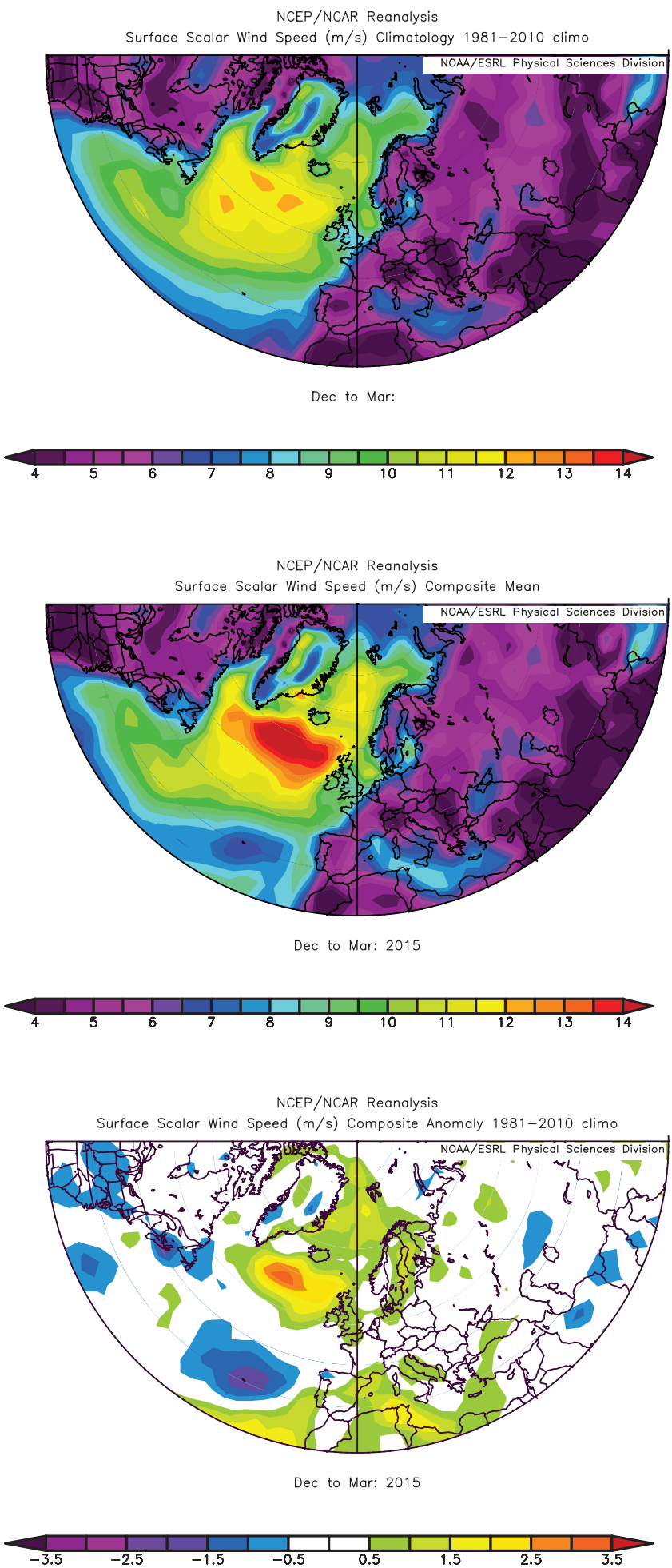

The pattern of sea-level pressure is closely related to patterns of wind. The geostrophic (or "gradient") wind blows parallel to the isobars, with lower pressure to the left; the closer the isobars, the stronger the wind. The strength of the winter mean surface wind averaged over the 30-year period (1981–2010) is shown in the upper panel of Figure 11, while the middle panel shows the mean surface wind for winter 2015 and the lower panel, the anomaly in winter 2015. Stronger-than-normal winds, associated with the strong northwest-to-southeast orientation of the isobars, were observed over the eastern North Atlantic centred between Scotland and Cape Farewell. The limited zonal extension of the strong anticyclonic anomaly over the Azores generated lower-than-normal windspeeds locally, but northerly winds over the Bay of Biscay and the Iberian Peninsula and southerly winds over the western North Atlantic between Newfoundland and the Azores.

Figure 11.
Winter (DJFM) surface windspeed. Top panel: surface windspeed averaged over 30 years (1981–2010). Middle panel: mean surface windspeed in winter 2015 (December 2014, January–March 2015). Bottom panel: winter 2014 surface windspeed anomaly—the difference between the top and middle panels. Images provided by the NOAA/ESRL Physical Sciences Division, Boulder, CO, USA (available online at http://www.cdc.noaa.gov/).

3.2 Surface air temperature

North Atlantic winter mean surface air temperatures are shown in Figure 12 (Kalnay *et al.*, 1996). The 1981–2010 mean conditions (Figure 12, top panel) show warm temperatures penetrating far to the north on the eastern side of the North Atlantic and the Nordic seas, caused by the northward movement of warm oceanic water. The middle panel of Figure 12 shows the conditions in winter (DJFM) 2014/2015, and the bottom panel shows the difference between the two.

Winter 2014/2015 was warmer than normal over the Nordic seas, Scandinavia, and central and eastern Europe. Over the continental area of the US, Canada, and Greenland, however, the winter was much colder than normal, and there was also an area of colder-than-normal air over the Subpolar Gyre region of the central North Atlantic, likely related to the sea surface temperature anomalies observed in this region.

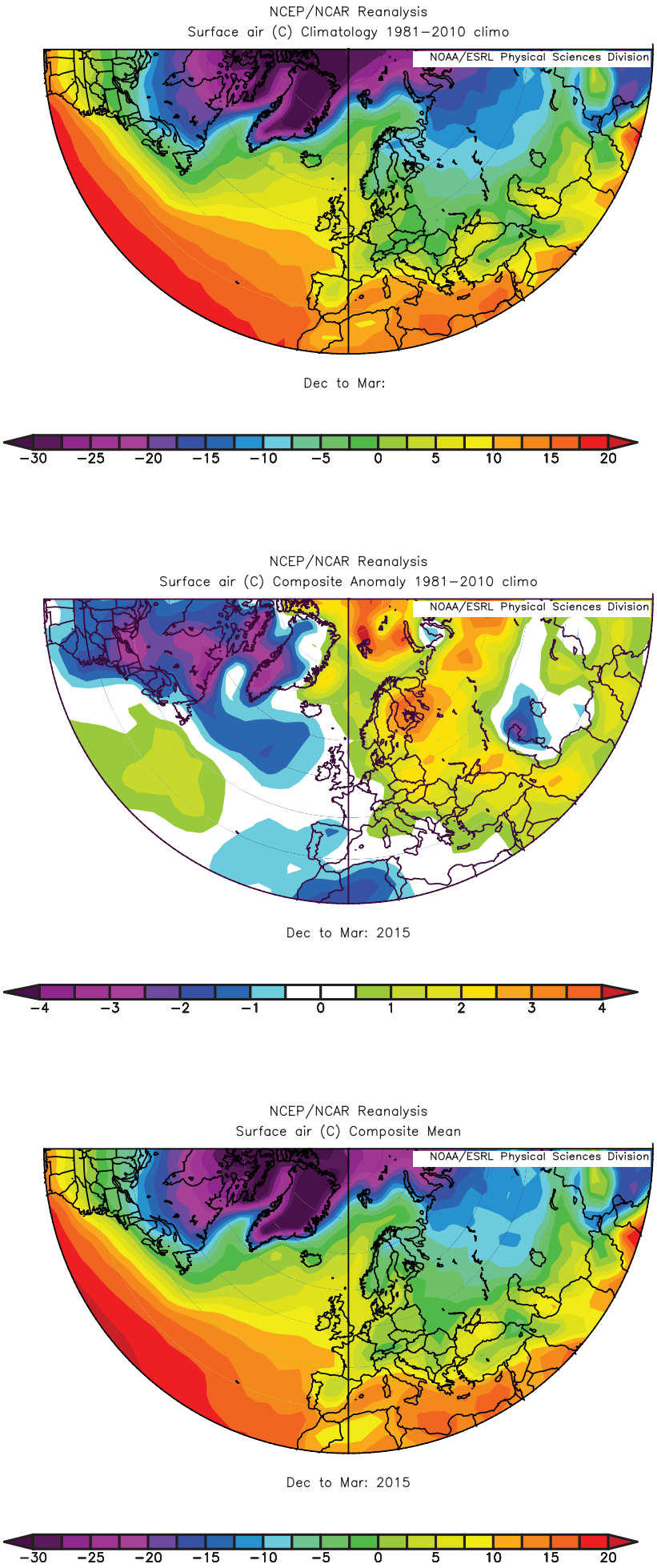

Figure 12.
Winter (DJFM) surface air temperature fields. Top panel: surface air temperature averaged over 30 years (1981–2010). Middle panel: temperatures in winter 2015 (December 2014, January–March 2015). Bottom panel: winter 2014 surface air temperature anomaly – the difference between the top and middle panels. Images provided by the NOAA/ESRL Physical Sciences Division, Boulder, CO, USA (available online at http://www.cdc.noaa.gov/).

4. DETAILED AREA DESCRIPTIONS, PART I: THE UPPER OCEAN

4.1 Introduction

This section presents time-series from many sustained observations in each of the ICES areas. The general pattern of oceanic circulation in the upper layers of the North Atlantic, relative to the areas described here, is given in Figure 13. In addition to temperature and salinity, other indices are presented where available, such as air temperature and sea ice extent. The regional context of the sections and stations is summarized, noting significant recent events.

Most standard sections or stations are sampled annually or more frequently. Often, the time-series presented here have been extracted from larger datasets and have been chosen as indicators of the conditions in a particular area. Where appropriate, data are presented as anomalies to demonstrate how the values compare with the average or "normal" conditions (usually the long-term mean of each parameter during 1981–2010). For datasets that do not extend as far back as 1981, average conditions have been calculated from the beginning of the dataset up to 2010.

In places, the seasonal cycle has been removed from a dataset, either by calculating the average seasonal cycle during 1981–2010 or by drawing on other sources, such as regional climatology datasets. Smoothed versions of most time-series are included using a "Loess smoother", a locally weighted regression with a two- or five-year window (chosen to be the most appropriate for each time-series).

In some areas, data are sampled regularly enough to allow a good description of the seasonal cycle. Where possible, monthly data from 2015 are presented and compared with the average seasonal conditions and statistics.

Although there are no real boundaries in the ocean, the aim is to use the data presented to represent conditions in a particular area (Figure 14). In setting out this chapter, datasets are grouped into areas based on existing definitions such as the ICES marine ecoregions[4] or NOAA Large Marine Ecosystems (LMEs)[5]. The bathymetry of ocean basins[6] and the general pattern of ocean circulation (Figure 13) are also taken into account.

[4]http://www.ices.dk/community/advisory-process/Pages/ICES-ecosystems-and-advisory-areas.aspx.

[5]http://www.lme.noaa.gov/

[6]http://www.gebco.net/data_and_products/undersea_feature_names/

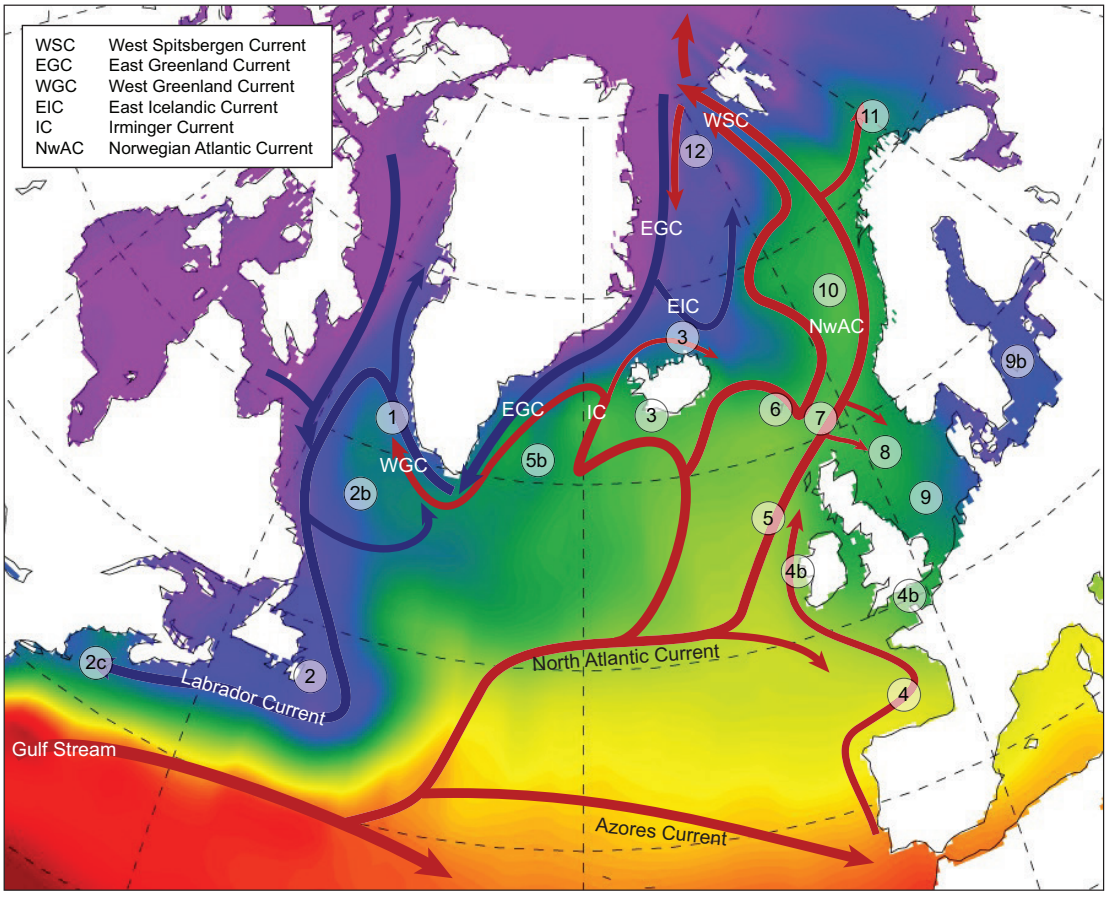

Figure 13.
Schematic of the general circulation of the upper ocean (0–1000 m) in the North Atlantic relative to the numbered areas presented below. Blue arrows = movement of cooler waters of the Subpolar Gyre; red arrows = movement of warmer waters of the Subtropical Gyre.

Where there is overlap, the ICES marine ecoregions and the NOAA LMEs generally align although there are some differences in the position of offshore boundaries. The offshore boundaries of the ICES marine ecoregions are often aligned to management areas, in most cases the 200 nautical mile fishery limits; accordingly, they are economic limits rather than truly ecosystem boundaries. The offshore boundaries of LMEs are more often aligned to bathymetric contours. Ocean currents tend to circulate around ocean basins and thus flow at the margins of a sea/ocean area. Shelf areas generally have waters of coastal origin farther onshore and of oceanic origin farther offshore; therefore, the offshore extent of ocean currents could be used to define the boundary. The dynamic nature of ocean currents ensures that this will never be a fixed boundary; for this reason, the areas defined here are nominal rather than definitive.

The data presented offer the best available indicative time-series within a region. However, it should be noted that in large areas with complex circulation patterns, consideration should be given to how representative these data can be of conditions across the entire ecoregion.

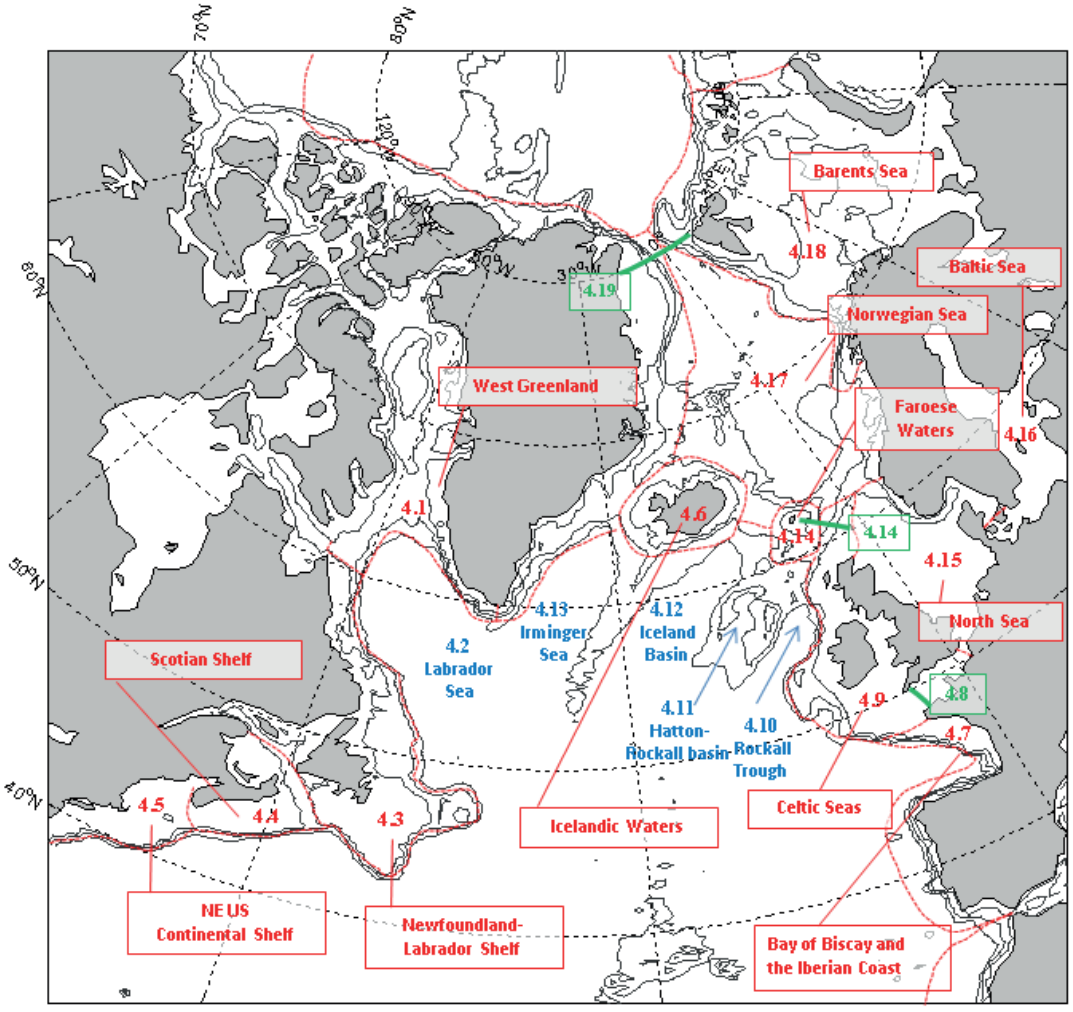

Figure 14.
Schematic of marine areas used to organize data presentation in this report. Numbers refer to the section number in this chapter. Regions are labelled in red. Ocean basins are labelled in blue. Straits are labelled in green. Region boundaries are nominal, but aligned where possible to the ICES marine ecoregions and the NOAA LMEs. Boundaries are modified where necessary to align better to hydrographic regions. For example, the offshore boundary of the Celtic Seas ecoregion is adjusted to separate it from the Rockall Trough. Bathymetric contours at 250, 1000, and 2000 m are plotted (black lines).

4.2 West Greenland

The NOAA Large Marine Ecosystems project identifies the ecosystem of the Canadian Eastern Arctic – Western Greenland. The hydrographic conditions presented here are monitored at two oceanographic sections across the continental slope of West Greenland in the southwestern part of the ecoregion, at a position influenced by the West Greenland Current.

The West Greenland Current (WGC) carries water northward along the west coast of Greenland and consists of two components: a cold and fresh inshore component, which is a mixture of polar water and melt water, and a warmer, saltier offshore component called Irminger Sea water. Being part of the cyclonic Subpolar Gyre, the WGC is subject to hydrographic variations at a range of time-scales associated with variability in the Subpolar Gyre.

In 2015, the NAO index was positive (3.56), representing the highest value since 1995. The annual mean air temperature at Nuuk Weather Station in West Greenland was –2.9°C in 2015, which was 1.5°C below the long-term mean (1981–2010).

The water properties between 0 and 50 m at Fyllas Bank Station 4 are used to monitor the variability of the fresh polar water component of the West Greenland Current. In 2015, the temperature of this water mass was 2.31°C, 0.33°C below its long-term mean (1983–2010). Salinity decreased in 2015, being 0.17 above its long-term mean.

The temperature and salinity of the Irminger Sea water component of the West Greenland Current has been increasing since the end of the 1990s, coinciding with the slowing down of the Subpolar Gyre. The warming trend lasted until 2014. However, water temperature in 2015 in the 75–200 m layer at Cape Desolation Station 3 was 5.41°C, which was 0.31°C below the long-term mean (1983–2010). Salinity in 2015 in the 75–200 m layer at Cape Desolation Station 3 was 34.93, which was 0.01 above the long-term mean.

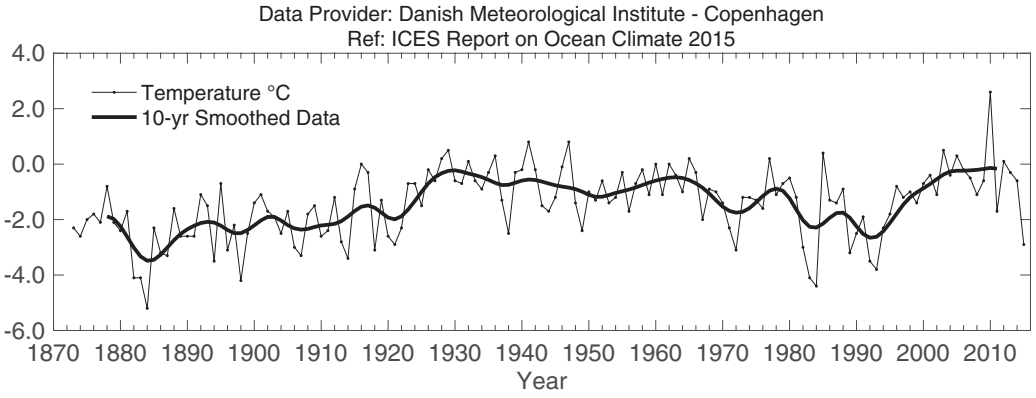

Figure 15.
West Greenland. Annual mean air temperature at Nuuk Station (64.16°N 51.75°W). Data source: Cappelen (2013).

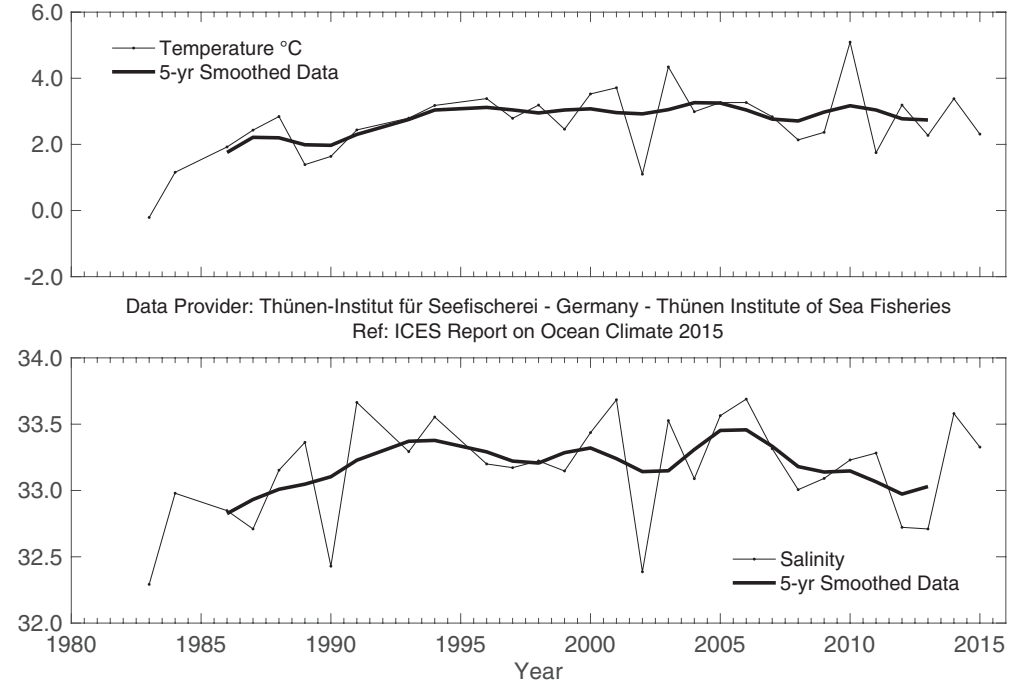

Figure 16.
West Greenland. Mean temperature (upper panel) and salinity (lower panel) in the 0–50 m water layer at Fyllas Bank Station 4 (63.88°N 53.37°W).

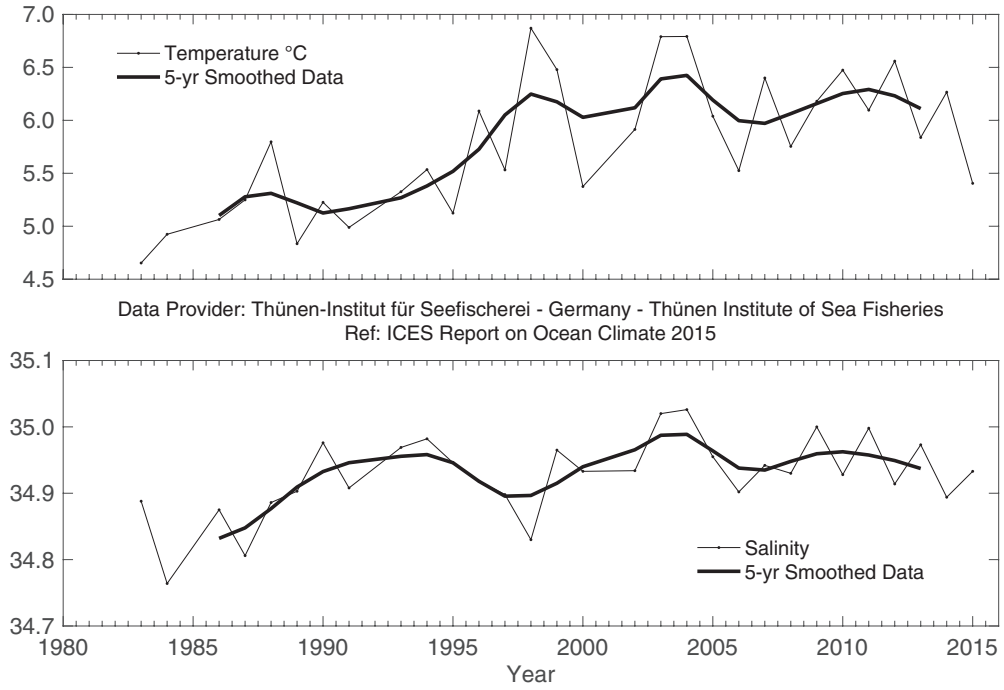

Figure 17.
West Greenland. Temperature (upper panel) and salinity (lower panel) in the 75–200 m water layer at Cape Desolation Station 3 (60.47°N 50°W).

4.3 Labrador Sea

The Labrador Sea is located between Greenland and the Labrador coast of eastern Canada. It is an ocean basin that lies offshore from the ecoregions of West Greenland and the Newfoundland–Labrador Shelf. Cold, low-salinity waters of polar origin circle the Labrador Sea in an anticlockwise current system that includes both the north-flowing West Greenland Current on the eastern side and the south-flowing Labrador Current on the western side. Warm and saline Atlantic waters originating in the subtropics flow north into the Labrador Sea on the Greenland side and become colder and fresher as they circulate.

Changes in Labrador Sea hydrographic conditions on interannual time-scales depend on the variable influences of heat loss to the atmosphere, heat and salt gain from Atlantic waters, and freshwater gain from Arctic outflow, melting sea ice, precipitation, and run-off. In the Labrador Sea, surface heat losses in winter result in the formation of dense waters, which drive the global ocean overturning circulation and ventilation of the deep layers.

The Atlantic Zone Off-Shelf Monitoring Program (AZOMP) of Fisheries and Oceans Canada provides observations of variability in the ocean climate and plankton affecting the regional climate and ecosystems of the North Atlantic and the global climate system. The 26th annual survey of the AR7W Line in the Labrador Sea (presently the core part of AZOMP) took place on CCGS "Hudson" during the period 4–26 May 2015.

A sequence of severe winters in the early 1990s led to deep convection that peaked in 1993–1994, filling the upper two kilometres of the water column with cold freshwater. Conditions have generally become milder since the mid-1990s. During 1995–2011, the upper levels of the Labrador Sea became warmer and more saline as heat losses to the atmosphere decreased and Atlantic waters became increasingly dominant. However, over the past five years, the upper and intermediate layers have exhibited a cooling and freshening trend.

In winter 2014–2015, the mid-high latitude North Atlantic experienced the most extreme heat loss in the region since 1979; this was primarily forced by strong westerly and northerly winds. This heat loss from the ocean to the atmosphere led to the most significant formation, in terms of volume, of Labrador Sea water (LSW) since 1994. Temperature and salinity profiles indicate that the winter mixed layer and hence convective overturning in the central Labrador Sea reached a maximum depth exceeding 1800 m in 2015, following the maximum of 1700 m observed in 2014. A reservoir filled with this newly ventilated, cold, and fairly fresh LSW is also rich in carbon dioxide and other dissolved gases, suggesting that the strong winter convection in 2014–2015 led to increased gas uptakes (dissolved oxygen, anthropogenic gases,

and carbon dioxide) in the Labrador Sea that spread to, and even below 1800 m.

Sea surface temperature (SST) anomalies in the Labrador Sea were near normal in winter, while positive anomalies were dominant in summer. The surface freshening observed in 2012–2013 in the central Labrador Sea was reduced and reversed in 2014, and the upper-layer salinity continued to increase in 2015. However, the intermediate waters between 400 and 1000 m experienced significant cooling after 2012, especially in 2014 and 2015, while their salinity remained nearly unchanged since 2014. In a similar manner to the last significant renewal of LSW (winter 2007–2008), the deep and intense winter mixing of two consecutive winters of 2013–2014 and 2014–2015 interrupted the general warming trend that has persisted in the intermediate waters of the Labrador Sea since the mid-1990s.

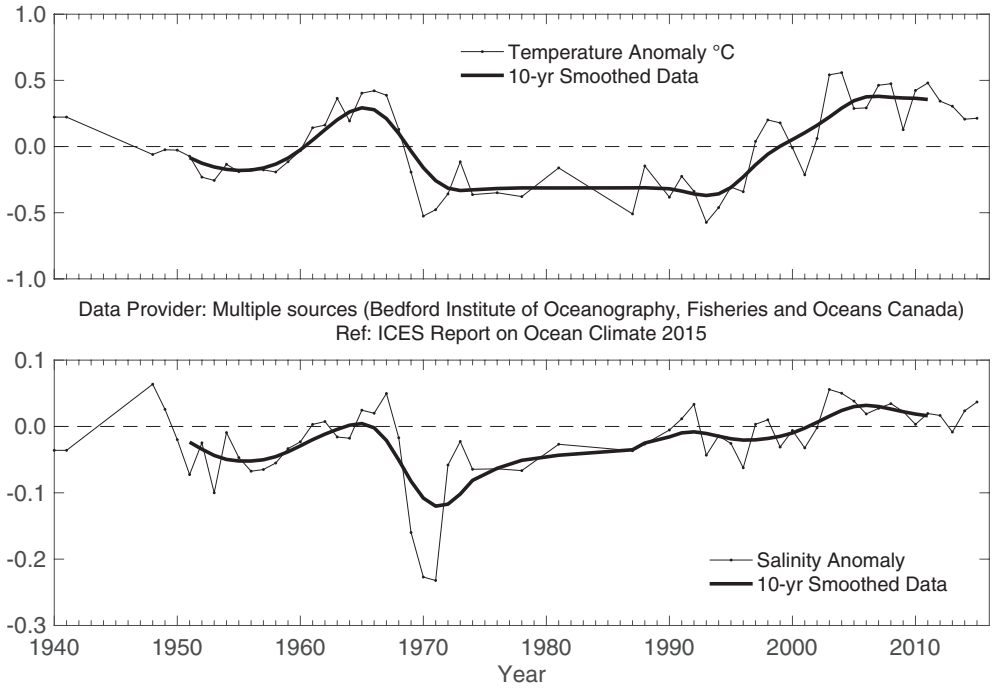

Figure 18.
Labrador Sea. Potential temperature (upper panel) and salinity (lower panel) anomalies at 50–200 m from CTD and Argo data in the west-central Labrador Sea (centred at 56.7°N 52.5°W). Estimates of seasonal cycle (derived from all data in the time-series) have been removed from the observations.

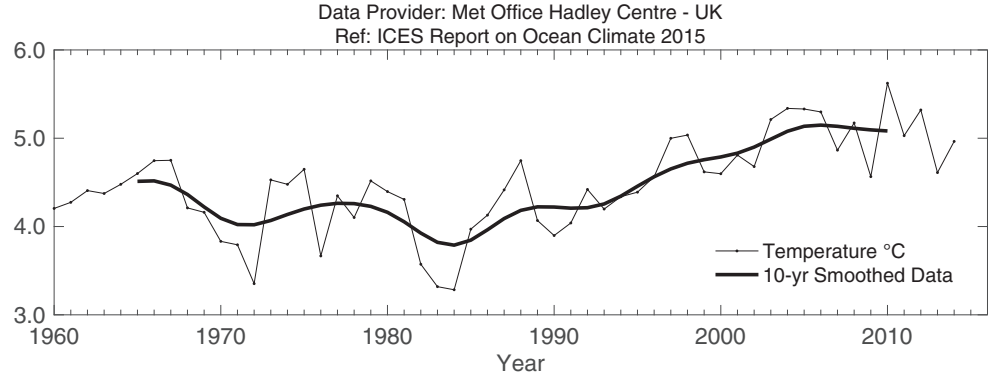

Figure 19.
Labrador Sea. Annual mean sea surface temperature data from the west-central Labrador Sea (56.5°N 52.5°W). Data obtained from the HadISST1.1 sea ice and sea surface temperature dataset, UK Meteorological Office, Hadley Centre. (Data to 2014.)

4.4 Newfoundland–Labrador shelf

The Newfoundland–Labrador (NL) shelf is identified as a NOAA Large Marine Ecosystem. This ecoregion is situated on the western side of the Labrador Sea, from the Hudson Strait in the north to the Grand Banks in the south. The Newfoundland–Labrador shelf is dominated by shallow banks, cross-shelf channels or saddles, and deep marginal troughs near the coast. Circulation is dominated by the south-flowing Labrador Current, which brings cold freshwater from the north as well as sea ice and icebergs to southern areas of the Grand Banks.

Hydrographic conditions are determined in part by the strength of the winter atmospheric circulation over the Northwest Atlantic (NAO), advection by the Labrador Current, cross-shelf exchange with warmer continental slope water, and bottom topography. Superimposed are large seasonal and interannual variations in solar heat input, sea ice cover, and storm-forced mixing. The resulting water mass on the shelf exhibits large annual cycles with strong horizontal and vertical temperature and salinity gradients.

The annual NAO index (Iceland–Azores), a key indicator of climate conditions in the Northwest Atlantic, remained in a positive phase in 2015 at 2 s.d. above normal, the highest in 120 years. As a result, Arctic air outflow to the Northwest Atlantic increased in most areas during winter 2015.

Annual air temperatures over Labrador at Cartwright decreased from near normal in 2014 to 1.5°C (1.2 s.d.) below normal in 2015. Farther south at St. John's, air temperature anomalies were also below normal at 0.6°C (0.7 s.d.). The winter sea ice extent on the NL shelf was about normal; however, the southern extent in March and April was above normal. As a result of these and other factors, local water temperatures on the NL shelf in 2015 continued to decrease during spring 2015.

At the standard monitoring site off eastern Newfoundland (Station 27), the depth-averaged annual water temperature has experienced a decreasing trend during the past three years from the record high in 2011, when it was +1.1°C (2.8 s.d.) above normal. In 2015, while the water-column-averaged temperature was above normal, bottom temperatures were –0.2°C (0.7 s.d.) below normal, the lowest since 1995.

A robust index of ocean climate conditions in eastern Canadian waters is the extent of the cold intermediate layer (CIL) of < 0°C water overlying the continental shelf. This winter-cooled water remains isolated between the seasonally heated upper layer and the warmer shelf-slope water throughout summer and early autumn. During the 1960s, when the NAO was well below normal and at its lowest value ever in the 20th century, the volume of CIL water was at a minimum (warmer-than-normal conditions), and during the high NAO years of the early 1990s, the CIL volume reached near record-high values (colder-than-normal conditions). Since the late 1990s, as ocean temperatures increased, the area of CIL water experienced a downward trend lasting until 2011. Since then, however, the CIL area has trended upward and, in 2015, reached its highest level since 1970 on the Grand Bank (2.2 s.d. above normal) during spring. The CIL continued above normal during summer, but had eroded significantly by late autumn.

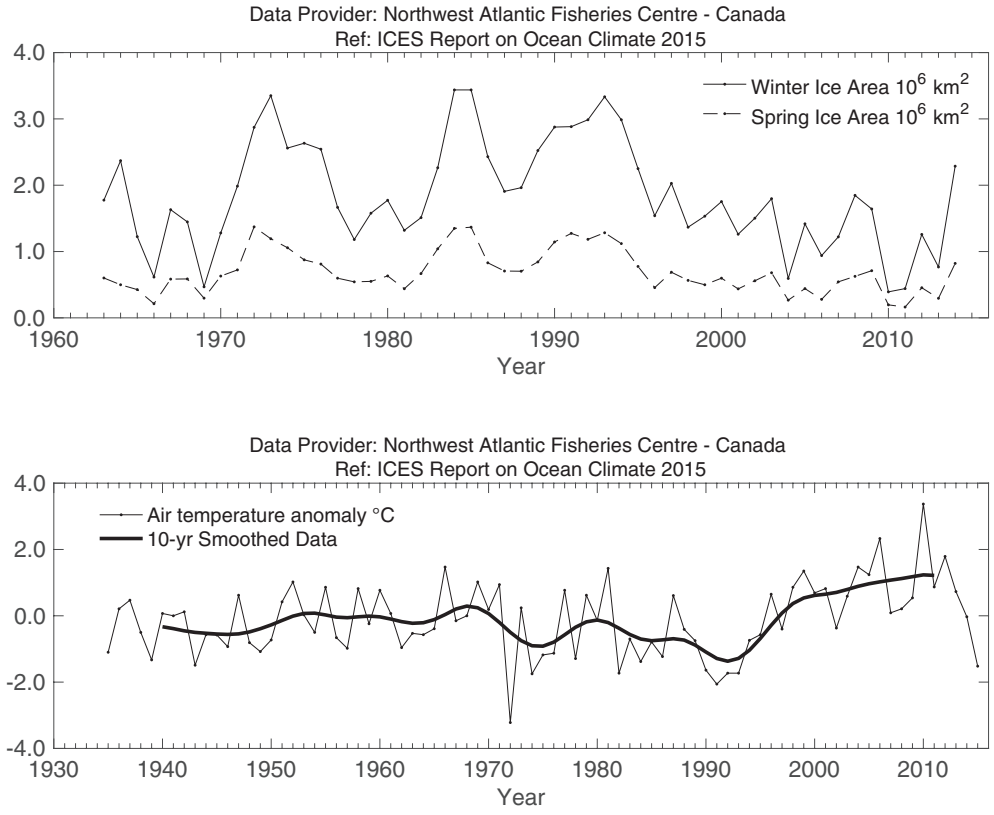

Figure 20.
Newfoundland–Labrador shelf. Winter and spring sea ice areas off Newfoundland–Labrador between 45° and 55°N (upper panel). Annual air temperature anomalies at Cartwright on the Labrador coast (lower panel).

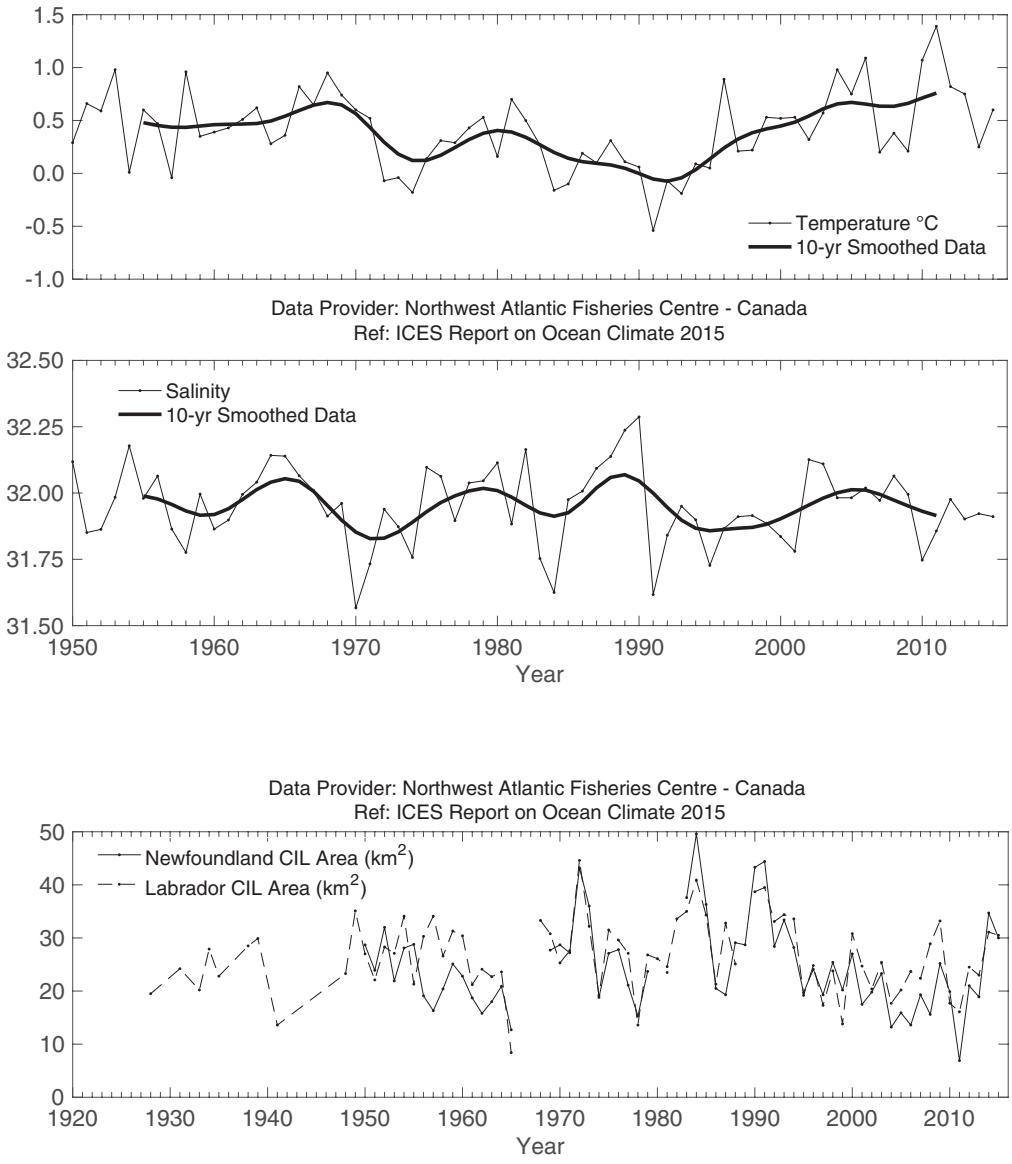

Figure 21.
Newfoundland–Labrador shelf. Annual depth-averaged Newfoundland shelf temperature (top panel) and salinity (middle panel) anomalies at Station 27 (47.55°N 52.59°W), and spatial extent of the cold intermediate layer (CIL; bottom panel).

THE AREA OF COLD INTERMEDIATE LAYER (CIL) WATER ON THE GRAND BANKS OF NEWFOUNDLAND DURING SPRING 2015 WAS AT ITS HIGHEST LEVEL SINCE 1970.

Photo: Simon Cooper, ICES.

4.5 Scotian shelf

The Scotian shelf is the continental shelf off the coast of Nova Scotia and is identified as a NOAA Large Marine Ecosystem. It is characterized by complex topography consisting of many offshore shallow banks and deep mid-shelf basins. It is separated from the Newfoundland shelf in the northeast by the Laurentian Channel and borders the Gulf of Maine to the southwest. Surface circulation is dominated by a general flow towards the southwest, interrupted by a clockwise movement around the banks and an anticlockwise movement around the basins, with the strengths varying seasonally.

Hydrographic conditions on the Scotian shelf are determined by heat transfer between the ocean and the atmosphere, inflow from the Gulf of St Lawrence and the Newfoundland shelf, and exchange with offshore slope waters. Water properties have large seasonal cycles and are modified by freshwater run-off, precipitation, and melting of sea ice. Temperature and salinity exhibit strong horizontal and vertical gradients that are modified by diffusion, mixing, currents, and shelf topography.

In 2015, annual mean air temperature over the Scotian shelf, represented by Sable Island observations, was +0.5°C (corresponding to +0.7 s.d.) above the long-term mean (1981–2010). The amount of sea ice on the Scotian shelf in 2015, as measured by the total area of ice seaward of Cabot Strait between Nova Scotia and Newfoundland from January to April, was 55 800 km^2. This is above the long-term mean coverage of 32 000 km^2 and unlike the 2010–2013 period which had extremely low coverage.

Topography separates the northeastern Scotian shelf from the rest of the shelf. In the northeast, the bottom tends to be covered by relatively cold waters (1–4°C), whereas the basins in the central and southwestern regions typically have bottom temperatures of 8–10°C. The origin of the latter is the offshore slope waters, whereas water in the northeast comes principally from the Gulf of St Lawrence. Interannual variability of the two water masses differs.

Measurements of temperatures at 100 m at the Misaine Bank station captured the changes in the northeast. They revealed conditions well above average in 2015, with temperature and salinity above normal, +0.9°C (+1.4 s.d.) and +0.26 (+2.0 s.d.), respectively. The deep Emerald Basin anomalies represent the slope water intrusions onto the shelf that are subsequently trapped in the inner basins. In 2014, the 250 m temperature and salinity anomalies were well above normal by +1.4°C (+1.7 s.d.) and +0.32 (+2.1 s.d.), respectively. The temperature and salinity anomalies were well above normal in 2015, +1.2°C (+1.4 s.d.) and +0.21 (+1.4 s.d.), respectively, but not as large as in 2014. Model simulations of the region showed a large flux of warm salty water from the slope region.

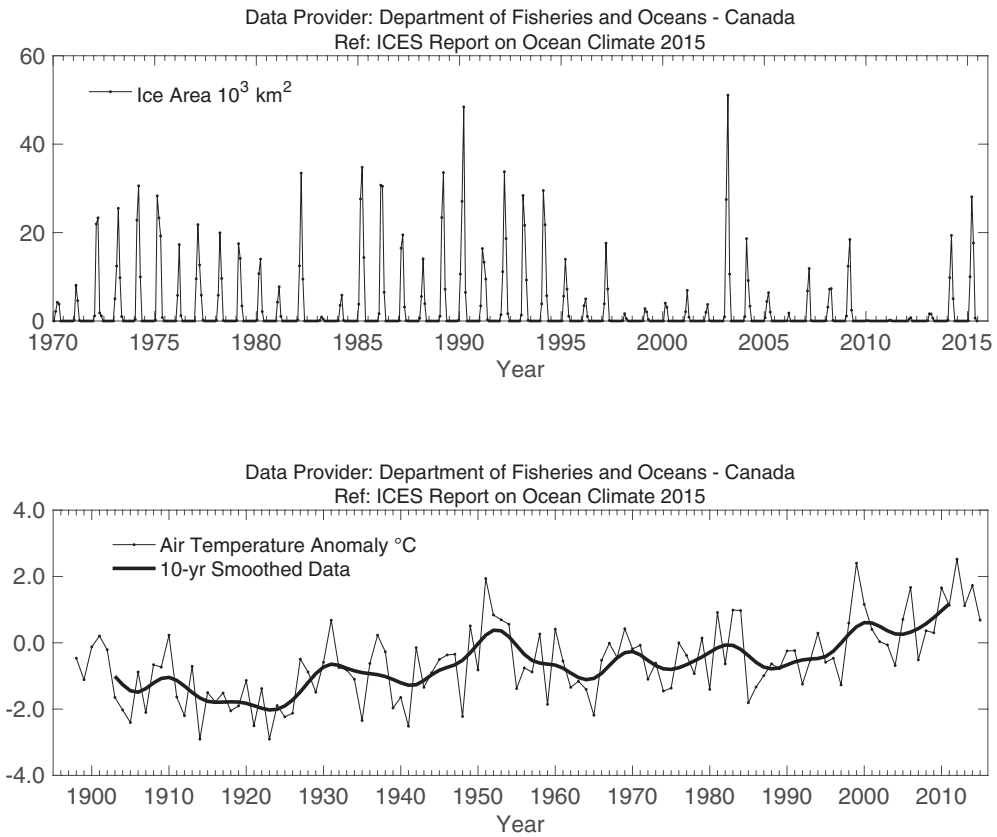

Figure 22.
Scotian shelf. Monthly means of ice area seaward of Cabot Strait (upper panel) and air temperature anomalies at Sable Island on the Scotian shelf (lower panel).

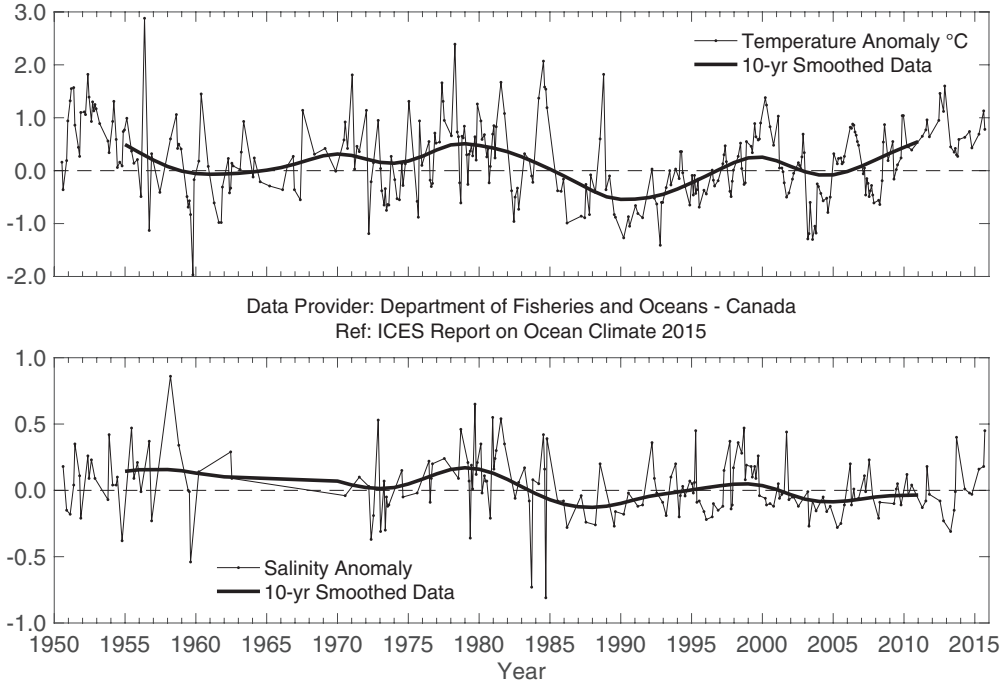

Figure 23.
Scotian shelf. Near-bottom temperature (upper panel) and salinity (lower panel) anomalies at Misaine Bank (100 m).

WARM WATER CONTINUED ON THE SCOTIAN SHELF AND SEA ICE LEVELS WERE ABOVE NORMAL.

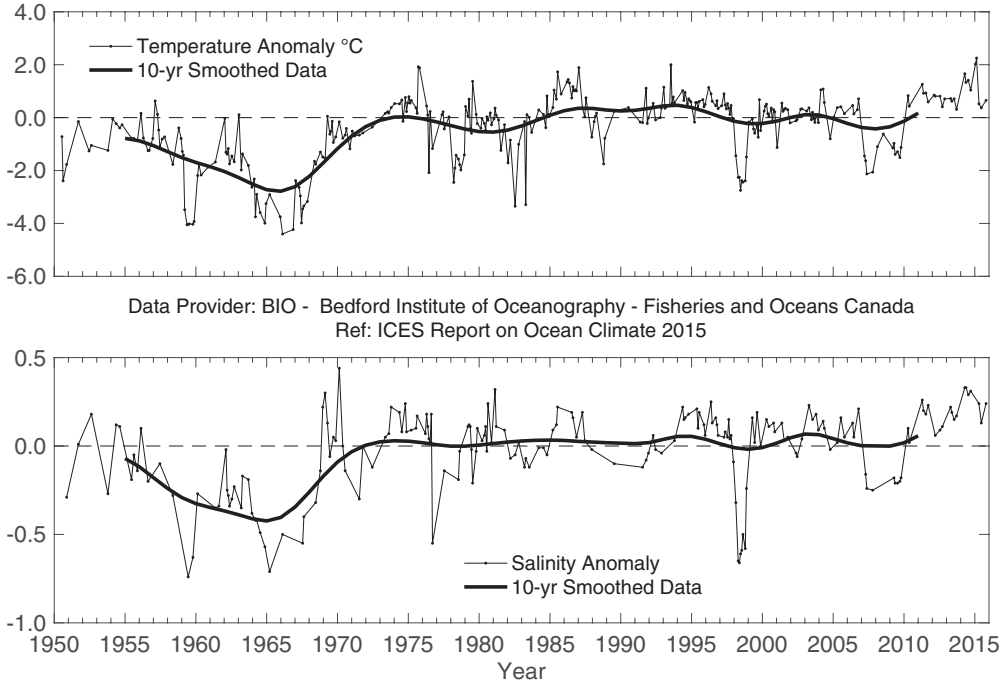

Figure 24.
Scotian shelf. Near-bottom temperature (upper panel) and salinity (lower panel) anomalies in the central Scotian shelf (Emerald Basin, 250 m).

4.6 Northeast US continental shelf

The northeast US continental shelf is the southernmost of the ecoregions along the North American coastline covered by this report. Hydrographic conditions in this region depend on the supply of waters from the Labrador Sea, flowing equatorward along the shelf and continental slope, as well as the offshore Gulf Stream flowing in the opposite direction. Shelf-wide, hydrographic conditions have been monitored annually since 1977 as part of the quarterly ecosystem monitoring and twice-yearly bottom-trawl surveys conducted by the US National Marine Fisheries Service, Northeast Fisheries Science Center. The surveys extend from Cape Hatteras into the Gulf of Maine, including Georges Bank and the Northeast Channel.

Observations indicate that the entire northeast US shelf was warmer and more saline in 2015 than the mean for the period 1981–2010. Annually, 0–30 m temperatures were between 0.3 and 1.4°C warmer than normal everywhere, with the largest anomalies observed in the Mid-Atlantic Bight. Seasonally, warming was most pronounced during late summer to early autumn. Upper level (0–30 m) waters were anomalously salty, with the largest annual anomalies observed in the Mid-Atlantic Bight. Extreme temperature anomalies observed during summer/autumn coincided with extremes in salinity as well, particularly in the Mid-Atlantic Bight. Extreme conditions observed during summer/autumn were caused by a procession of Gulf Stream warm-core rings, whose interaction with the topography at the shelf break drove an incursion of Gulf Stream water onto the inner shelf between spring and autumn of this year.

Temperature and salinity anomalies derived from hydrographic observations collected within the deep layer (150–200 m) in the Northeast Channel indicate that deep inflow to the Gulf of Maine remained warmer and saltier in 2015 compared with the long-term mean. These deep waters are not influenced by seasonal atmospheric forcing and represent deep inflow conditions for one of the dominant water mass sources to the Gulf of Maine (the slope waters).

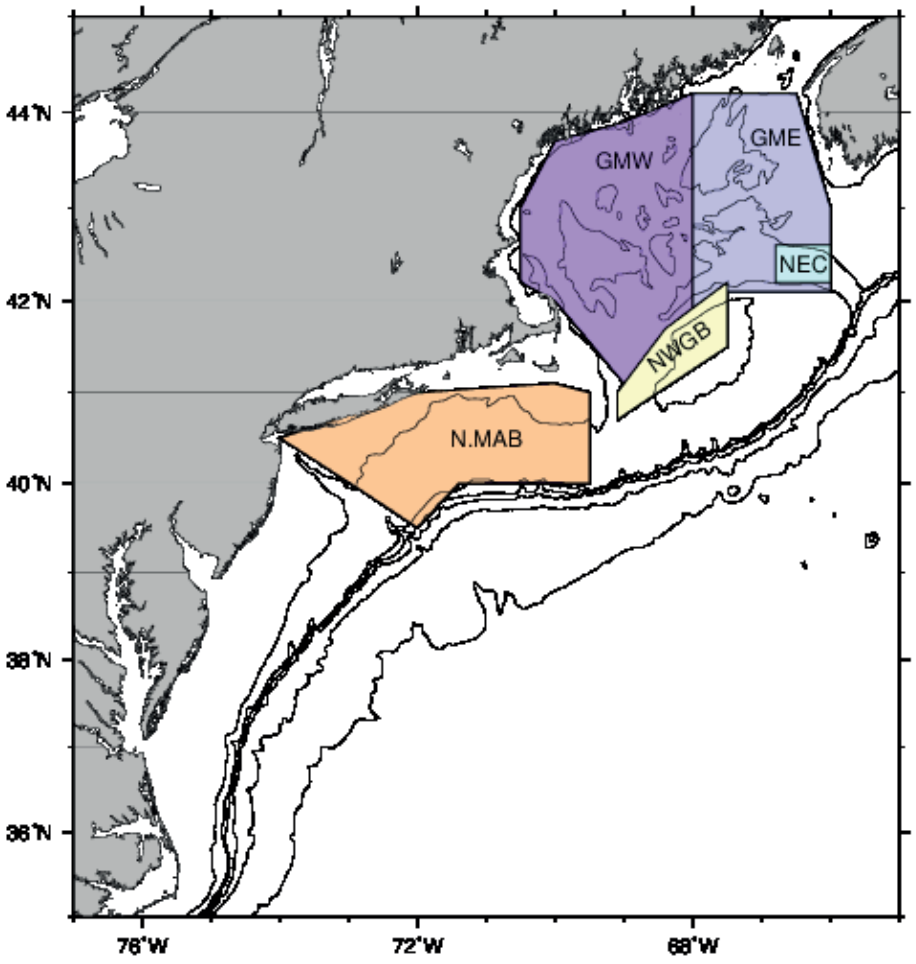

Figure 25.
NE US continental shelf. The five regions within which CTD observations are used to compute regional average time-series: GME and GMW = eastern and western Gulf of Maine; N.MAB = northern Mid-Atlantic Bight; NEC = Northeast Channel; and NWGB = Northwest Georges Bank. The 50, 100, 500, 1000, 2000, and 3000 m isobaths are also shown.

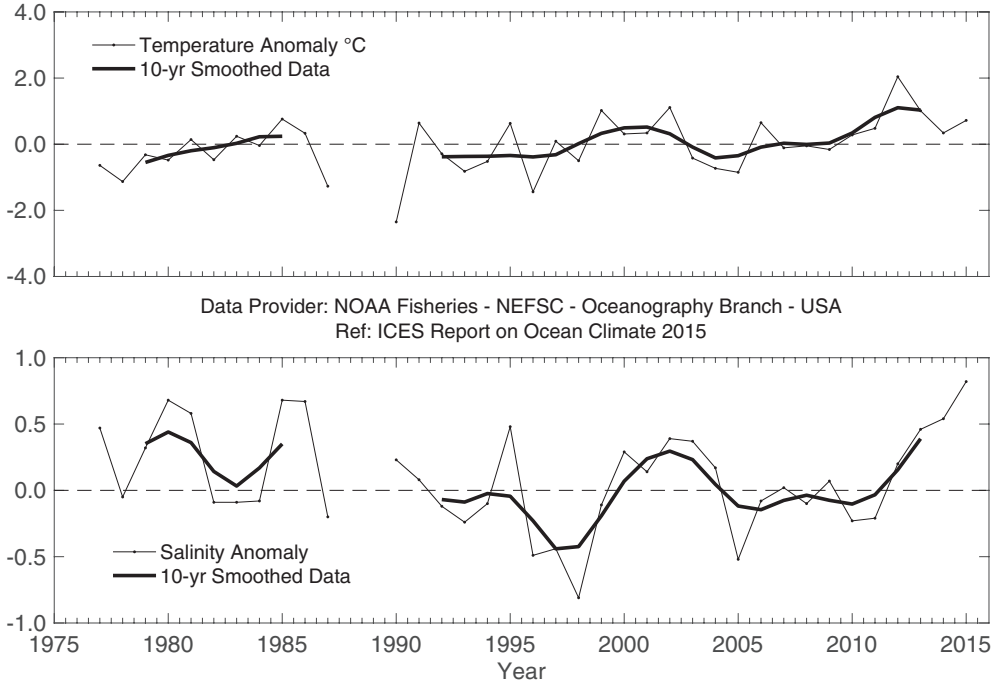

Figure 26.
NE US continental shelf. Time-series plots of 0–30 m averaged temperature anomaly (upper panel) and salinity anomaly (lower panel) in the region between Hudson Canyon and Cape Cod, Massachusetts. Anomalies are calculated relative to the period 1981–2010 using hydrographic data from shelf-wide surveys.

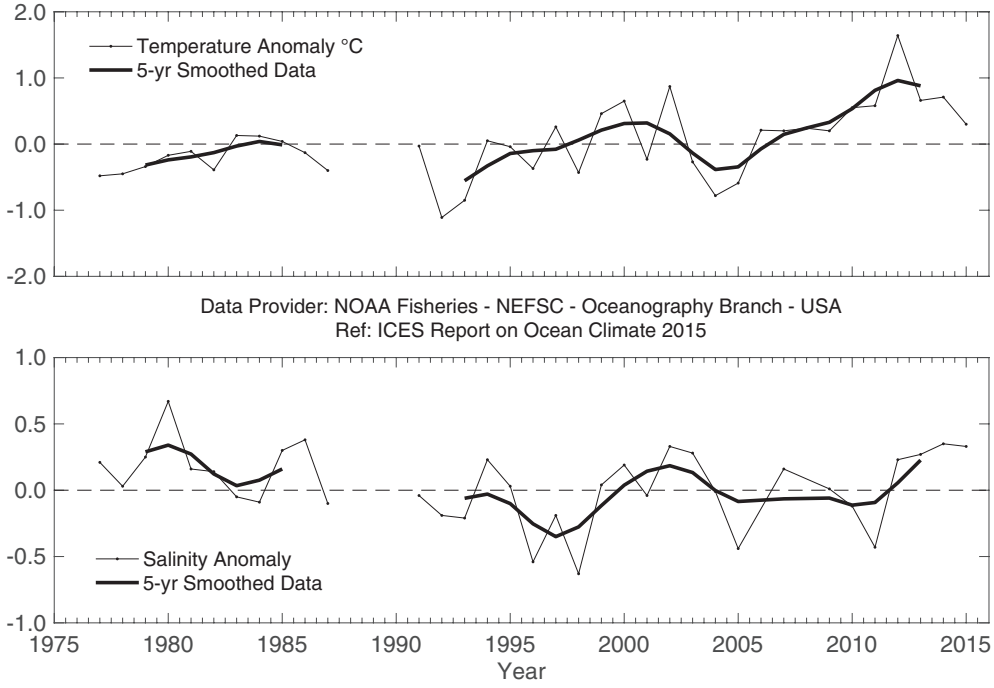

Figure 27.
NE US continental shelf. Time-series plots of 0–30 m averaged temperature anomaly (upper panel) and salinity anomaly (lower panel) in the western Gulf of Maine. Anomalies are calculated relative to the period 1981–2010 using hydrographic data from shelf-wide surveys.

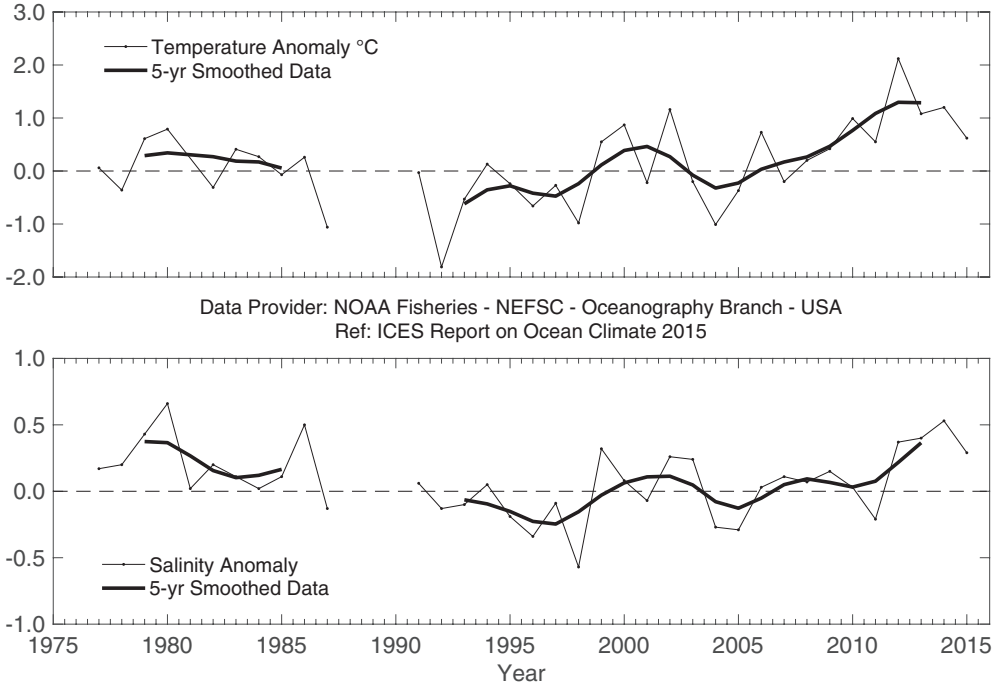

Figure 28.
NE US continental shelf. Time-series plots of 0–30 m averaged temperature anomaly (upper panel) and salinity anomaly (lower panel) in the eastern Gulf of Maine. Anomalies are calculated relative to the period 1981–2010 using hydrographic data from shelf-wide surveys.

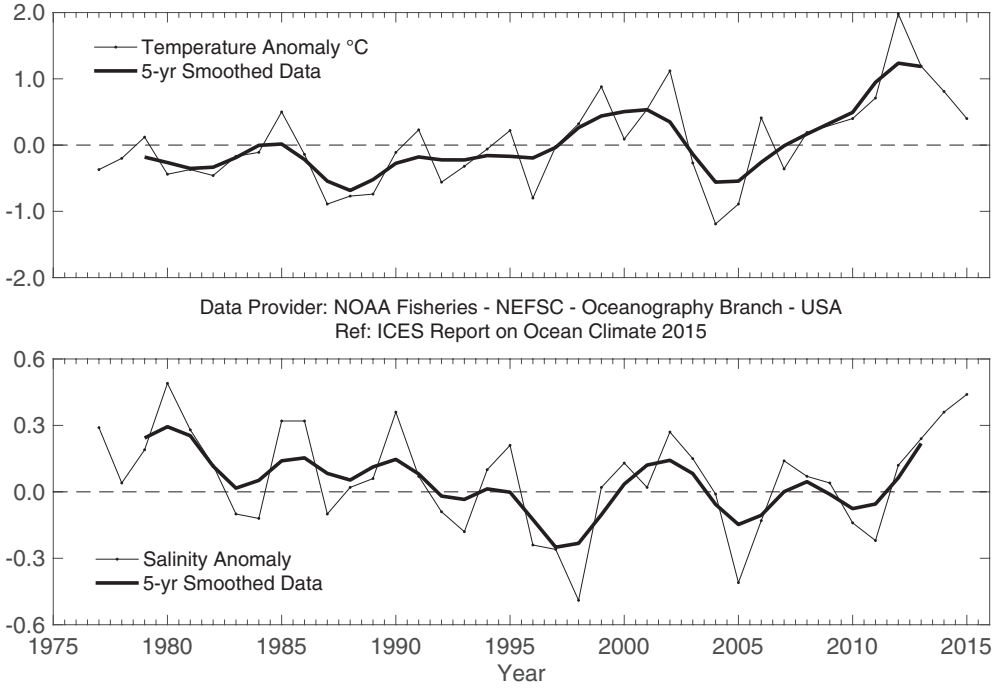

Figure 29.
NE US continental shelf. Time-series plots of 0–30 m averaged temperature anomaly (upper panel) and salinity anomaly (lower panel) on northwest Georges Bank. Anomalies are calculated relative to the period 1981–2010 using hydrographic data from shelf-wide surveys.

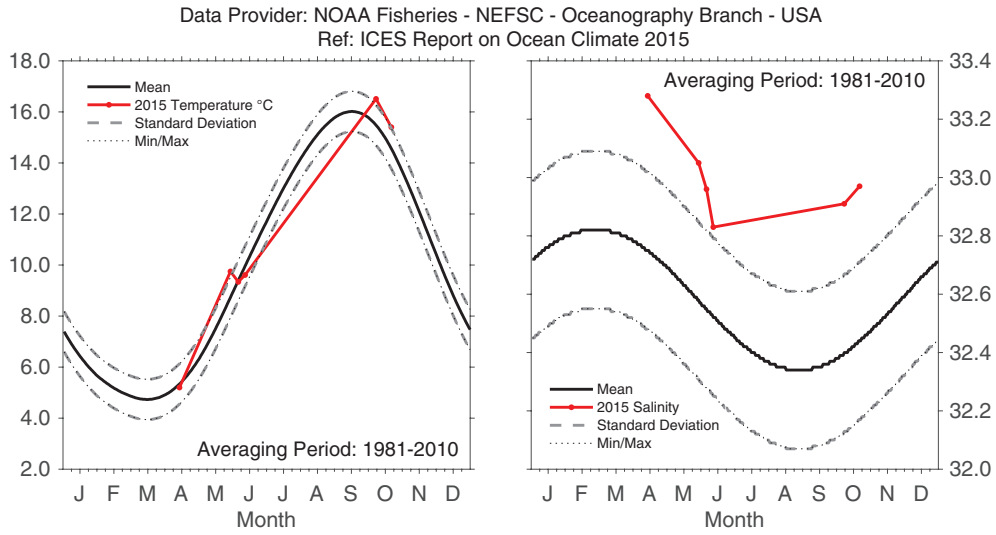

Figure 30.
NE US continental shelf. 2015 temperature (left) and salinity (right) averaged over 0–30 m at northwest Georges Bank, relative to the annual cycle calculated for 1981–2010. The envelope corresponding to the monthly range and one standard deviation are shown.

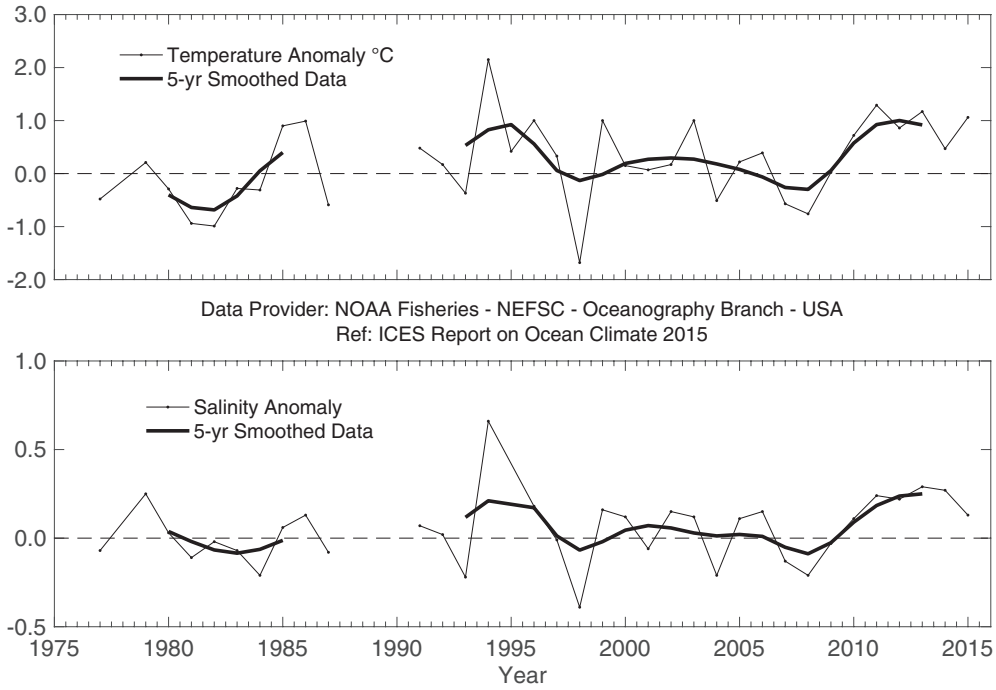

Figure 31.
NE US continental shelf. Time-series plots of 150–200 m averaged temperature anomaly (upper panel) and salinity anomaly (lower panel) in the Northeast Channel. Anomalies are calculated relative to the period 1981–2010 using hydrographic data from shelf-wide surveys.

4.7 Icelandic waters

The Iceland shelf and seas are identified as a NOAA Large Marine Ecosystem and an ICES ecoregion. Iceland is the meeting place of warm and cold currents that converge in an area of submarine ridges (Greenland–Scotland Ridge, Reykjanes Ridge, Kolbeinsey Ridge), forming natural barriers to the main ocean currents. The warm Irminger Current (6–8°C), a branch of the North Atlantic Current, flows from the south, and the cold East Greenland and East Icelandic currents (–1°C to 2°C) flow from the north. Deep and bottom currents in the seas around Iceland are principally the overflow of cold water from the Nordic seas and the Arctic Ocean over the submarine ridges into the North Atlantic.

Hydrographic conditions in Icelandic waters are generally closely related to atmospheric or climatic conditions in and over the country and the surrounding seas, mainly through the Icelandic low-pressure and the Greenland high-pressure systems. These conditions in the atmosphere and the surrounding seas affect biological conditions, expressed through the food chain in the waters, including recruitment and abundance of commercially important fish stocks.

In 2015, mean air temperature in the south (Reykjavik) and north (Akureyri) was lower in than previous years and around the long-term average. Temperature and salinity in the Atlantic water from the south was lower in 2015 than it has been since before year 2000, and around or below the long-term mean in the upper layers. Salinity and temperature in the East Icelandic Current in spring 2015 were both above average. In 2015, upper-layer temperature and salinity north of Iceland were slightly above the long-term mean.

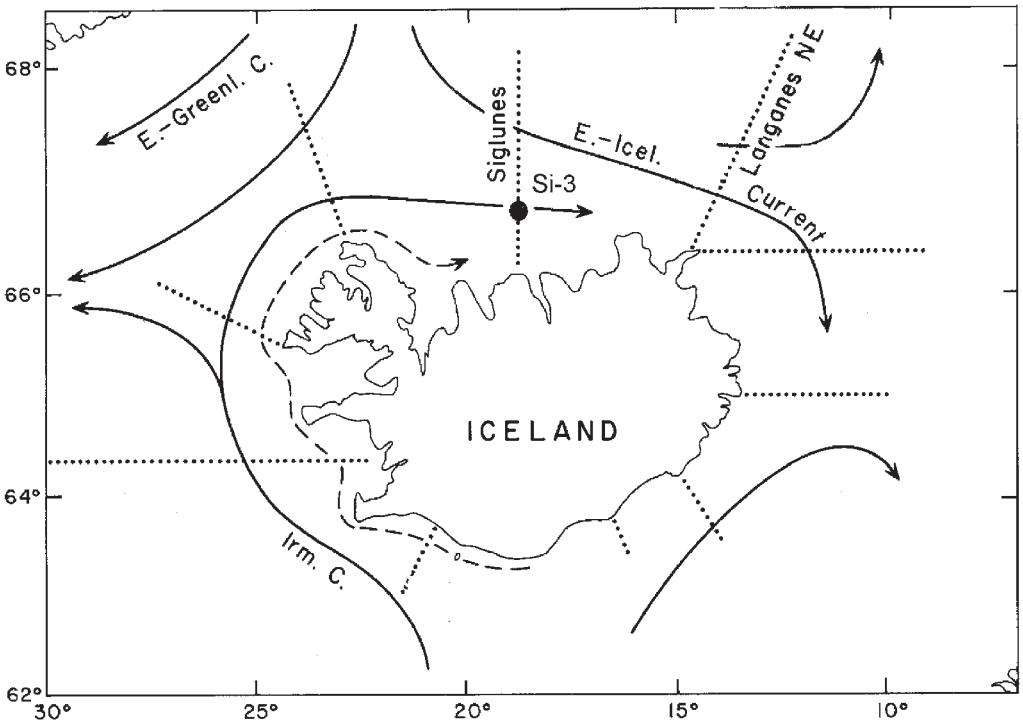

Figure 32.
Icelandic waters. Main currents and location of standard sections in Icelandic waters.

Photo: Simon Cooper, ICES.

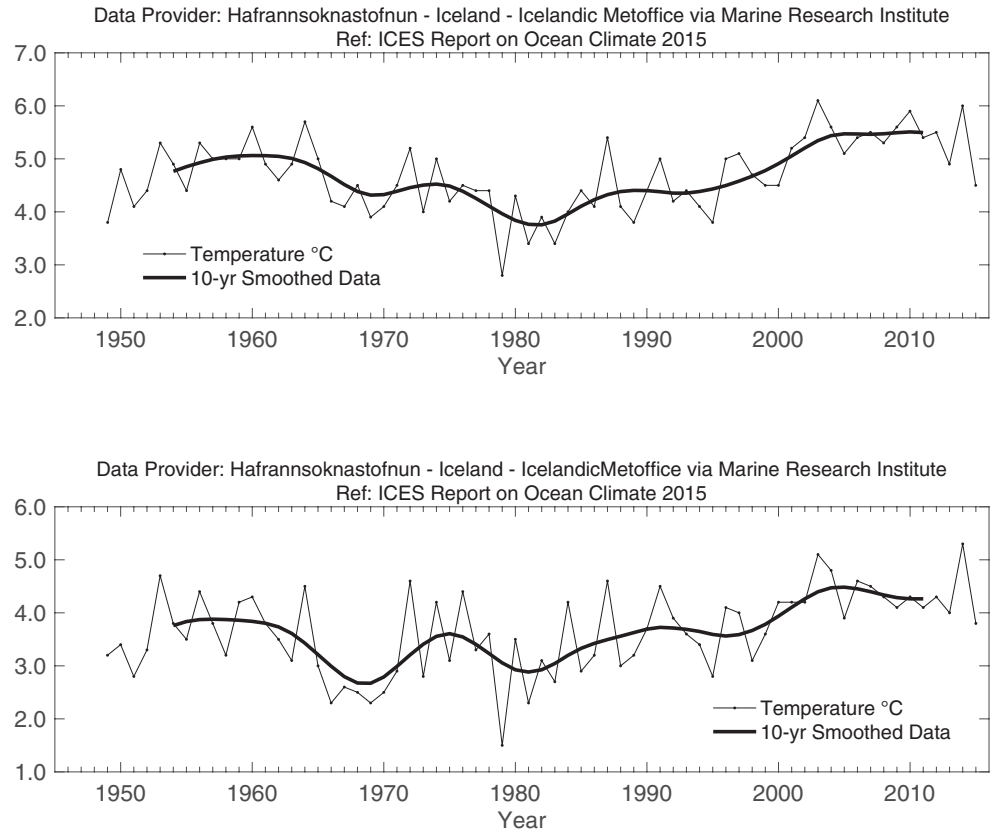

Figure 33.
Icelandic waters. Mean annual air temperature at Reykjavík (upper panel) and Akureyri (lower panel).

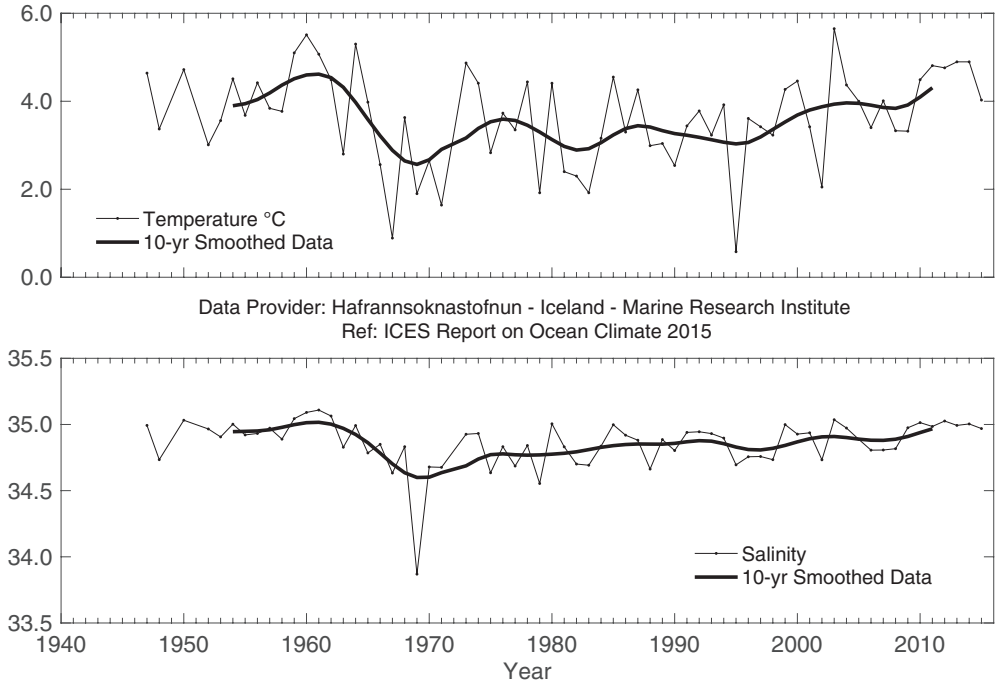

Figure 34.
Icelandic waters. Temperature (upper panel) and salinity (lower panel) at 50–150 m at Siglunes Stations 2–4 in North Icelandic waters.

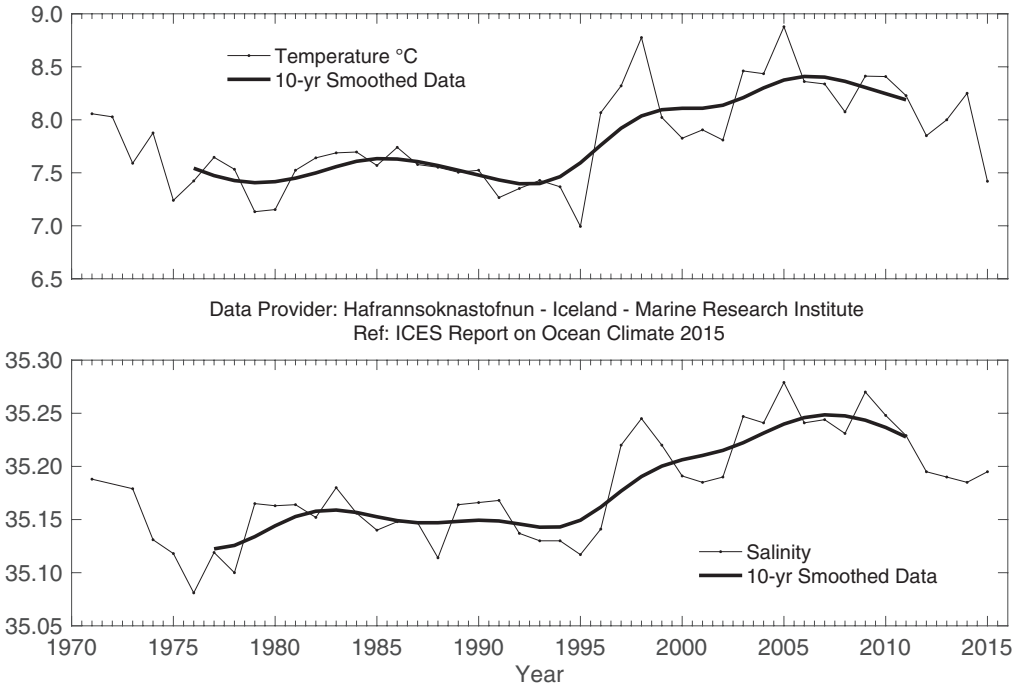

Figure 35.
Icelandic waters. Temperature (upper panel) and salinity (lower panel) at 0–200 m at Selvogsbanki Station 5 in South Icelandic waters.

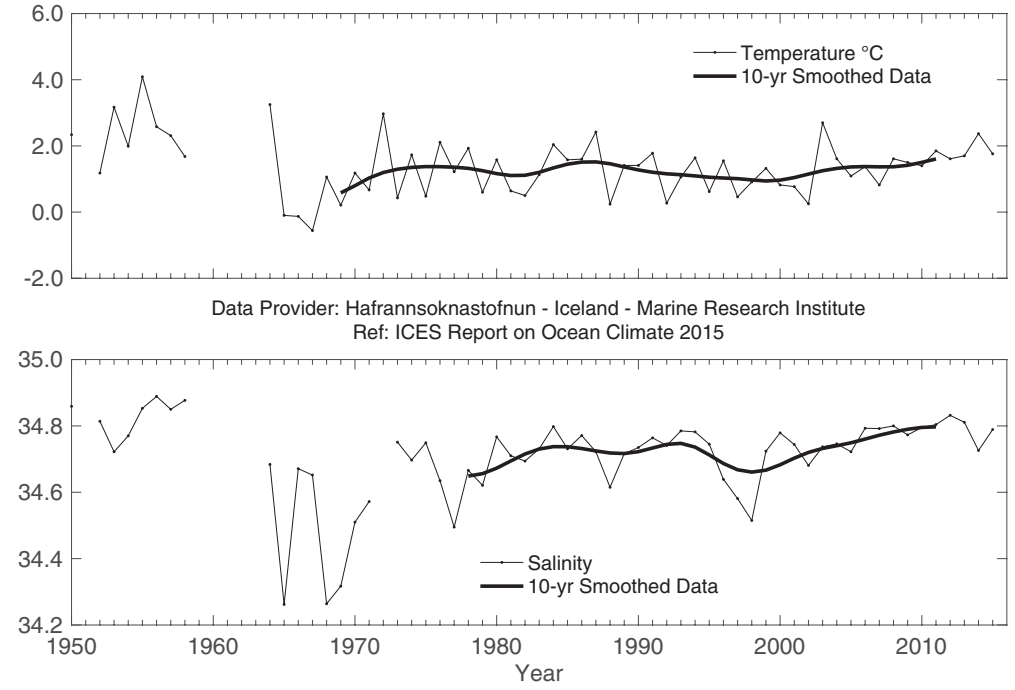

Figure 36.
Icelandic waters. Temperature (upper panel) and salinity (lower panel) at 0–50 m in the East Icelandic Current (Langanes Stations 2–6).

4.8 Bay of Biscay and Iberian coast

The Bay of Biscay and the Iberian coast is defined as an ICES ecoregion. The NOAA Large Marine Ecosystem definition identifies the Iberian coast as a separate region and includes the Bay of Biscay and the Celtic seas. This region is located in the eastern North Atlantic at the northeastern edge of the subtropical, anticyclonic gyre or within the intergyre area. It could be considered an adjacent sea with a weak anticyclonic circulation. Shelf and slope currents are important in the system, characterized by coastal upwelling events in spring–summer and the dominance of a geostrophic balanced poleward flow (known as the Iberian Poleward Current) in autumn and winter.

From the atmospheric point of view, the year 2015 can be considered warm relative to the long-term mean on the Iberian coast and the southern Bay of Biscay. Overall, average temperatures exceeded 0.7°C relative to the reference period 1981–2010, being slightly colder than in 2014.

The seasonal cycle pattern showed a cold winter, especially in February, and warm conditions the remainder of the year, reaching a late-autumn and early-winter warmth record. In terms of precipitation, 2015 can be considered normal to slightly dry, especially compared to the wet previous two years. Surface temperature did not tightly respond to local atmospheric forcing as in other years; despite warm atmospheric conditions, surface waters were fresh, while a positive SST anomaly remained below 0.4°C, roughly half of the 2014 value.

The subsurface water column continued to freshen; therefore, the sequence follows a return to the long-term average in 2013 after record-high salinity conditions, weak negative anomaly in 2014, and fresh conditions in 2015. Temperature remained average to low. This behavior is again in contrast to regional atmospheric conditions (warm and dry), but consistent with a lack of a strong signature of the Iberian Poleward Current, specific upwelling pulses during summer, and a general further advective influence of northern regions, implying more presence of subpolar-origin central waters.

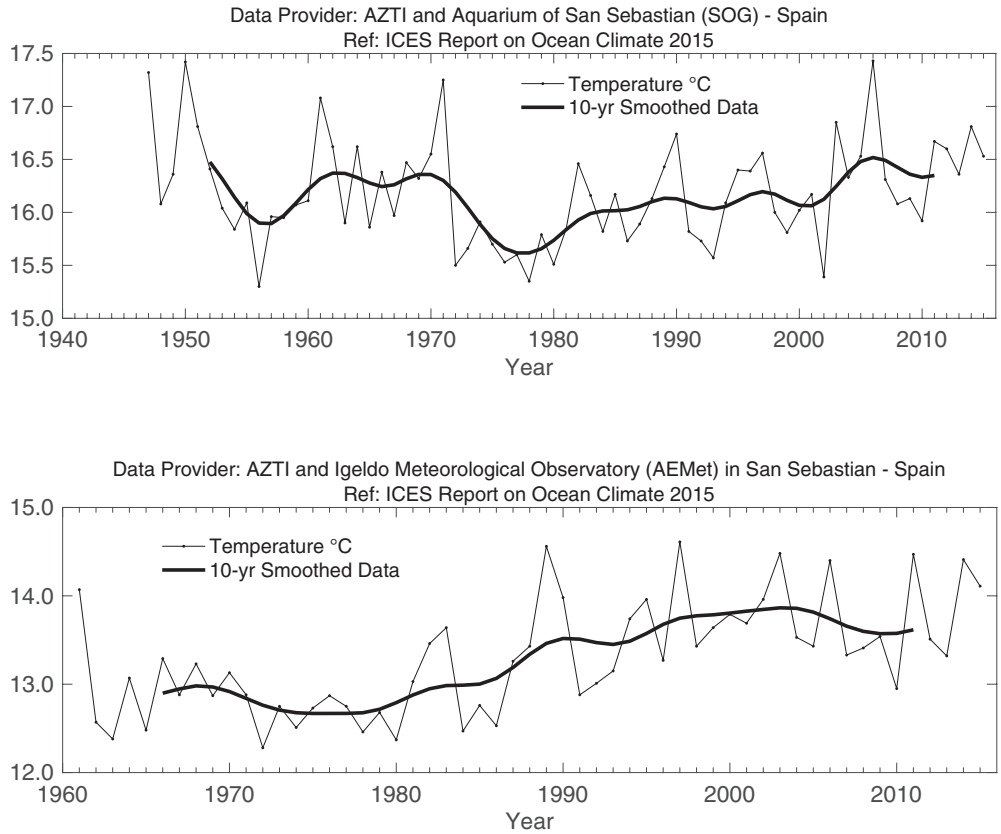

Figure 37.
Biscay and Iberian coast. Sea surface temperature (upper panel) and air temperature (lower panel) at San Sebastian (43°18.5′N 02°2.37′W).

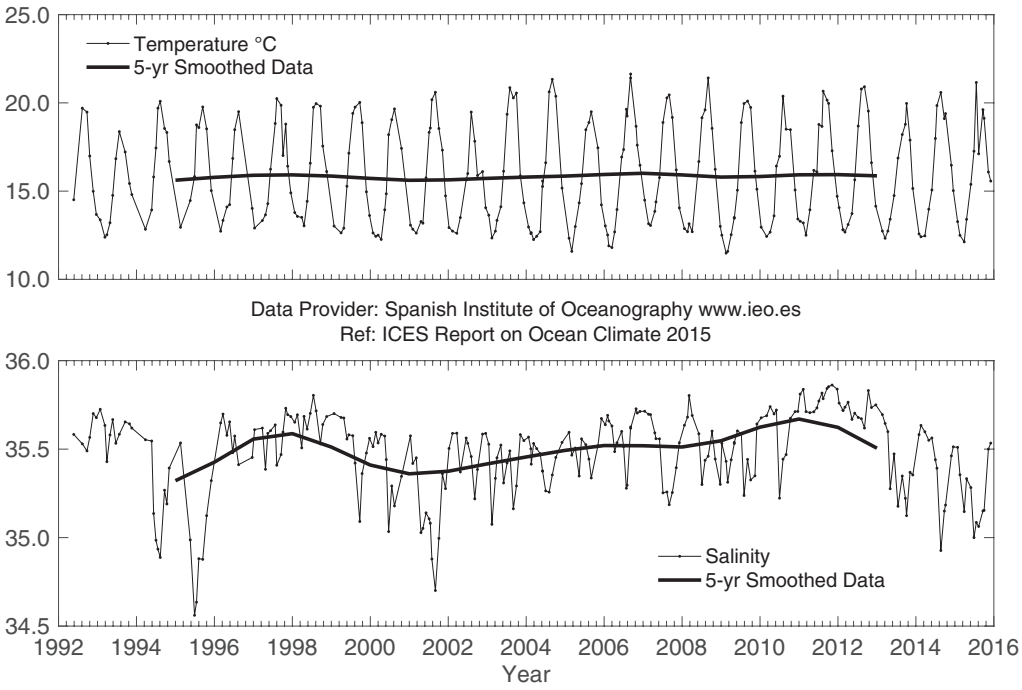

Figure 38.
Bay of Biscay and Iberian coast. Potential temperature (upper panel) and salinity (lower panel) at Santander Station 6 (5–30 m).

DESPITE REGIONAL WARM AND DRY CONDITIONS IN THE AREA FOR MOST OF THE YEAR, THE UPPER OCEAN REMAINED RELATIVELY COOL. THE FRESHENING INITIATED AROUND 2013 CONTINUED AND WAS ENHANCED THROUGHOUT 2015.

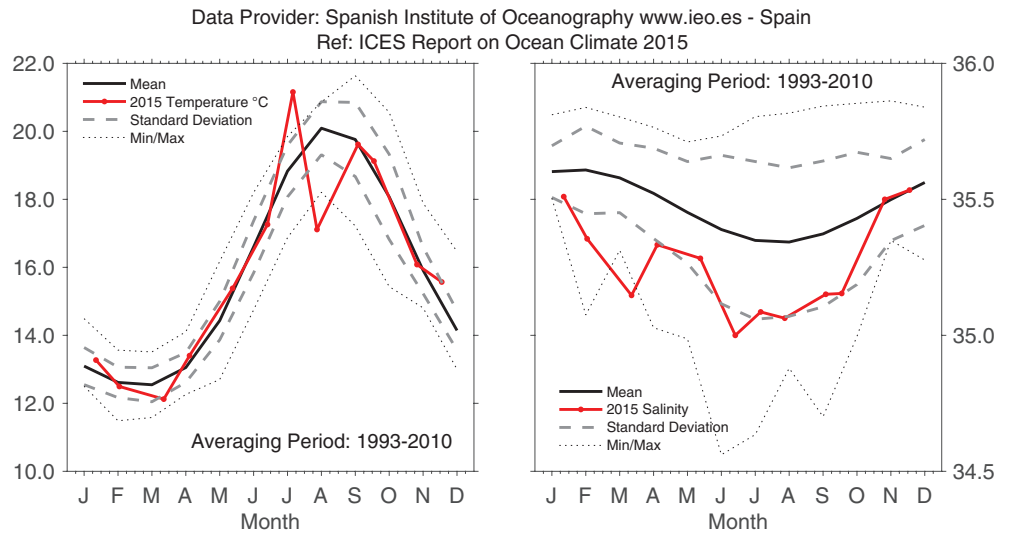

Figure 39.
Bay of Biscay and Iberian coast. 2015 monthly temperature (left panel) and salinity (right panel) at Santander Station 6 (5–30 m).

4.9 Southwest Approaches

The datasets presented here are derived from the western end of the English Channel and the boundary of the Celtic Seas and the Bay of Biscay ecoregions. The area is commonly referred to as the Southwest (SW) Approaches, which relates to the shipping passage through the English Channel. As these data lie on a boundary of the different ecoregions, this terminology has been adopted here and relates to the region forming a pathway for Atlantic water to enter the southern North Sea.

The Astan Site (48.77°N 3.94°N) is located in the western English Channel, 3.5 km offshore of the northern coast of Brittany, France. Measurements began in 2000 and are collected twice a month at this coastal station. Properties at this site are typical of western Channel waters. Bottom depth is ca. 60 m, and the water column is well mixed for most of the surveys.

At Astan Station, temperatures in 2015 were higher than the climatology values in winter, spring, and summer, being lower than average only in September and October. The main anomalies occurred in winter and late autumn. The overall anomaly is 0.29°C above the long-term (2000–2015) mean. The salinity cycle was atypical compared to the average pattern; no low salinity values were observed in winter and spring, but there was a constant increase throughout the year. Average 2015 salinity was slightly higher (< 0.1) than the long-term mean. As normally observed in this area, western Channel waters were well-mixed over the entire water column during the whole year since no temperature or salinity differences between surface and bottom waters were observed.

Station E1 (50.03°N 4.37°W) is situated on the southern coast of England in the western English Channel. Water depth is 75 m, and the station is tidally influenced by a 1.1-knot maximum surface stream at mean spring tide. The seabed is mainly sand, resulting in low bottom stress (1–2 ergs cm^{-2} s^{-1}). The station may be described as oceanic with the development of a seasonal thermocline. Stratification typically starts in early April, persists throughout summer, and is eroded by the end of October. The typical depth of the summer thermocline is around 20 m. The station is greatly affected by ambient weather.

Measurements have been taken at this station since the end of the 19th century, with data currently available since 1903. The series is unbroken, apart from the gaps for the two world wars and a hiatus in funding between 1985 and 2002. Data include vertical profiles of temperature and salinity. Early measurements were taken with reversing mercury-in-glass thermometers and discrete salinity bottles. More recently, electronic equipment (Seabird CTD) has been utilized.

The time-series demonstrates considerable interannual variability in temperature. In 2015, the monthly average surface temperature was below the long-term mean between April and early September. During winter 2014/2015, the temperature was anomalously warm, and markedly anomalously warm in December 2015. This pattern was repeated at 50 m depth, in a modulated fashion as this is beneath the seasonal thermocline.

The salinity recorded in 2015 was consistently 0.1 psu above the long-term mean (~35.4) in the entire water column.

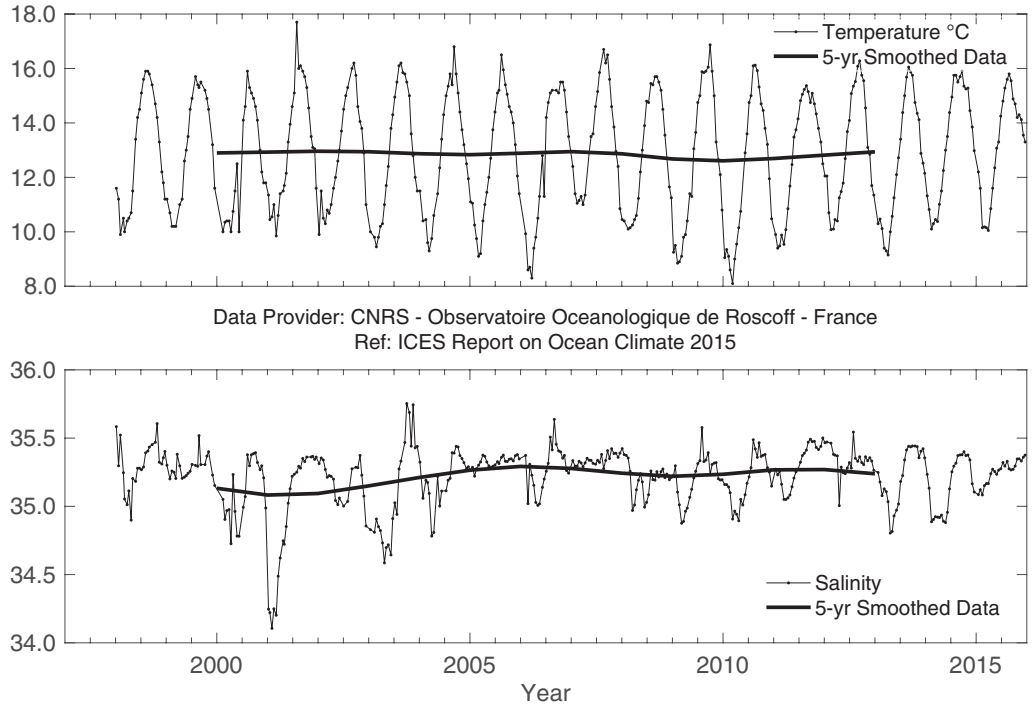

Figure 40.
SW Approaches. Temperature (upper panel) and salinity (lower panel) of surface water at the Astan Station (48.77°N 3.94°W). Base period 1998–2010.

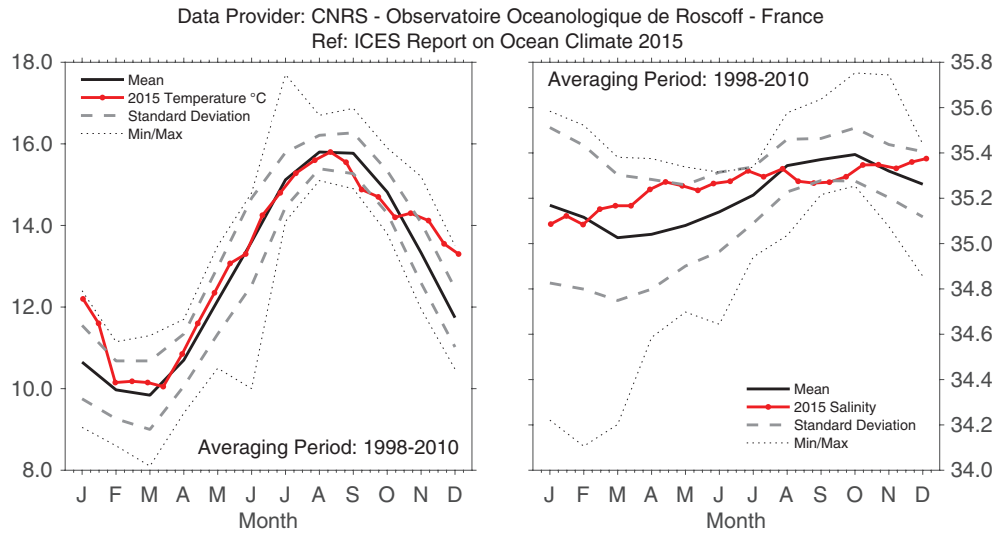

Figure 41.
SW Approaches. Monthly average seasonal cycle with 2015 temperature (left panel) and salinity (right panel) observations of surface water at the Astan Station (48.77°N 3.94°W) (NB: month markers are placed mid-month).

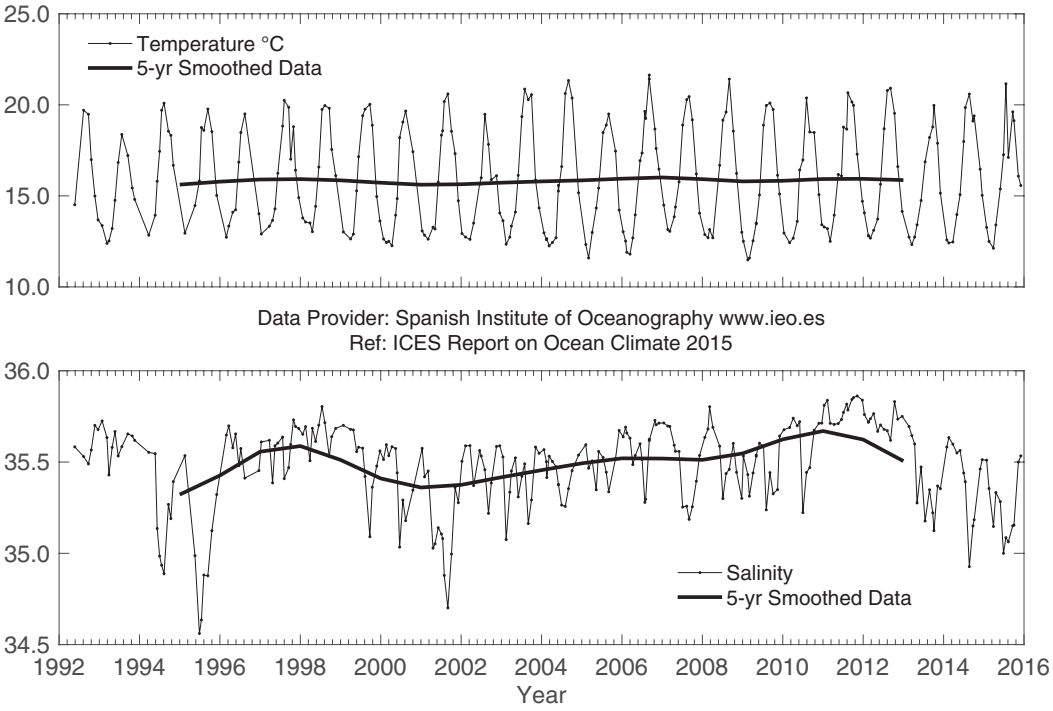

Figure 42.
SW Approaches. Temperature (upper panel) and salinity (lower panel) anomalies of surface (0–40 m) water at Station E1 in the western English Channel (50.03°N 4.37°W).

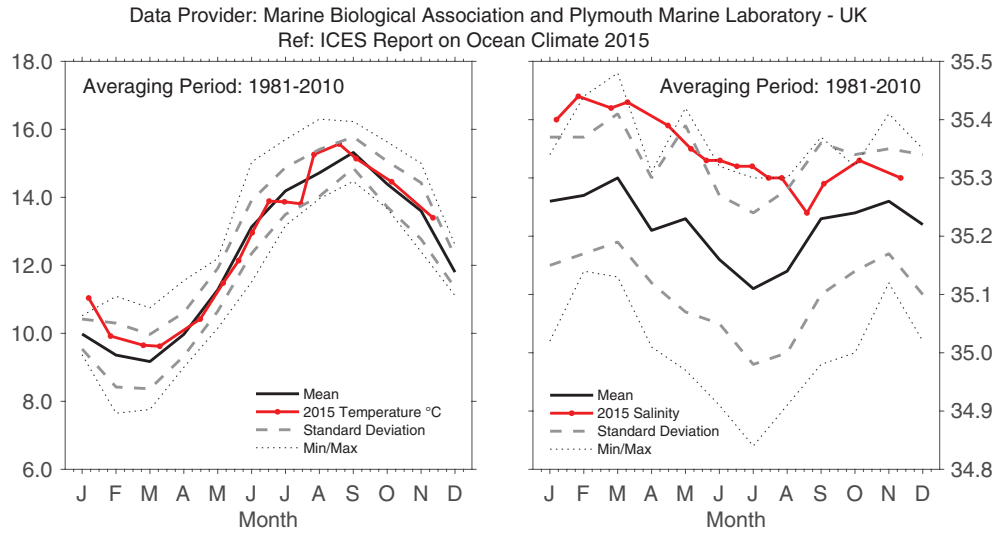

Figure 43.
SW Approaches. Monthly average seasonal cycle with observations of 2015 temperature (left panel) and salinity (right panel) of surface (0–40 m) water at Station E1 in the western English Channel (50.03°N 4.37°W).

4.10 Celtic seas

The Celtic Seas ecoregion relates to the area west of the UK and Ireland, and also to the Irish Sea. It is bounded by France in the south and the Faroes in the north. In addition to the influence of coastal waters on the shelf, the area is strongly influenced by the poleward transport of Atlantic water as well as the continental slope current which brings waters northward from the Biscay region.

The time-series of surface temperature observations at the Malin Head coastal station (the most northerly point of Ireland) is inshore of coastal currents and influenced by run-off. The temperature record between 1959 and 2006 was constructed using manual measurements (i.e. water temperature measured using handheld thermometer). From mid-2008 onward, temperature has been measured by an *in situ* SBE 39 temperature sensor. An offshore weather buoy (M3) has been maintained at 51.22°N 10.55°W, ca. 50 km off the southwest coast of Ireland (water depth of 155 m) since mid-2002. Sea surface temperature is collected hourly at this buoy.

Sea surface temperature at Malin Head has undergone quite a dramatic rise since the end of the 1980s. However, since the mid-2000s, there is some evidence of the rate of increase slowing down. The average sea surface temperature for 2015 was 1.02°C above the mean of 1981–2010.

At the M3 buoy, there is considerable interannual variability. Over the last six years, the annual mean sea surface temperature was lower than average. However, this trend needs to be treated with caution since the "long-term mean" used to calculate the anomalies only covers the last eight years of the 1981–2010 period. The average sea surface temperature for 2015 was 1.00°C below average; however, higher monthly sea surface temperatures were evident at the end of the year.

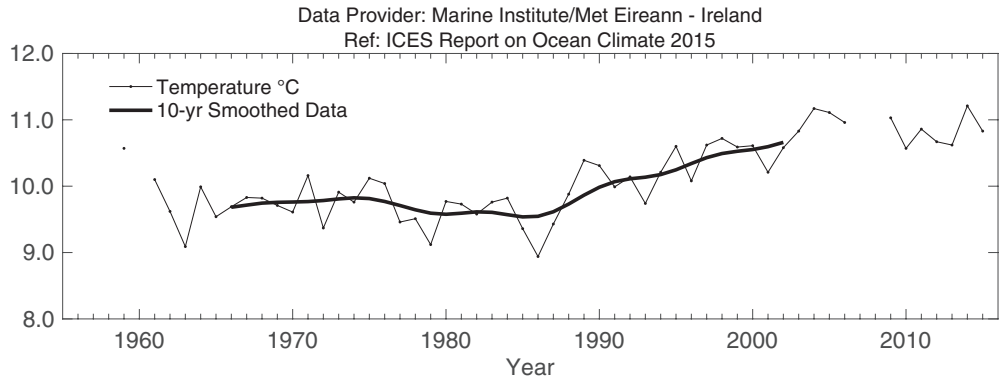

Figure 44.
Celtic seas. Temperature at the Malin Head coastal station (55.39°N 7.38°W).

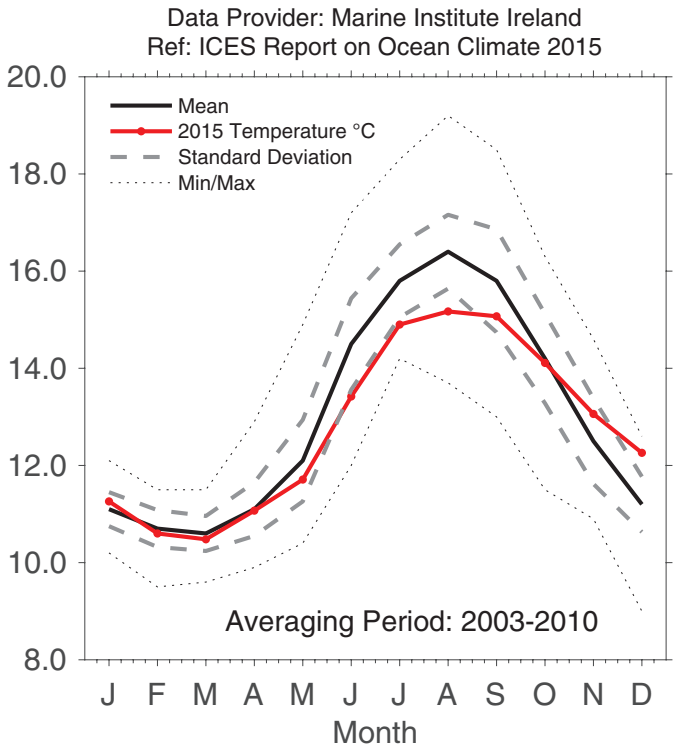

Figure 45.
Celtic seas. Monthly average seasonal cycle with 2015 monthly temperature at the M3 Weather Buoy southwest of Ireland (51.22°N 10.55°W).

4.11 Rockall Trough

Rockall Trough is a deep ocean basin situated west of Britain and Ireland and is within the Celtic Seas ecoregion. With significantly different oceanographic characteristics than the shallower shelf sea areas, Rockall Trough is separated from the Iceland Basin by Hatton and Rockall banks and from the Nordic seas by the shallow (500 m) Wyville–Thomson Ridge. It allows warm North Atlantic upper water to reach the Norwegian Sea, where it is converted into cold, dense overflow water as part of the thermohaline overturning in the North Atlantic. The upper water column is characterized by poleward-moving eastern North Atlantic water, which is warmer and more saline than waters of the Iceland Basin, which also contribute to the Nordic sea inflow.

The potential temperature of the upper 800 m remains higher than the 1981–2010 mean. The upper ocean has been cooling relative to the peak in 2007. The 2015 temperature was the lowest since 2001. The salinity of the upper 800 m decreased sharply from the end of the 2000s, but after returning close to the long-term mean in 2014, the 2015 salinity was greater than the mean.

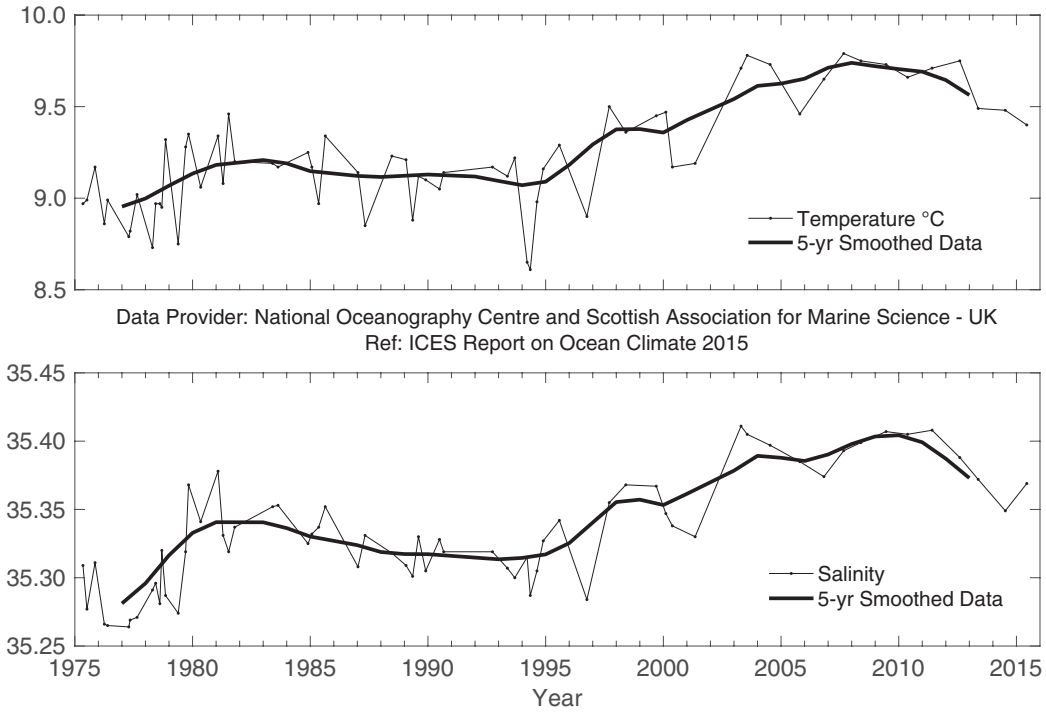

Figure 46.
Rockall Trough. Temperature (upper panel) and salinity (lower panel) for the upper ocean (potential density 27.2–27.50, representing the top 800 m, but excluding the seasonally warmed surface layer).

4.12 Hatton–Rockall Basin

The shallow Hatton–Rockall Basin (1000 m) lies between the Iceland Basin to the west and Rockall Trough to the east and is bounded by the Hatton and Rockall banks. The basin is filled with well-mixed subpolar-mode water moving northward as part of the North Atlantic Current (NAC) complex. Winter mixing reaches 800–1000 m here. Temperature and salinity vary considerably depending on the type of NAC water that enters the basin. The region is in the transition zone between cold, fresh, central subpolar water and warm, saline, eastern subpolar water. When the NAC fronts shift westward, the basin becomes warmer and more saline.

The range of basin mean temperature and salinity in the upper 1000 m is more than 1°C and 0.1 psu, rather higher than the Iceland Basin to the west and Rockall Trough to the east. The lowest values were seen in 1996, followed by a steady rise to maximum values in the late 2000s. Since 2010, there has been a decrease in temperature and salinity; in 2015, both were lower than the 1996–2010 average, and the magnitude of these anomalies is second only to the 1996 values.

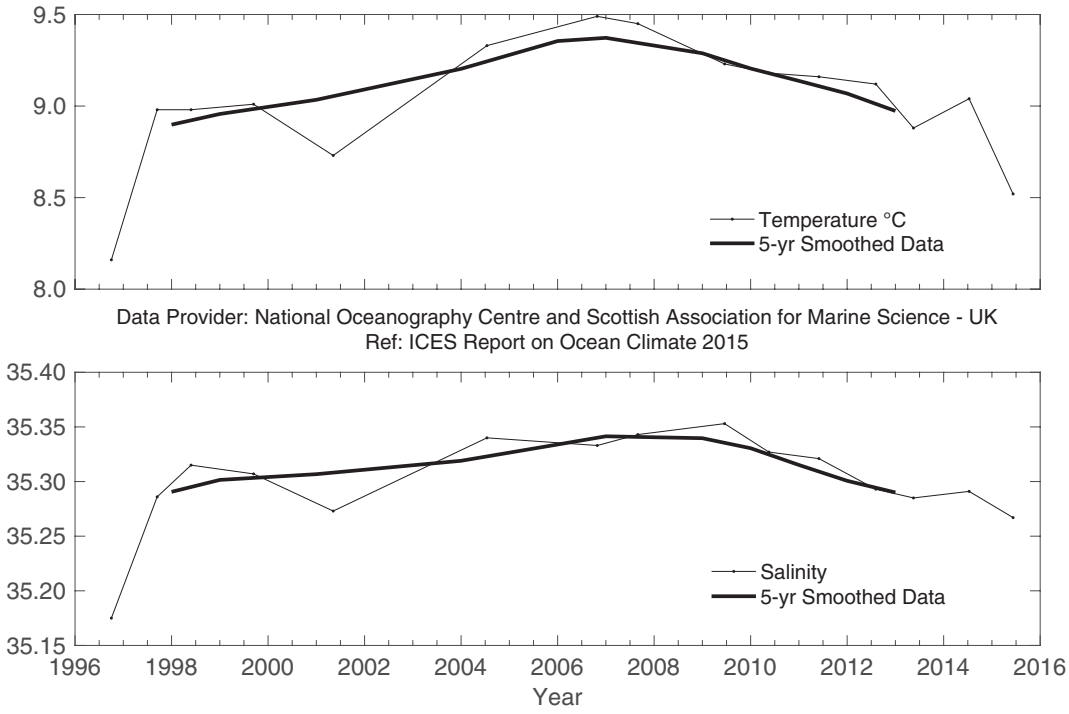

Figure 47.
Hatton–Rockall Basin. Temperature (upper panel) and salinity (lower panel) for the upper ocean (potential density 27.20–27.50, representing the top 600 m and excluding the seasonally warmed surface layer).

4.13 Iceland Basin

A major part of the North Atlantic Current (NAC) flows into the Iceland Basin adjacent to the shallow Hatton Bank on the southeast side of the basin. The NAC typically consists of one or two fronts between warmer and more saline water in the east and colder, fresher water to the north and west. The region is rich in eddy activity, and the water properties are quite variable in time and space. Most of the water entering the Iceland Basin from the south flows through into the Nordic seas over the Iceland–Scotland Ridge. A smaller fraction of the NAC water recirculates south of Iceland in the boundary currents of the main anticlockwise circulation of the Subpolar Gyre.

The temperature and salinity of the upper ocean (ca. the top 500–600 m) vary from year to year, but also exhibit multiyear changes. From 1996 to the late 2000s, both temperature and salinity were increasing, but have since been decreasing. In 2015, the temperature and salinity values were the lowest recorded since 1996. The 2015 temperature anomaly is particularly strong, more than four standard deviations below the 1996–2010 mean. This change implies that the basin is receiving more water originating in the west and central subpolar region and less warm, saline water from the eastern intergyre regions.

THE 2015 TEMPERATURE ANOMALY IN THE ICELAND BASIN IS MORE THAN FOUR STANDARD DEVIATIONS BELOW THE 1996–2010 MEAN.

Photo: Jannica Haldin, ICES.

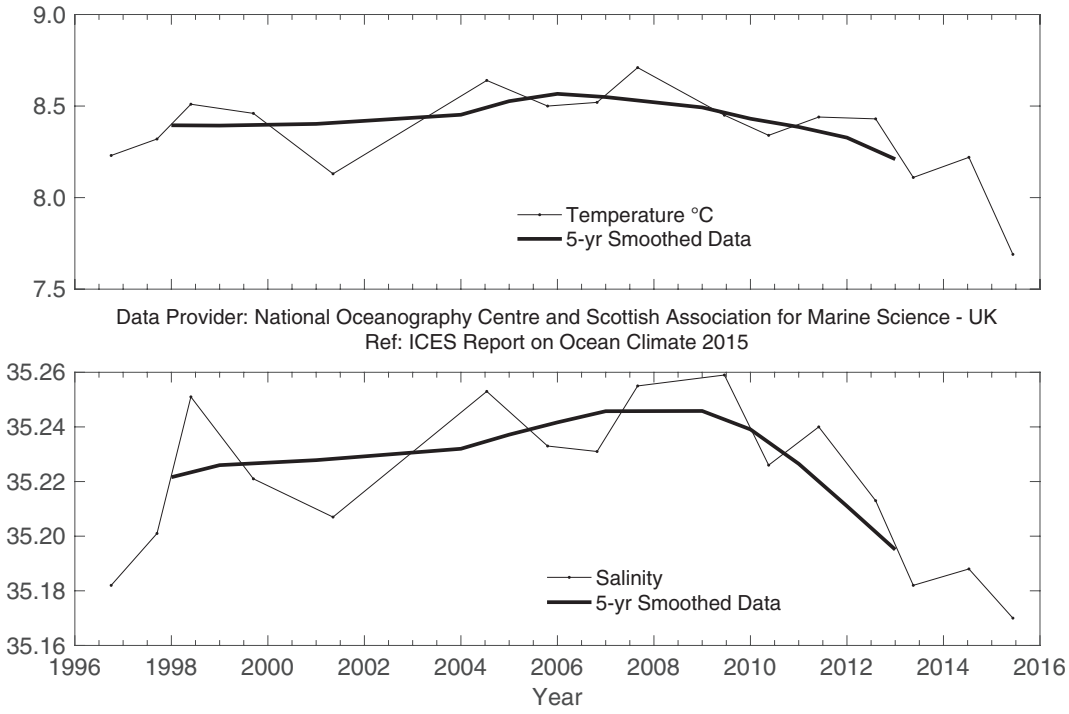

Figure 48.
Iceland Basin. Temperature (upper panel) and salinity (lower panel) for the upper ocean (potential density 27.20–27.50, representing the top 500 m and excluding the seasonally warmed surface layer).

4.14 Irminger Sea

The Irminger Sea is the ocean basin between southern Greenland, the Reykjanes Ridge, and Iceland. This area forms part of the North Atlantic subarctic cyclonic gyre. Due to this gyre, the exchange of water between the Irminger and Labrador seas proceeds relatively fast. In the bottom layers of the Irminger Sea, cold water originating from the (sub)arctic seas flows from Denmark Strait southwards over the continental slope of Greenland.

In 2004, subpolar-mode water (SPMW) in the centre of the Irminger Sea in the pressure interval 200–400 dbar reached its highest temperature and salinity since 1991. Since then, temperature has exhibited well-correlated interannual variations, suggesting that variations in wind-driven circulation were the main cause of this hydrographic variability. However, with the time-series extended to 2015, there appears to be a small downward trend in temperature, but not in salinity.

Updates carried out for 2014 showed that the temperature of SPMW in the central Irminger Sea was 0.006°C below the long-term mean, and salinity was 0.011 above the long-term mean (Note: these are corrections from the 2014 report). In 2015, this trend continued, with the temperature of the SPMW in the central Irminger Sea 0.226°C below the long-term mean, while salinity of the SPMW was 0.022 above the long-term mean. Hence, there was slightly colder, but more saline, SPMW water relative to 2014. The cold winter of 2014–2015 caused deep convection in the Irminger Sea; however, the resulting SPMW temperature was not as cold as in the first half of the 1990s.

Photo: Jannica Haldin, ICES.

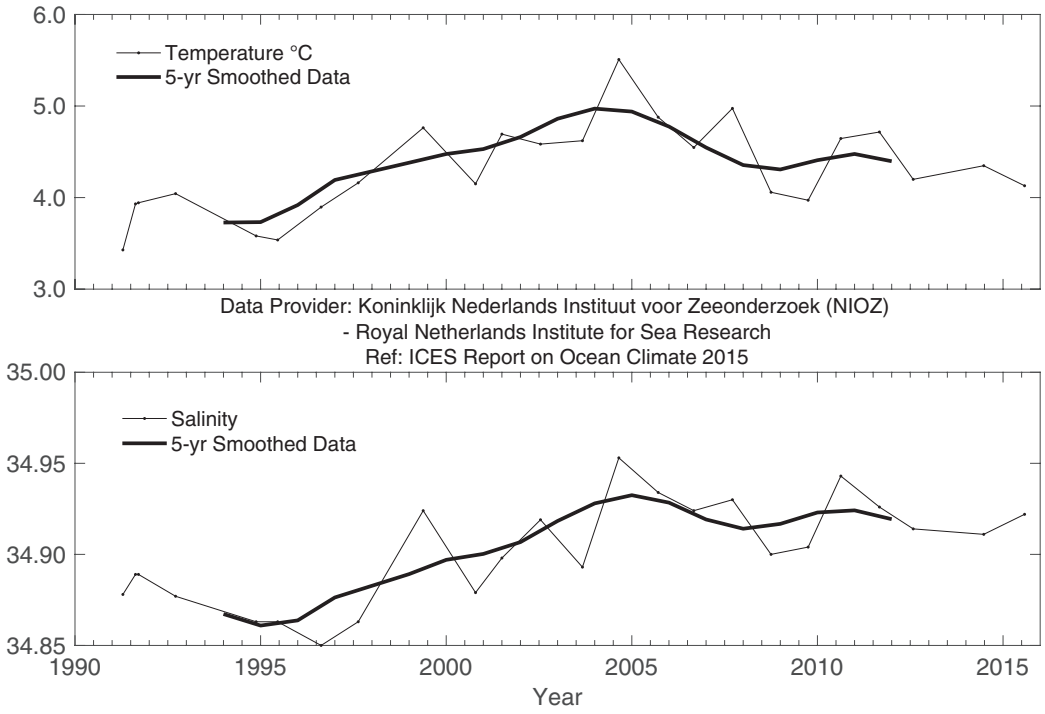

Figure 49.
Irminger Sea. Temperature (upper panel) and salinity (lower panel) of subpolar-mode water in the central Irminger Sea (averaged over 200–400 m).

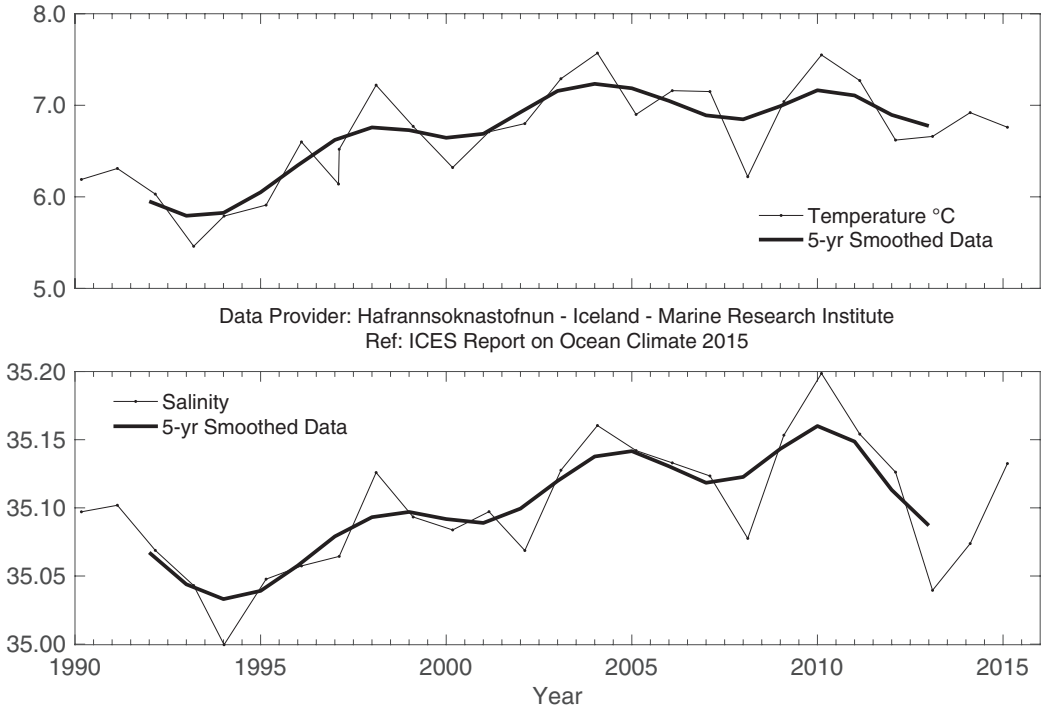

Figure 50.
Irminger Sea. Temperature (upper panel) and salinity (lower panel) of subpolar–mode water in the northern Irminger Sea (Station FX9, 64.33°N 28°W), from winter observations averaged over 200–500 m).

4.15 Faroese waters and the Faroe–Shetland Channel

Data from Faroese waters are here grouped together with data from the Faroe–Shetland Channel. This small region is at the boundary between the Celtic Seas, North Sea, and Norwegian Sea ecoregions and also the boundary between the North Atlantic and Nordic seas.

One branch of the North Atlantic Current crosses the Greenland–Scotland Ridge, flowing on either side of the Faroes. Measurements made in the Faroe Bank Channel are, therefore, of the water in the NAC before it crosses the Greenland–Scotland Ridge. Once the NAC has crossed the ridge, its properties change due to mixing with other water masses. Some of this water, now referred to as Modified North Atlantic Water (MNAW) recirculates into the Faroe–Shetland Channel.

Farther to the east, the continental slope current flows along the edge of the northwest European continental shelf. Originating in the southern Rockall Trough, it carries warm, saline Atlantic water (AW) into the Faroe–Shetland Channel. A proportion of this AW crosses onto the shelf itself and enters the North Sea, where it is diluted with coastal water and eventually leaves in the Norwegian Coastal Current. The remainder enters the Norwegian Sea and joins the water coming from north of the Faroes to become the Norwegian Atlantic water.

Generally, both temperature and salinity in all upper-layer waters around the Faroes and the Faroe–Shetland Channel increased markedly during the 1990s and 2000s. Both temperature and salinity decreased during the first half of the 2010s.

After the record-high salinities observed in the Faroe Bank Channel and the Faroe Current in November 2009, salinities decreased at both locations, but then levelled off in the Faroe Bank Channel. In the Faroe Current, there was a slight increase in salinity in 2015 compared to 2014. Temperatures in the Faroe Bank Channel have been relatively high and stable since the mid-2000s and into the early 2010s. In 2012, they decreased and have been more variable; temperature decreased from 2014 to 2015, but remained slightly above the long-term mean. Normally the characteristics of water in the Faroe Current change in the same way as the characteristics of the Faroe Bank Channel, but with a delay; thus, in the Faroe Current, a similar temperature variability was observed, but the temperature in 2015 was slightly below the long-term mean.

On the Faroe shelf, the annual average temperature has been relatively high since the early 2000s, but in 2015, the annual averaged temperature was the lowest observed since 2000. The main reason for this was the unusually cold spring and summer air temperatures that were observed everywhere in the Northwest Atlantic. The long-term trend in salinity on the Faroe shelf follows the trend observed in off-shelf waters. Thus, salinities increased from the start of the observations in 1995 to record-high values in 2010. Since 2010, salinities have been decreasing and are now close to the values observed in the beginning of the series.

The temperature and salinity of the surface waters of the Faroe–Shetland Channel have generally increased over the past two decades. Water on the western slopes of the Channel, known as modified North Atlantic water, experienced record-high temperature and salinity in 2010. Temperature and salinity of Atlantic water masses on both sides of the Faroe–Shetland Channel have decreased slightly since then, and values are now lower than the long-term mean.

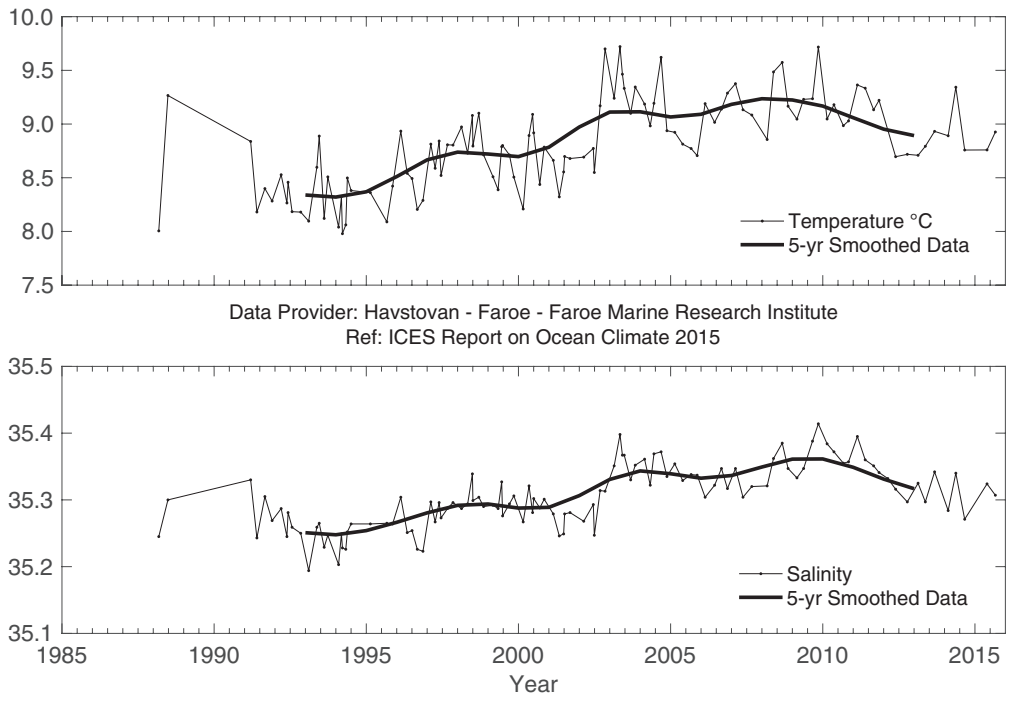

Figure 51.
Faroese waters. Temperature (upper panel) and salinity (lower panel) in the high salinity core of the Atlantic water over the Faroe Bank Channel (maximum salinity averaged over a 50 m deep layer).

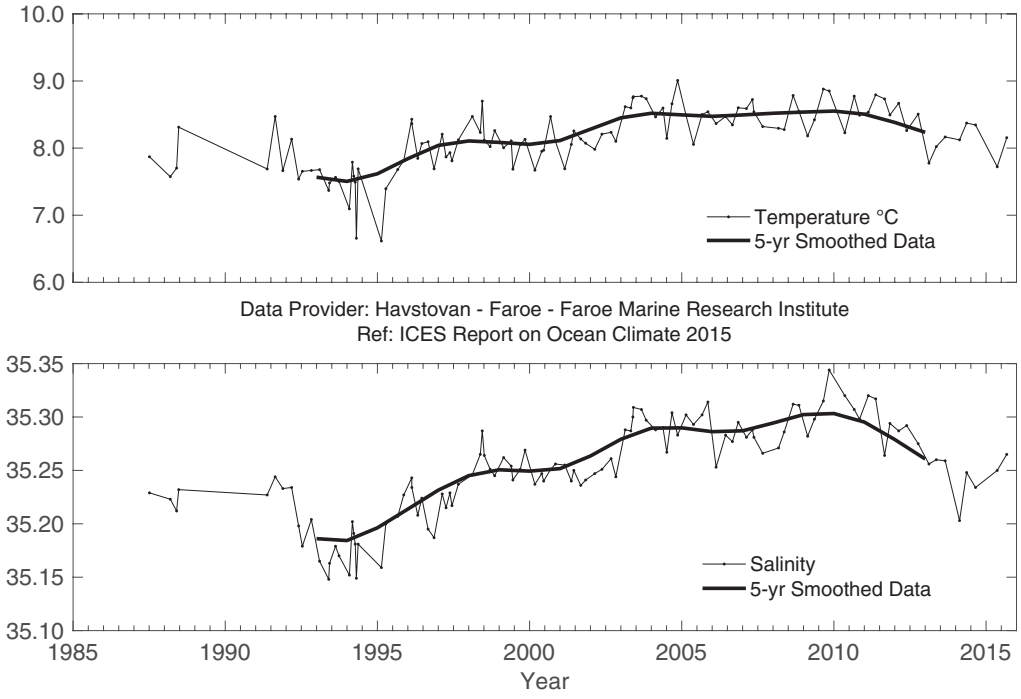

Figure 52.
Faroese waters. Temperature (upper panel) and salinity (lower panel) in the high salinity core of the Faroe Current north of the Faroes (maximum salinity averaged over a 50 m deep layer).

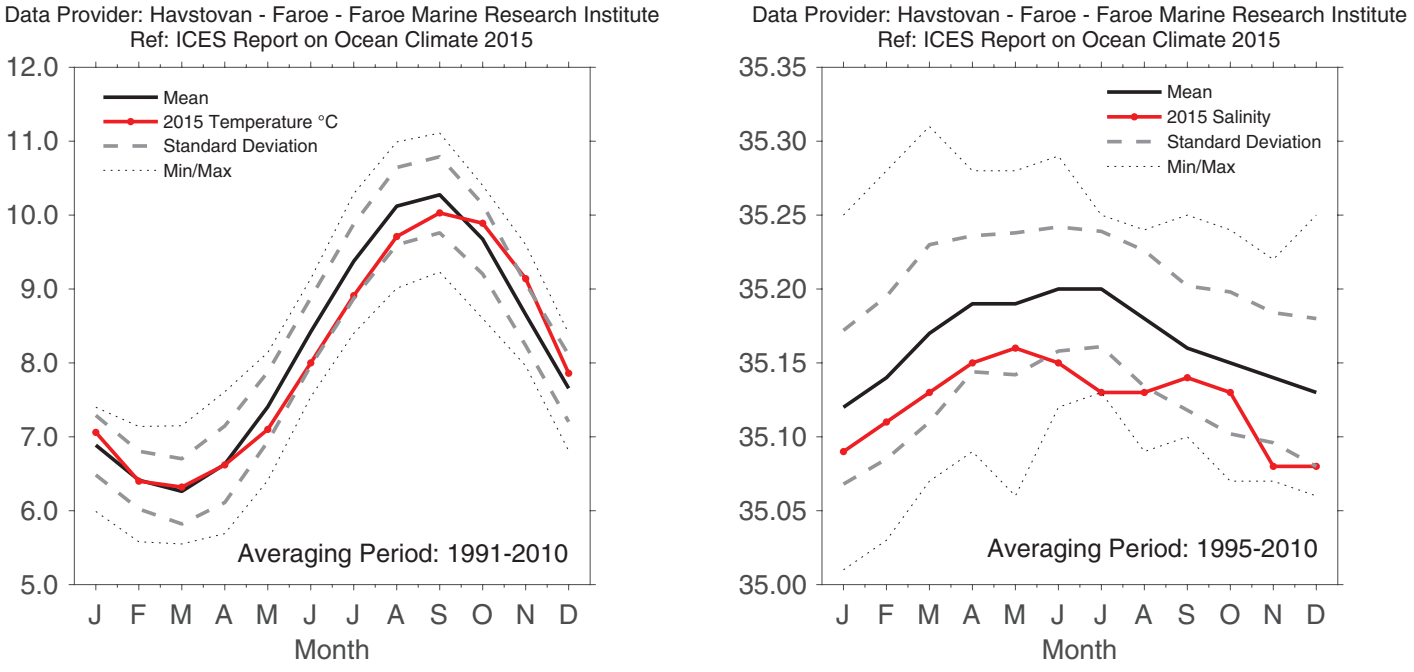

Figure 53.
Faroese waters. 2015 monthly temperature (left) from the Faroe coastal station at Oyrargjogv (62.12°N 7.17°W) and monthly salinity (right) from the Faroe coastal station at Skopun (61.91°N 6.88°W). Note that the temperature averaging period has been changed and is now based on data from Oyrargjogv in the period 1991–2010. The salinity averaging period is 1995–2015.

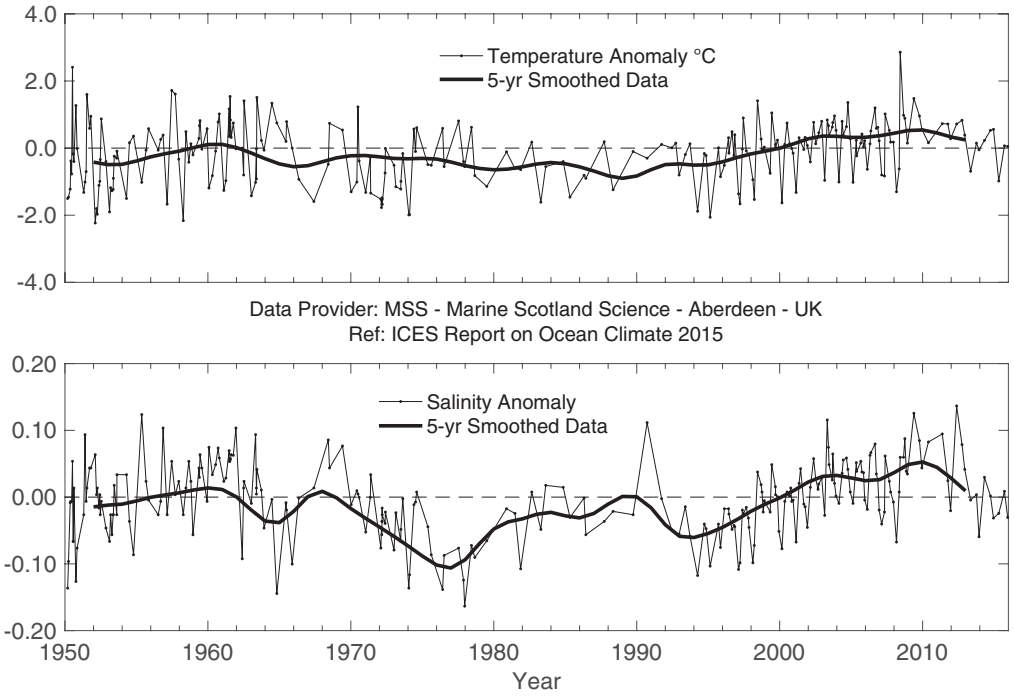

Figure 54.
Faroe–Shetland Channel. Temperature anomaly (upper panel) and salinity anomaly (lower panel) in the modified Atlantic water entering the Faroe–Shetland Channel from the north after circulating around the Faroes.

TEMPERATURES AND SALINITIES HAVE BEEN DECREASING DURING THE 2010s AND ARE NOW CLOSE TO OR BELOW THE LONG-TERM MEAN.

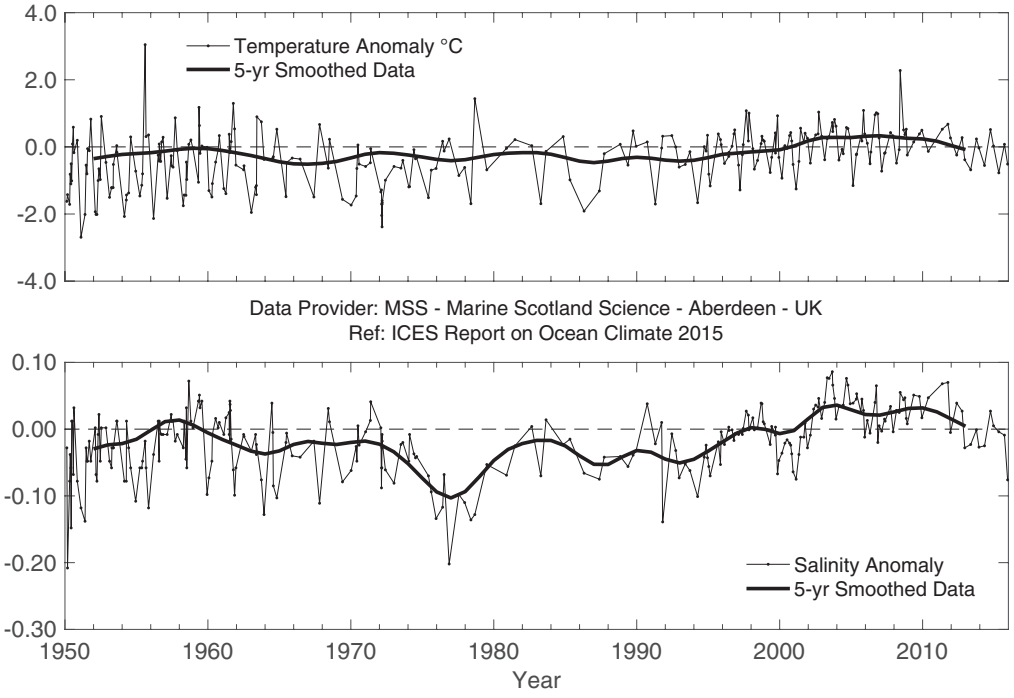

Figure 55.
Faroe–Shetland Channel. Temperature anomaly (upper panel) and salinity anomaly (lower panel) in the Atlantic water in the slope current.

4.16 North Sea

North Sea oceanographic conditions are determined by the inflow of saline Atlantic water (AW) and the ocean–atmosphere heat exchange. The inflow through the northern entrances (and, to a lesser degree, through the English Channel) can be strongly influenced by the NAO. Numerical-model simulations also demonstrate strong differences in the North Sea circulation, depending on the state of the NAO. The AW mixes with river run-off and lower salinity Baltic outflow along the Norwegian coast. A balance of tidal mixing and local heating forces the development of a seasonal stratification from April/May to September in most parts of the North Sea.

Between January and October, the monthly means of area-averaged North Sea SST were close to normal in the reference period (RP) 1981–2010, but in the last months of the year, SST increased and exceeded the long-term mean significantly. At 9.5°C the 2015 December mean is, together with 2006, the warmest December since 1971 (anomaly +1.3°C). After a maximum of 11.4°C in 2014, the annual SST mean dropped back to 10.6°C in 2015, which is still 0.4°C above the annual mean of the RP. In addition to the inflow of warmer Atlantic water at the northern boundary and through the English Channel, much of the SST variability is caused by the local ocean–atmosphere heat flux.

In 2015, the large-scale horizontal temperature distribution in the surface layer differed significantly from the RP. The southern part was slightly warmer, while the area north of 55°N was clearly colder, with negative anomalies up to –2°C west of Utsira. In the bottom layer, the pattern was different, with positive anomalies over large areas of the North Sea and a local maximum of +3.5°C over Dogger Bank. Small negative anomalies up to –1°C occurred west of Dogger Bank, in the Skagerrak, along the eastern coast, and around the Shetlands.

The maximum difference between surface and bottom temperatures was generally much lower than in previous years, with a maximum of 8°C within a small patch north of Dogger Bank. The maximum vertical temperature gradient in the thermocline was 1.5°C m^{-1}, the depth of the thermocline varied between 16 and 55 m, and its strength was weakening from south to north. Compared to 2014, the total heat content decreased to 1.663×10^{21} J and exceeded the reference mean of 1.631×10^{21} J by only 0.4 standard deviations.

The southern boundary of Atlantic water (AW) >35 psu intruding from the northern boundary into the North Sea was located at about 58°N at the surface and at about 57°N in the bottom layer. The general pattern showed a positive anomaly in the eastern and a negative anomaly in the western North Sea. At the surface, a local positive anomaly of >2 psu was observed west of Utsira. The area covered by AW was larger than in 2014 at the surface and comparable to 2014 in the bottom layer. Nevertheless, the total salt content decreased to 1.039×10^{12} t, which is the lowest value since 2001. This is caused by the bottom layer in the central North Sea, with salinities between 34 and 35 psu, being fresher than in previous years and having a reduced vertical extension.

With the exception of January, the monthly run-off volumes of the River Elbe were below the reference period 1981–2010. However, the annual run-off volume of 15 km^3 $year^{-1}$ (long-term mean 22 km^3 $year^{-1}$) was still within the 95%, and no significant impacts on salinity in the German Bight have been observed.

Temperature and salinity at two positions in the northern North Sea illustrate conditions in the Atlantic inflow (Figure 56). The first (Location A) is at the near-bottom in the northwestern part of the North Sea, and the second (Location B) is in the core of the AW at the western shelf edge of the Norwegian Trench. Measurements were taken during summer and represent the previous winter's conditions. The average temperature at Location A was 1–2°C lower than at Location B, and salinity was also slightly lower. Above-average temperatures and salinities were shown at both locations in 2009, and there has been an increase in both salinities and temperatures since 2008.

IN 2015, ANNUAL AREA-AVERAGED NORTH SEA SST STILL EXCEEDED THE CLIMATOLOGICAL MEANS. THE DECEMBER SST MEAN SHOWS, TOGETHER WITH 2006, THE WARMEST DECEMBER SINCE RECORDS BEGAN IN 1971, WITH AN ANOMALY OF +1.3°C.

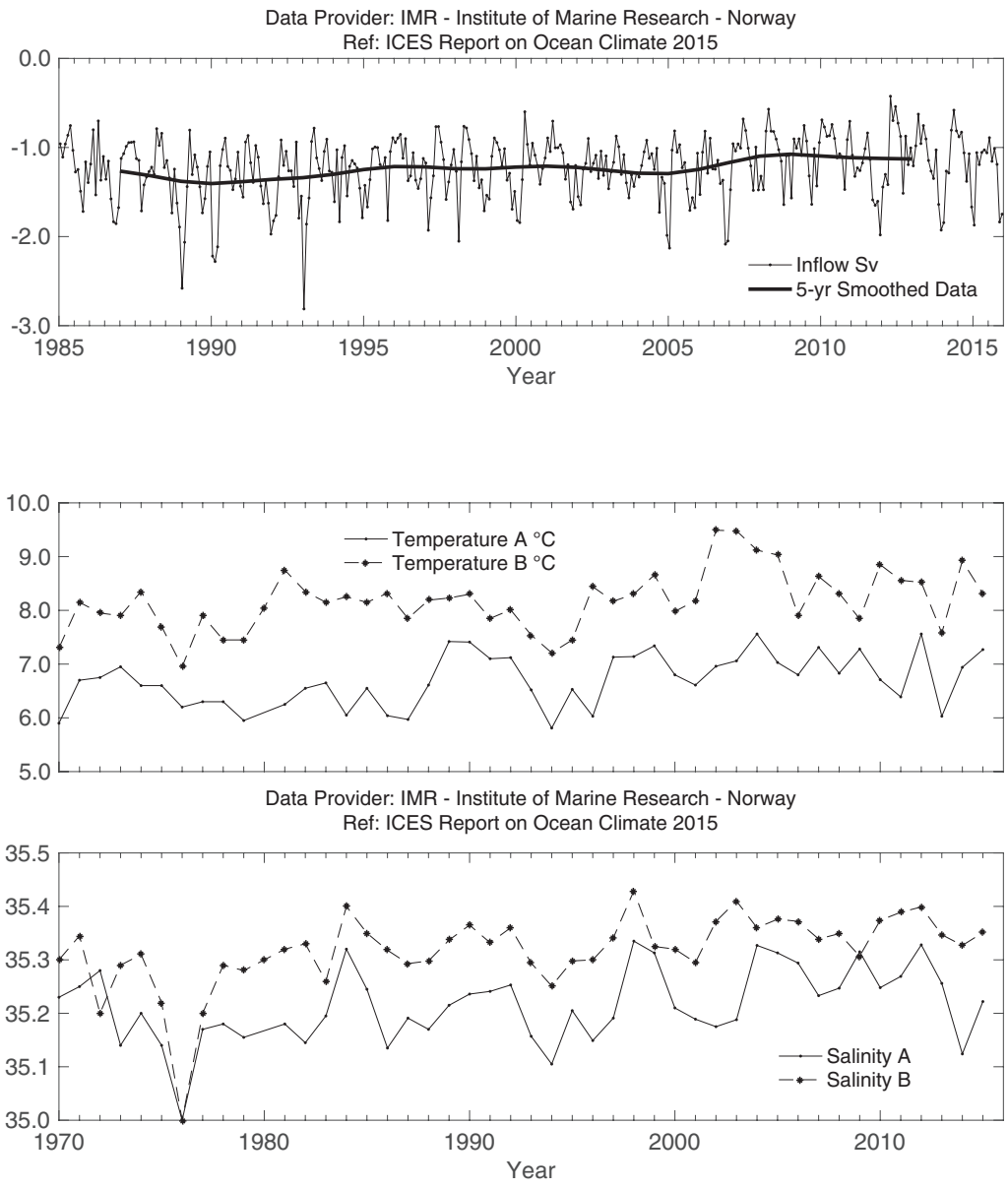

Figure 56.
North Sea. Modelled annual mean (bold) and monthly mean volume transport of Atlantic water into the northern and central North Sea southwards between the Orkney Islands and Utsira, Norway (top panel). Temperature (middle panel) and salinity (bottom panel) near the seabed in the northwestern part of the North Sea (Location A) and in the core of AW at the western shelf edge of the Norwegian Trench (Location B) during the summers of 1970–2015.

Photo: Jannica Haldin, ICES.

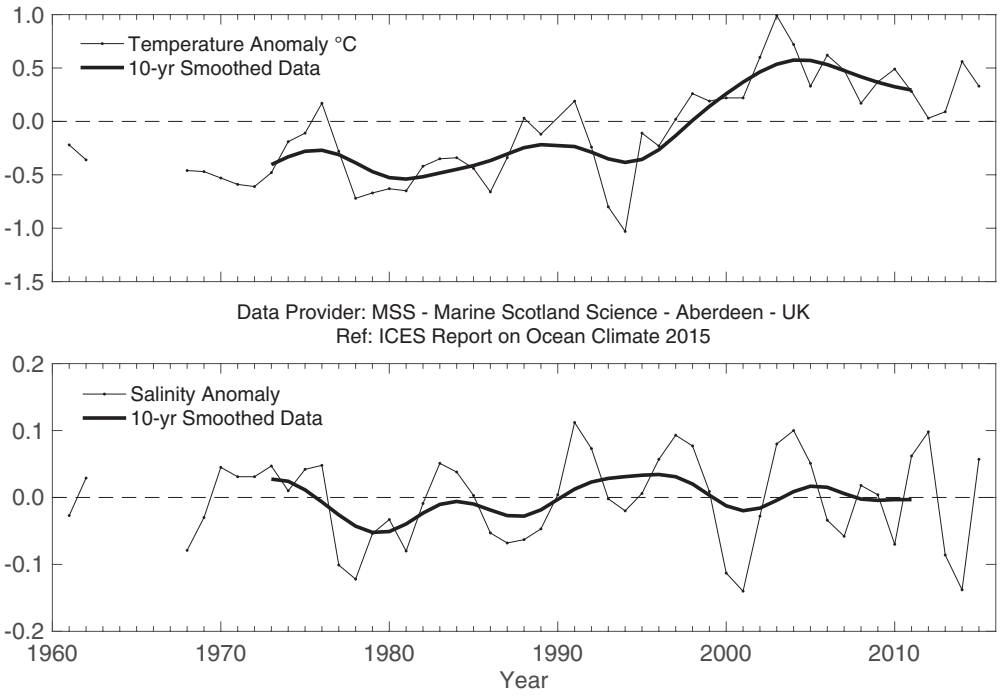

Figure 57.
North Sea. Temperature anomaly (upper panel) and salinity anomaly (lower panel) in the Fair Isle Current entering the North Sea from the North Atlantic.

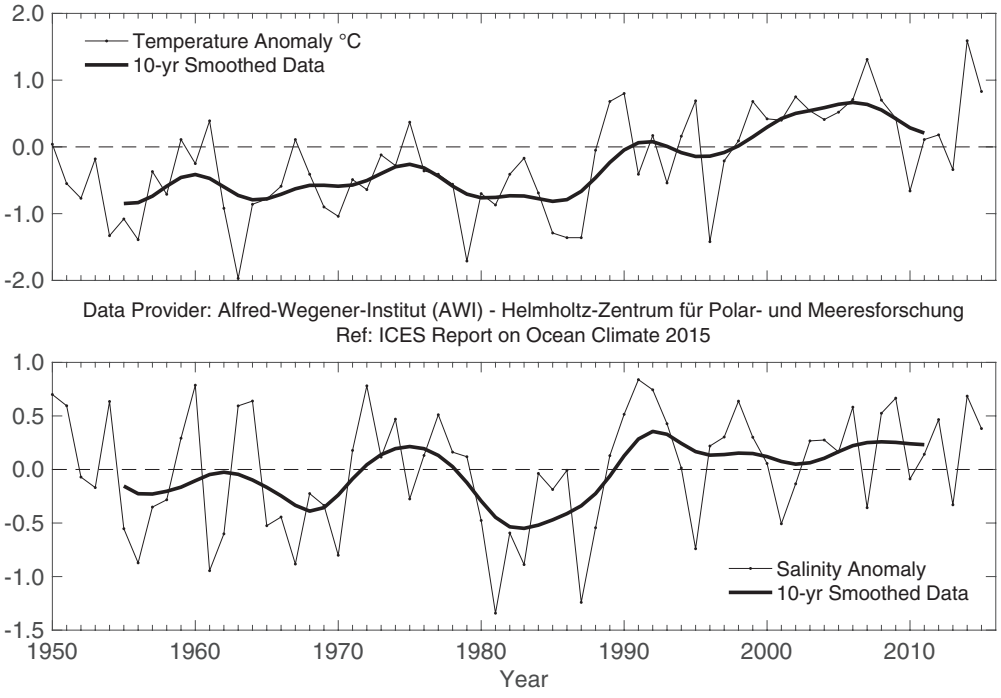

Figure 58.
North Sea. Annual mean surface temperature anomaly (upper panel) and salinity anomaly (lower panel) at Station Helgoland Roads.

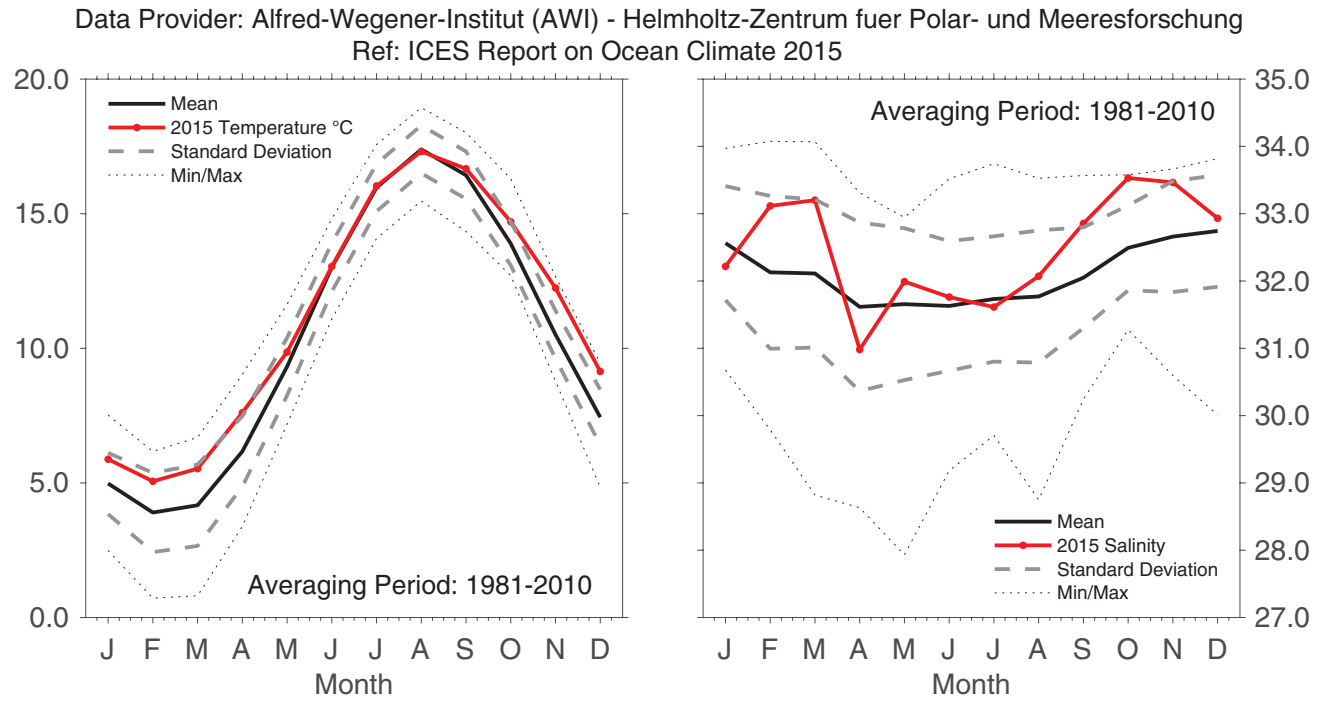

Figure 59.

North Sea. Monthly surface temperature (left panel) and salinity (right panel) at Station Helgoland Roads.

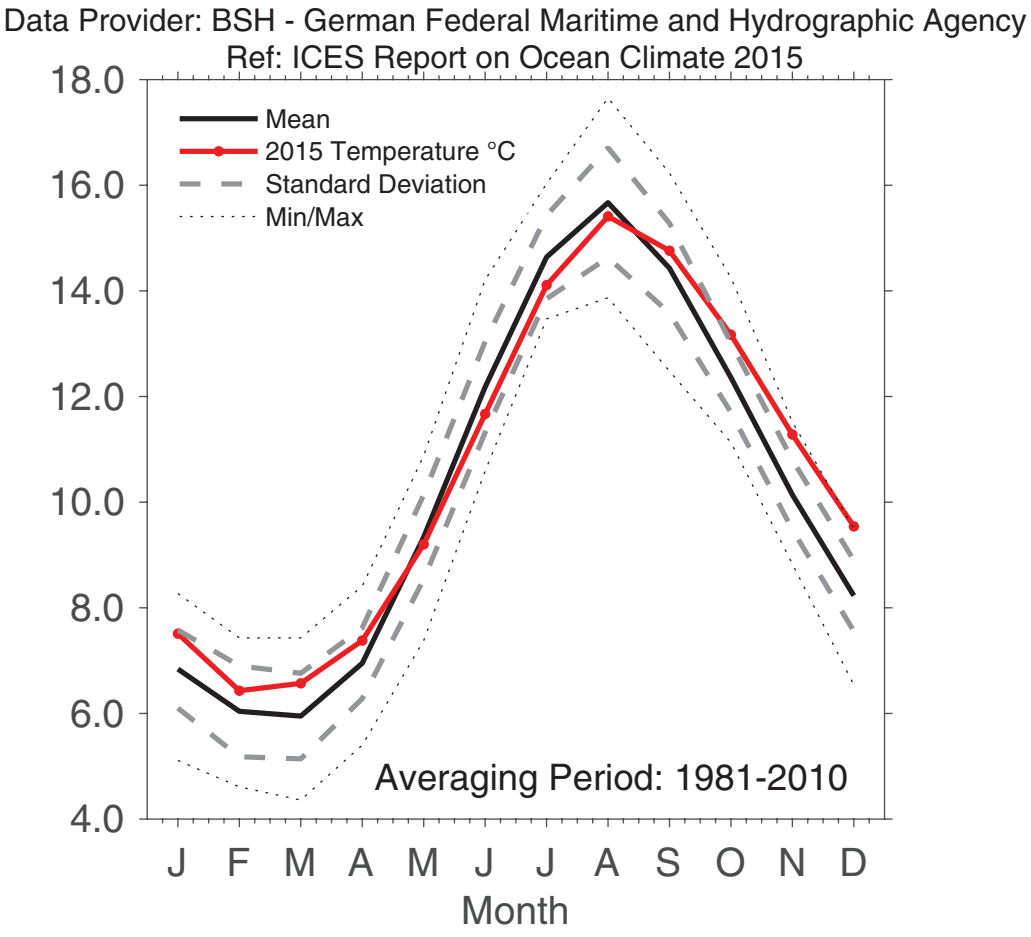

Figure 60.

Northern and southern North Sea. North Sea area-averaged sea surface temperature (SST) annual cycle; 2015 monthly means based on operational weekly North Sea SST maps.

4.17 Skagerrak, Kattegat, and the Baltic

The shallow seas of the Skagerrak, Kattegat, and the Baltic are characterized by large salinity variations. In the Skagerrak, water masses from different parts of the North Sea are present. The Kattegat is a transition area between the Baltic and the Skagerrak. Water is strongly stratified, with a permanent halocline (sharp change in salinity at depth). The deep water in the Baltic Proper, which enters through the Belts and the Sound, can be stagnant for long periods in the inner basins. In the relatively shallow area in the southern Baltic, smaller inflows pass relatively quickly, and conditions in the deep water are quite variable. Surface salinity is very low in the Baltic Proper and its gulfs. The Gulf of Bothnia and the Gulf of Finland are ice covered during winter.

Owing to its central location relative to the Skagerrak, Kattegat, and Baltic, the weather in Sweden can be considered representative for the area. Since 1860, only two years, 1935 and 2014, have had mean temperatures higher than in 2015. All months, except May, June, and July, were warmer than normal. Mean precipitation was somewhat higher than normal in most parts of the country. October was, however, a very dry month. The number of sun hours was close to normal in the north, but was above normal elsewhere.

Sea surface temperatures were above normal at the beginning and end of the year in most areas. Only in the Skagerrak did the year start with temperatures close to normal. In summer, water temperatures were below normal because it took some time to warm up the surface layer after the cold weather in early summer.

Surface salinities were mostly normal in the Skagerrak and the Kattegat, except in August and October and also in September in some areas, when values were below normal. These low salinities were probably due to an increase in the discharge from the Baltic Sea. There were inflows of more-saline water into the Baltic at the beginning and at the end of the year. Consequently, there were higher-than-normal values for surface salinity in the southern parts of the Kattegat and the Baltic Proper. The rest of the Baltic Proper exhibited values close to normal.

The inflow that took place in December 2014 was monitored monthly as it proceeded into the deeper parts of the Baltic Sea. The effect of the inflow was not long-lasting, and oxygen rates have started to decrease again. The inflow never reached the northern and western parts of the Gotland Basin because the salinity of the inflowing water was too low. Furthermore, the warm autumn caused oxygen levels of the inflowing water to be lowered, which kept water temperatures above normal.

The ice season 2014/2015 had a late start because of higher-than-normal sea water temperatures at the end of 2014. Cold periods were then mixed with windy periods, which made it hard to establish an ice cover. The maximum ice extent of 45 000 km^2 was reached already on 24 January; this was the lowest value of the maximum ice cover ever recorded. The ice season ended as early as the first week of May. The Bothnian Bay was never fully ice covered during winter 2014/2015.

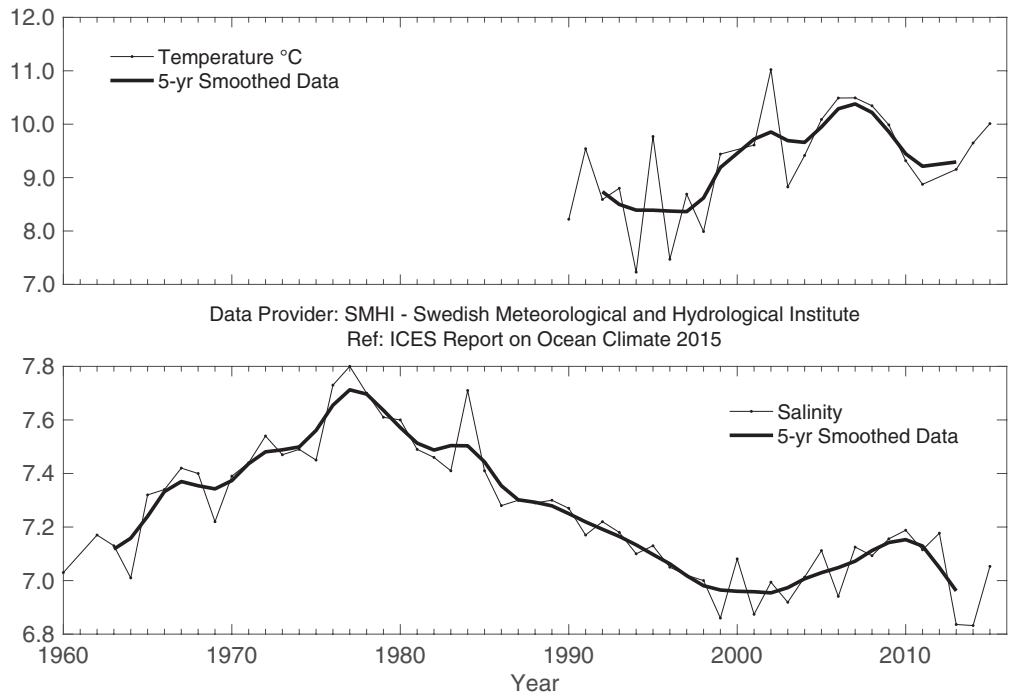

Figure 61.
Skagerrak, Kattegat, and the Baltic. Surface temperature, yearly mean (upper panel) and surface salinity, yearly mean (lower panel) at Station BY15 (east of Gotland) in the Baltic Proper.

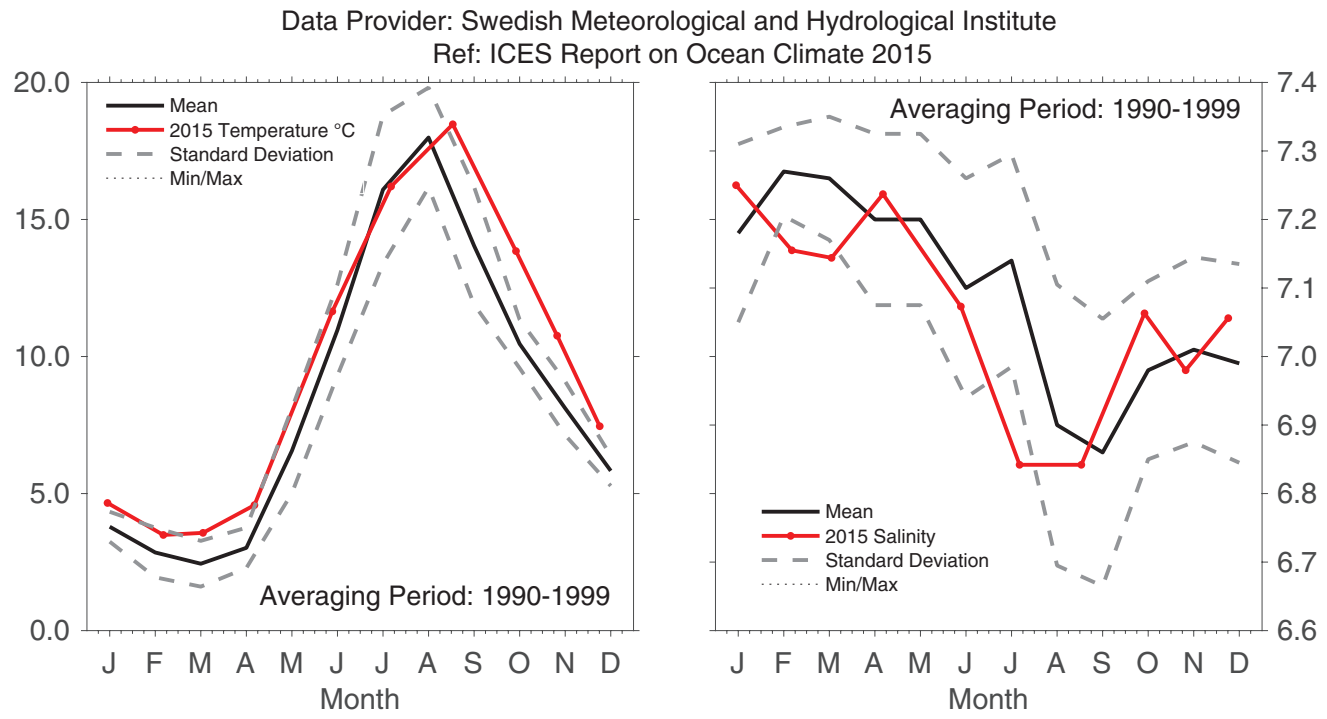

Figure 62.

Skagerrak, Kattegat, and the Baltic. Monthly surface temperature (left panel) and salinity (right panel) at Station BY15 (east of Gotland) in the Baltic Proper.

A WARM YEAR WITH A NEW RECORD-LOW ICE COVER IN THE BALTIC SEA.

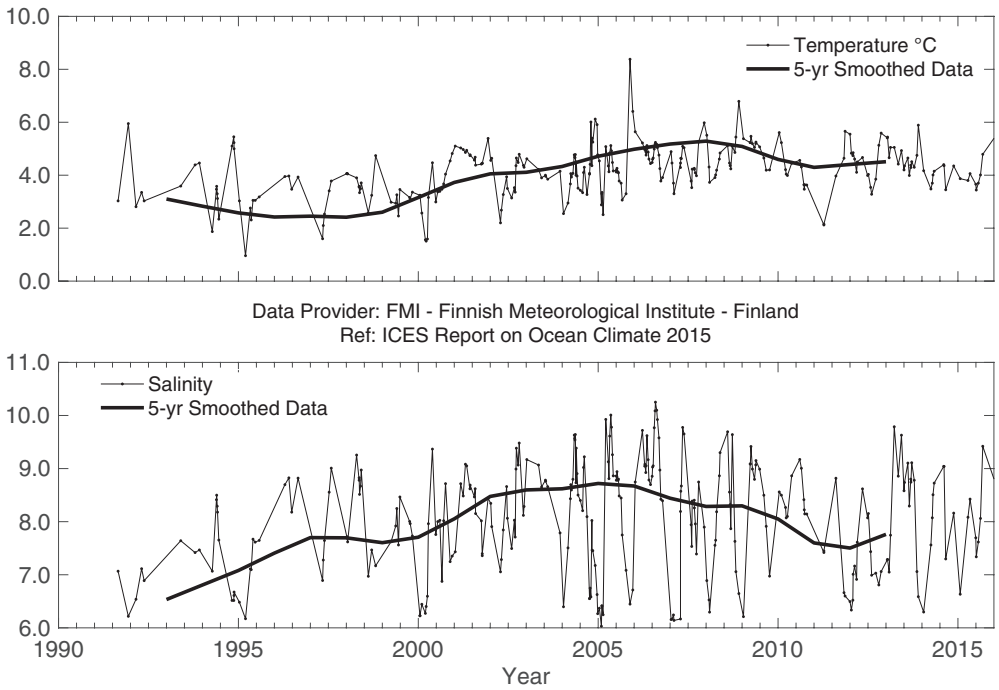

Figure 63.

Skagerrak, Kattegat, and the Baltic. Temperature (upper panel) and salinity (lower panel) at Station LL7 in the Gulf of Finland.

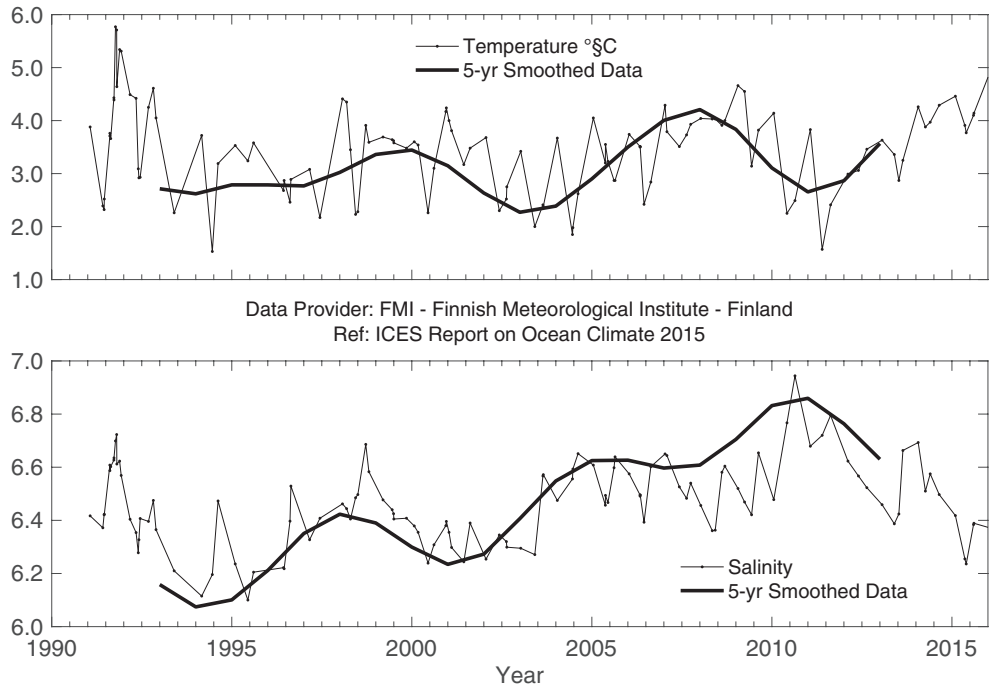

Figure 64.
Skagerrak, Kattegat, and the Baltic. Temperature (upper panel) and salinity (lower panel) at Station SR5 in the Bothnian Sea.

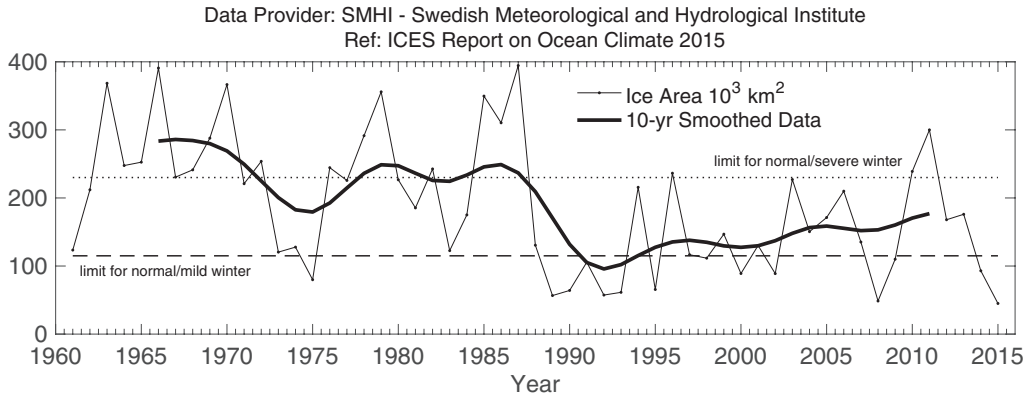

Figure 65.
Skagerrak, Kattegat, and the Baltic. The maximum ice extent in the Baltic starting from 1957.

Photo: Jannica Haldin, ICES.

4.18 Norwegian Sea

The Norwegian Sea is characterized by warm Atlantic water on the eastern side and cold Arctic water on the western side, separated by the Arctic front. Atlantic water enters the Norwegian Sea through the Faroe–Shetland Channel and between the Faroes and Iceland via the Faroe Front. A smaller branch, the North Icelandic Irminger Current, enters the Nordic seas on the western side of Iceland. Atlantic water flows north as the Norwegian Atlantic Current, which splits when it reaches northern Norway; some enters the Barents Sea, whereas the rest continues north into the Arctic Ocean as the West Spitsbergen Current.

Three sections from south to north in the eastern Norwegian Sea demonstrate the development of temperature and salinity in the core of the Atlantic water (AW) at Svinøy-NW, Gimsøy-NW, and Sørkapp-W. In general, there has been an increase in temperature and salinity in all three sections since the mid-1990s, except for the most recent years when both temperature and salinity declined. In 2015, salinity was close to normal, while temperature was still higher than the long-term averages in the two southernmost sections. Unfortunately, data for 2015 in the northernmost section, the Sørkapp section, were missing. Annual temperature averages in 2015 were 0.3 and 0.5°C above the long-term means at the Svinøy and Gimsøy sections, respectively. Salinity averages in 2015 were 0.01 and 0.02 above the long-term means in the Svinøy and Gimsøy sections, respectively.

The ocean heat and freshwater content of Atlantic water using hydrographic data during spring from 1951 describe the climate variability in the Norwegian Sea. The heat content of the Norwegian Sea has been above the long-term mean since 2000. The freshwater content has increased since 2010 and was close to the long-term mean in 2015.

THE HEAT CONTENT OF THE NORWEGIAN SEA HAS BEEN ABOVE THE LONG-TERM MEAN SINCE 2000.

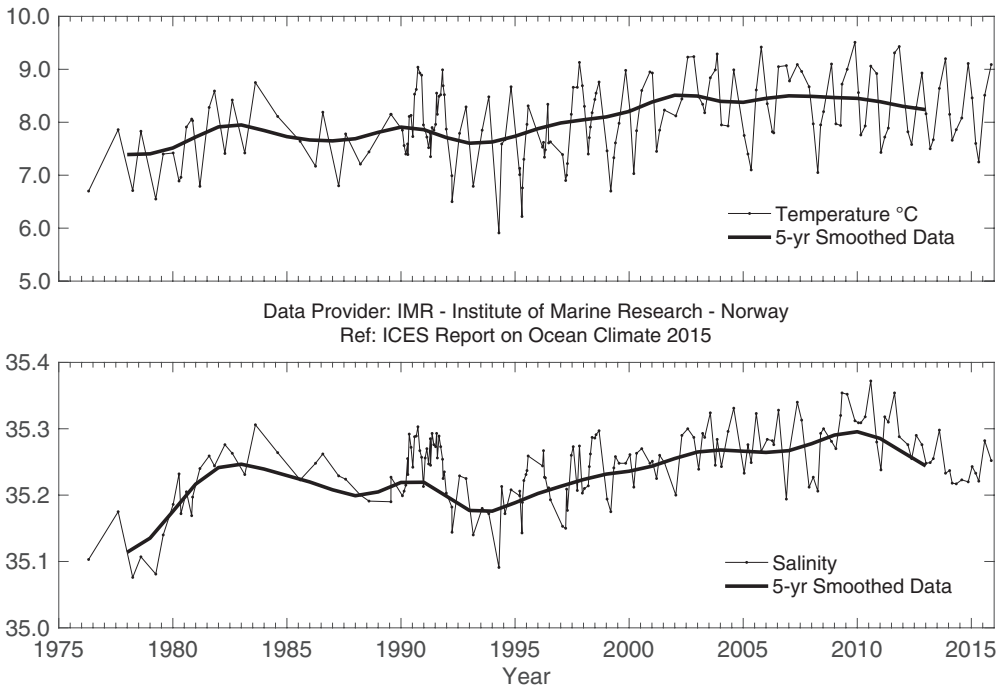

Figure 66.
Norwegian Sea. Temperature (upper panel) and salinity (lower panel) above the slope at Svinøy Section (63°N).

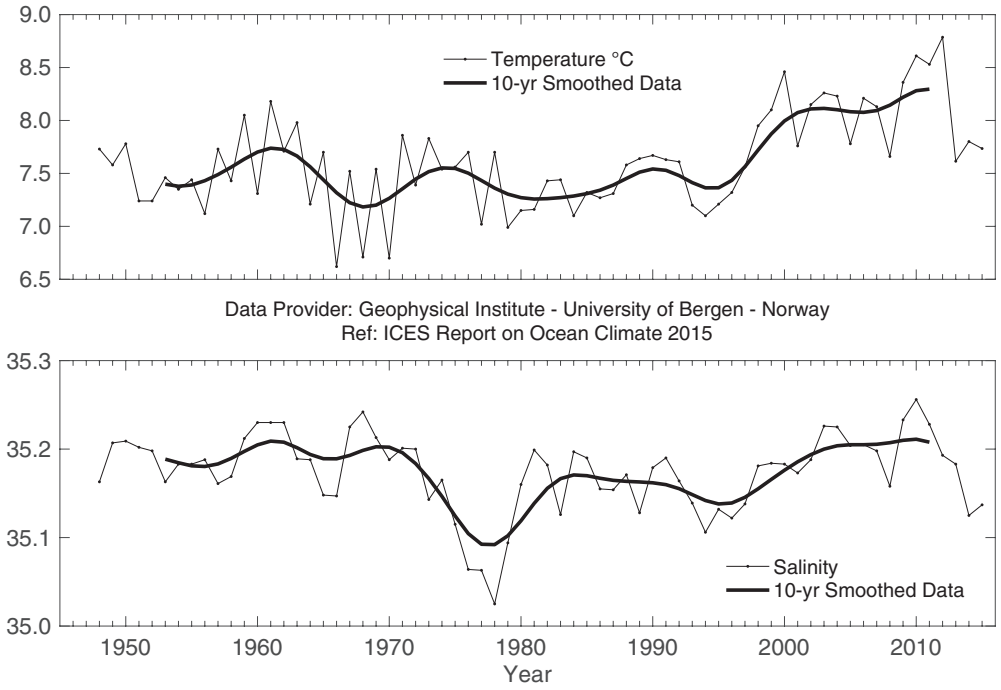

Figure 67.
Norwegian Sea. Temperature (upper panel) and salinity (lower panel) at 50 m at Ocean Weather Station "M" (66°N 2°E).

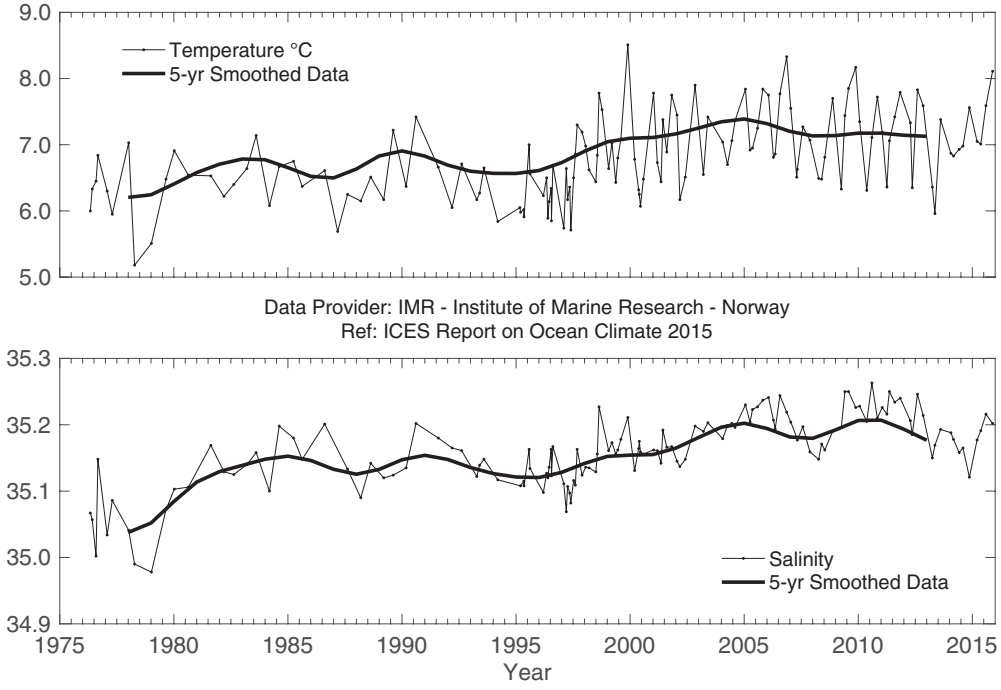

Figure 68.
Norwegian Sea. Temperature (upper panel) and salinity (lower panel) above the slope at Gimsøy Section (69°N).

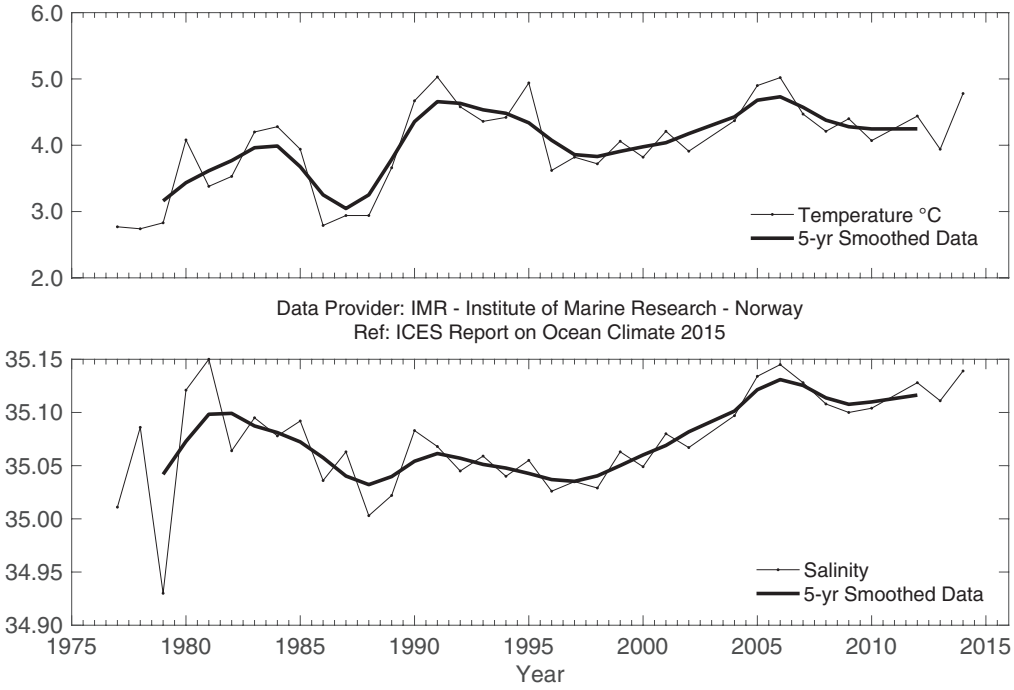

Figure 69.
Norwegian Sea. Temperature (upper panel) and salinity (lower panel) above the slope at Sørkapp Section (76°N). No data in 2015.

4.19 Barents Sea

The Barents Sea is a shelf sea, receiving an inflow of warm Atlantic water from the west. The inflow demonstrates considerable seasonal and interannual fluctuations in volume and water mass properties, causing high variability in heat content and ice coverage of the region.

In 1996 and 1997, after a period of high temperatures in the first half of the 1990s, temperatures in the Barents Sea dropped to values slightly below the long-term average. From March 1998, the temperature in the western Barents Sea increased to just above average, whereas the temperature in the eastern part remained below average during 1998. From the beginning of 1999, there was a rapid temperature increase in the western Barents Sea that also spread to the eastern part. Since then, temperature has remained above average.

In 2015, temperatures in the Barents Sea were still well above normal and typical of anomalously warm years. In the Kola Section (0–200 m), the Atlantic water was 0.5–1.1°C warmer than normal during 2015. Temperature anomalies were increasing from 0.5°C in February to 0.8°C in May. They remained high (0.8–1.1°C) the rest of the year and reached the highest (since 1951) values in November and December. Compared to 2014, the Atlantic water was warmer from April until the end of the year. The 2015 annual mean temperature of the Atlantic water in the Kola Section was 0.8°C higher than normal, which is typical of anomalously warm years and 0.3°C higher than in 2014. This is the third highest value since 1900 (after the record-warm years of 2006 and 2012). The 2015 annual mean salinity of the Atlantic water in the Kola Section was well below average and the lowest since 2001.

In August–September 2015, the surface, deeper, and bottom waters were still much warmer (by 1.2, 1.0, and 0.9°C, respectively) than the long-term mean (1930–2010) all over the Barents Sea. They were also warmer than in 2014 in most of the sea. Positive temperature anomalies were increasing from west to east. Negative anomalies were mainly found in the northwest Barents Sea, especially south and east of the Spitsbergen Archipelago. Surface and bottom waters were saltier than average (1930–2010) in most of the sea, with the largest positive salinity anomalies at the surface in the northern part. Negative anomalies were mainly found in the southern and northwestern Barents Sea. In autumn 2015, at depths of 50 and 100 m and near the bottom, the area of cold water was smaller than in the previous two years, whereas the area of warm water was larger. At 50 and 100 m, the area of warm water was as large as in the record-warm years 2006 and 2012. Ice coverage in 2015 was below average and also lower than that in 2014. The sea ice cover reached its maximum in February, two months earlier than normal, and the Barents Sea was totally free of ice from August through October.

The volume flux into the Barents Sea varies with periods of several years, and was significantly lower during 1997–2002 than during 2003–2006. In 2006, the volume flux was at a maximum during winter and very low during autumn. After 2006, the inflow has been relatively low. During autumn 2014, the inflow was lower than average, whereas at the start of 2015, the inflow increased to 1.5 Sv above the long-term average for the season. The data series presently stops in spring 2015; therefore no information about summer, autumn, and early winter 2015 is yet available.

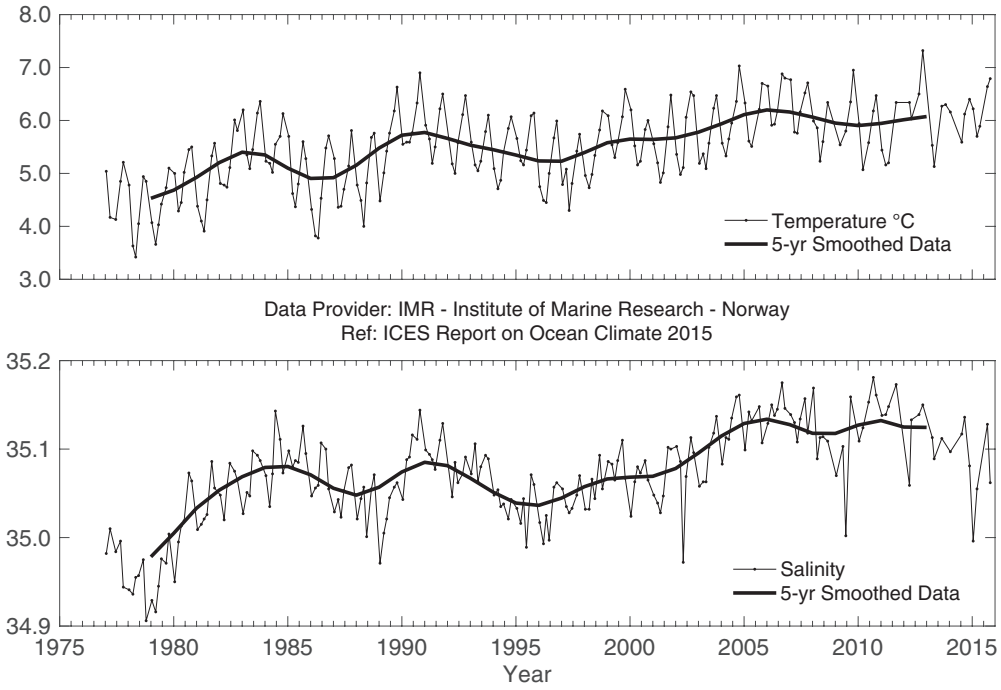

Figure 70.
Barents Sea. Temperature (upper panel) and salinity (lower panel) in the Fugløya–Bear Island Section.

STILL LOWER-THAN-NORMAL ICE COVERAGE, WITH MAXIMUM COVERAGE TWO MONTHS EARLIER THAN USUAL, AND WELL ABOVE-NORMAL TEMPERATURES IN 2015.

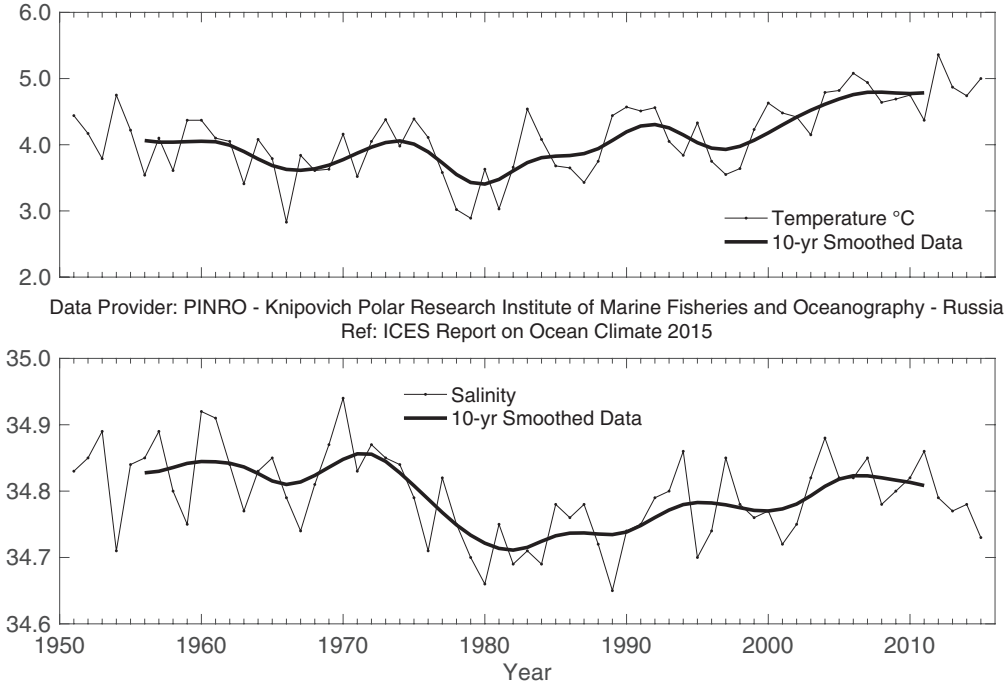

Figure 71.
Barents Sea. Temperature (upper panel) and salinity (lower panel) in the Kola Section (0–200 m).

4.20 Fram Strait

The Fram Strait is the northern border of the Nordic seas; its easternmost side is within the ecoregion of the Barents Sea and its westernmost side is within the ecoregion of the Greenland Sea. It is the only deep passage connecting the Arctic to the rest of the world ocean and is one of the main routes whereby Atlantic water (AW) enters the Arctic (the other is the Barents Sea). The AW is carried northwards by the West Spitsbergen Current, and AW temperature, volume, and heat fluxes exhibit strong seasonal and interannual variations. A significant part of the AW also recirculates within the Fram Strait and returns southwards (return Atlantic water). Polar water from the Arctic Ocean flows south in the East Greenland Current and affects water masses in the Nordic seas.

The temperature of Atlantic water (AW) at the eastern rim of the Greenland Sea (along the 75°N section between 10°E and 13°E) reached its highest value in 2005–2007, with a peak in 2006. After this period, AW temperature decreased significantly in 2008–2009 and remained below its long-term mean value until 2011. In the following three years (2012–2014), the temperature of AW in the eastern Greenland Sea recovered and remained relatively stable, with its values slightly exceeding its long-term mean (by 0.3°C). In 2015, the AW temperature increased further and reached 5.09°C (0.55°C warmer than average). A significant increase in the salinity of Atlantic water in the eastern Greenland Sea was observed in the period 2005–2006, with a maximum of 35.16 in 2006 (exceeding the long-term average by 0.07). This peak was followed by a sharp decrease in 2007 and further slow descent until 2009, when AW salinity returned to its long-term average. In 2010, salinity started to rise again and reached its second peak in 2012 (0.06 above its long-term mean). Since then, it has remained relatively steady, with a slight decrease in 2015 (down to 35.12, but still 0.03 above the long-term mean). Over more than a decade, since 2004, the salinity of Atlantic water in the eastern Greenland Sea has been above its long-term average (except in 2009 when it leveled out).

The western and central parts of the Greenland Sea section at 75°N have not been measured since 2010. The temperature of return Atlantic water (RAW) at the western rim of the Greenland Sea reached a maximum in 2006 (2.9°C) and has been slowly decreasing until the end of the observation period (2010). In 2008–2010, the temperature of RAW was slightly lower than its long-term average. The temperature maximum in 2006 was accompanied by a very strong peak in RAW salinity (0.13 above the long-term mean, more than threefold larger than the standard deviation of RAW salinity). In 2007, the salinity of RAW dropped again and remained slightly higher than its long-term average until 2008. In 2009 and 2010, it decreased further and was close to the average. Temperature and salinity in the upper layer of the central Greenland Basin, within the Greenland Gyre, were modified by the advection of AW and winter convection. The interface with enhanced temperature and salinity gradients has steadily descended (by more than 1000 m) since the beginning of measurements in 1993. After winter 2007/2008, a two-layer structure resulted from a mixed-layer type convection that supplied both salt and heat into the intermediate layers. In winter 2008/2009, almost half of the Greenland Sea had been shielded from convection because of the unusual western location of the Arctic Front (the boundary between the Atlantic and Greenland Sea waters).

In the southern Fram Strait at the standard section along 76.50°N (at the level of 200 dbar, spatially averaged between 9°E and 12°E), a record-high summer temperature for AW was observed in 2006 (a maximum of 4.5°C, exceeding the long-term average by 1.3°C), accompanied by the highest AW salinity (35.13) in the observation period. After that peak, temperature and salinity decreased rapidly in 2007 and 2008 before increasing again in the summers of 2009–2012. In 2011–2015, the temperature of AW in the southern Fram Strait remained relatively constant (3.7–3.8°C, exceeding its average by ca. 0.6°C) except in summer 2013 when it dropped to 3.22°C and levelled out at its long-term mean value. In 2011, 2012, and 2014, AW salinity in the southern Fram Strait was the same (35.13) as during the 2006 maximum, exceeding its long-term mean by 0.07. Slight decreases in salinity were observed in 2013 and 2015, but since 2004, the salinity of AW has remained higher than its long-term mean. Both temperature and salinity trends for the 1996–2015 period were positive.

THE TEMPERATURE OF THE ATLANTIC WATER IN THE FRAM STRAIT INCREASED THROUGH 2012–2014 AND IN 2015 EXCEEDED ITS PREVIOUS PEAK IN 2011. HOWEVER, IT WAS STILL BELOW THE 2006 MAXIMUM.

In the northern Fram Strait at the standard section along 78.83°N, three characteristic areas can be distinguished relative to the main flows: the West Spitsbergen Current (WSC) between the shelf edge and 5°E, the Return Atlantic Current (RAC) between 3°W and 5°E, and the polar water in the East Greenland Current (EGC) between 3°W and the Greenland shelf. The spatially averaged mean temperature of the upper 500 m layer in the WSC reached its peak in 2006 (4.54°C) and decreased afterwards, varying during 2007–2011 within the range of ±0.4°C from the long-term average. In 2012–2013, temperature in the WSC dropped further, reaching 0.7–0.8°C below its long-term mean. Since 2014, it has again been rising and, in 2015, it reached the second highest value in the observation period (4.24°C, exceeding the long-term mean by 1.13°C). It was 1.5°C warmer than the RAC, which was only slightly warmer (0.5°C) than its long-term mean. The highest temperatures in the RAC were observed in 2005 (3°C) and in 2009–2010 (slightly above 2.9°C);

since 2011, temperatures have remained close to the long-term average of 2.2°C. The RAC temperature increased slightly in 2015 to 2.7°C. In the EGC domain, temperature reached its peak in 2007 (1.9°C), decreased significantly to 0.3°C in 2008, and since then has remained relatively stable (within ±0.3°C from its long-term mean), with a slight decrease to 0.3°C in 2014 and returning to 1.0°C in 2015.

The highest salinity in the upper 500 m in the WSC was observed in 2006 (35.11), followed by a decrease to the long-term average in 2007–2008. Between 2009 and 2011, the WSC salinity increased, reaching 0.5 above the long-term mean in 2011. After a slight decrease in 2012–2013, salinity in the WSC reached its second maximum (35.09) in 2014, followed by a slightly lower value of 35.07 in 2015. Maximum salinity in the RAC was observed in 2010 and in subsequent years (2011, 2012, and 2014) exceeded its long-term mean by about 0.05, but leveled out in 2015. Salinity in the EGC was highest in 2007 (34.90) and dropped afterwards below its long-term average except for the intermediate peak (34.72) in 2011. In 2008 and 2014, the EGC salinity reached the lowest value during the last decade (34.50, compared to the record-low minimum of 34.45 observed in 2000 and 2002), while in 2015, it returned to its long-term average.

In 2015, the Atlantic water at the standard section along 78.83°N occupied the core of the West Spitsbergen Current much deeper than in 2014. In 2015, the isotherm of 2°C nearly reached a depth of 800 m in the WSC core located over the upper shelf slope, while one year earlier, it was found at a depth of 400–600 m. The AW mean temperature in the WSC (defined after Rudels *et al.*, 2005 with T >2°C and 27.7< σ_θ <27.97) was 3.54°C in 2015 compared to 3.51°C in 2014 and 3.36°C in 2013. It was lower (by more than 1.3°C) than the maximum of 4.88°C observed in 2006. In the offshore branch of the WSC located over the lower shelf slope, the AW layer was much shallower in 2015 compared to 2014, with the isotherm of 2°C found at a depth of about 300 m (only about half of the AW layer thickness in 2014 when water warmer than 2°C was observed down to 600 m). The low salinity surface layer, covering the upper 50 m of the WSC offshore branch in 2014, was less pronounced in 2015.

In the western deep part of the strait, recirculating AW with temperatures above 3°C extended far westward, reaching 2°W. Smaller patches of the Arctic Atlantic water (AAW) warmer than 2°C were found over the upper continental slope east of Greenland (between 2°W and 6°W), occupying the 200–500 m layer located below the polar water in the southward flowing EGC. The AAW in 2015 was significantly warmer and more saline than in 2014. The position of the Arctic front between the Arctic-derived polar water and Atlantic water at the surface was near 1°W in 2015, similar to 2013 and in contrast with 2014, when it was observed much farther east (about 1°E). The temperature, salinity, and thickness of the polar water surface layer observed in 2015 were similar to 2014.

The continuous measurements from moorings along 78°50′N were only partially recovered in 2013–2015, so the annual temperature evolution and volume transport cannot be updated from 2012 onward. Based on the last available data, the winter-centred annual mean volume transport in the West Spitsbergen Current was 6.4 Sv in 2011–2012, close to the transport observed in 2010–2011 (6.3 Sv) and slightly higher than the long-term mean of 6 Sv.

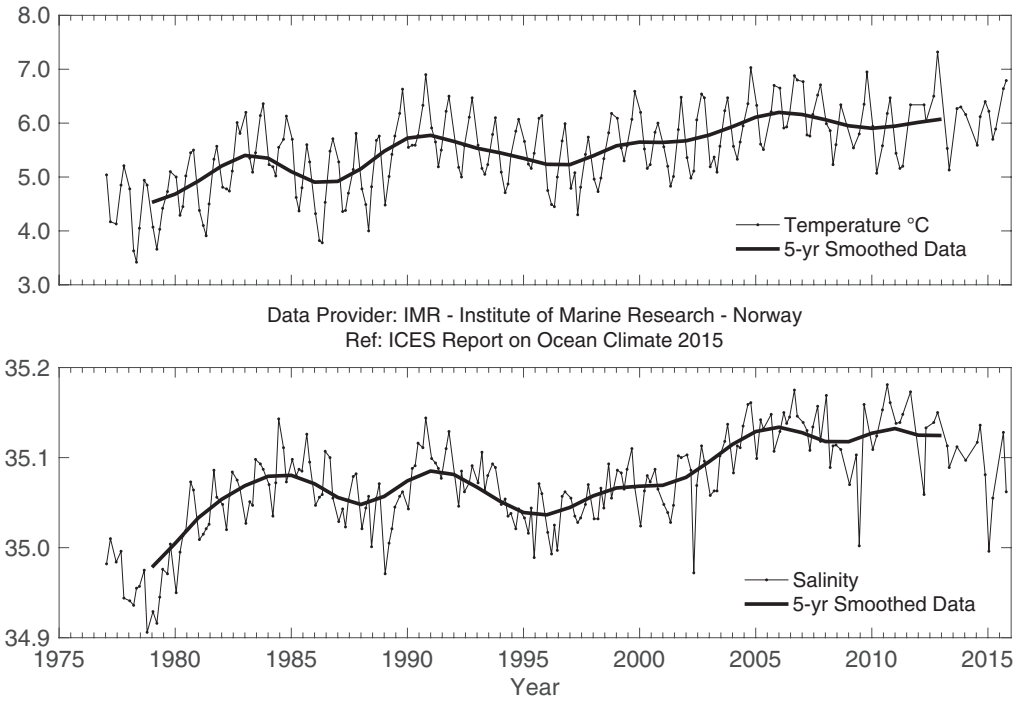

Figure 72.
Fram Strait. Temperature (upper panel) and salinity (lower panel) of Atlantic water (AW) and Return Atlantic Water (RAW) in the Greenland Sea Section at 75°N. AW properties are 50–150 m averages at 10–13°E. The RAW is characterized by temperature and salinity maxima below 50 m averaged over three stations west of 11.5°W.

SALINITY OF THE ATLANTIC INFLOW TO THE ARCTIC OCEAN SLIGHTLY DECREASED IN 2015 COMPARED TO 2014, BUT IT HAS CONSISTENTLY REMAINED ABOVE ITS LONG-TERM AVERAGE OVER THE LAST DECADE.

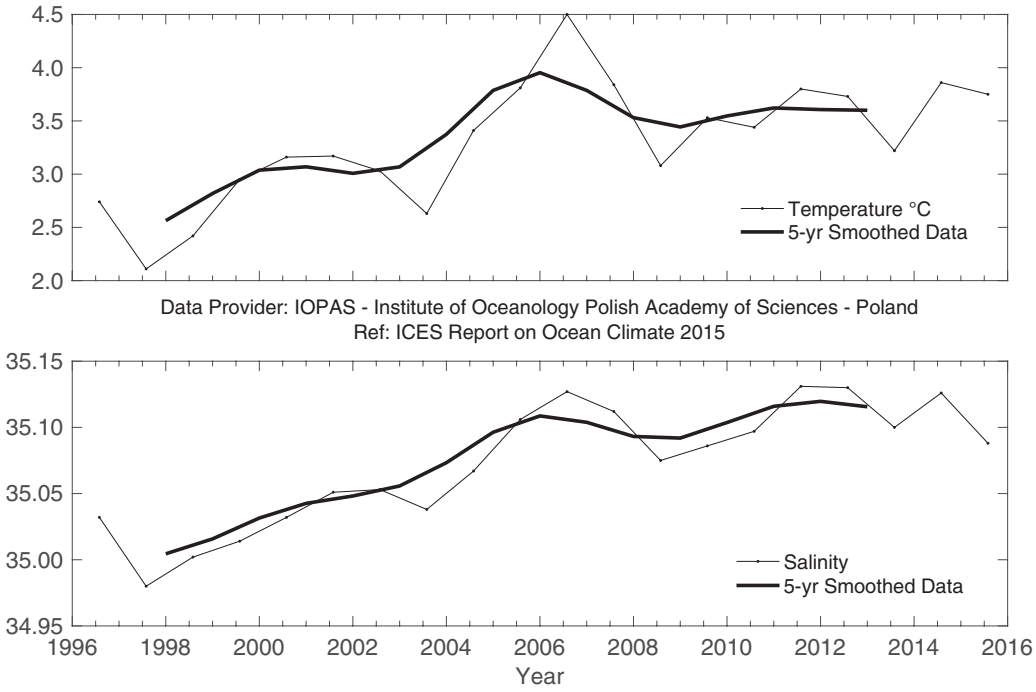

Figure 73.
Fram Strait. Temperature (upper panel) and salinity (lower panel) at 200 m in the southern Spitsbergen Section (76.50°N).

THE RECIRCULATING ATLANTIC WATER IN THE FRAM STRAIT, FLOWING WESTWARD AND ULTIMATELY TO THE SOUTH, WAS WARMER AND MORE SALINE IN 2015 THAN IN PREVIOUS YEARS.

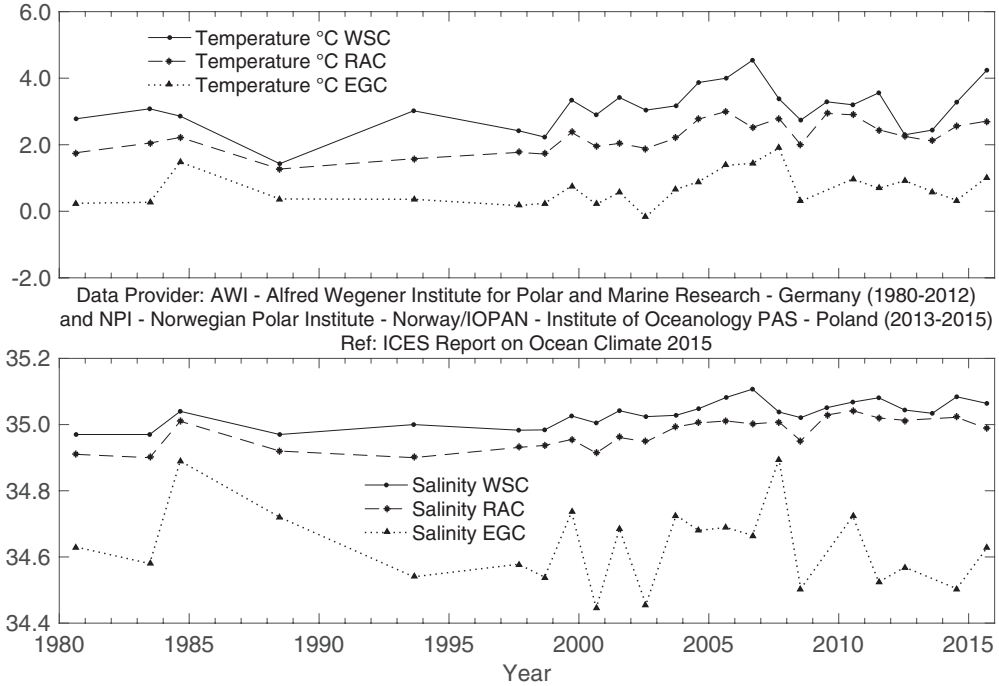

Figure 74.
Fram Strait. Temperature (upper panel) and salinity (lower panel) in the Fram Strait (78.83°N) at 50–500 m: in the Atlantic water in the West Spitsbergen Current (WSC; between the shelf edge and 5°E), in the Return Atlantic Current (RAC; between 3°W and 5°E), and in the polar water in the East Greenland Current (EGC; between 3°W and the Greenland Shelf).

5. DETAILED AREA DESCRIPTIONS, PART II: THE DEEP OCEAN

5.1 Introduction

In this section the focus is on the deeper waters of the Nordic seas and the North Atlantic, typically below 1000 m. The general circulation scheme and dominant water masses are given in Figure 75.

At the northern boundary of the area of interest, the cold and dense outflow from the Arctic Ocean enters Fram Strait along its western side and reaches the Greenland Sea. The outflow is a mixture of Eurasian Basin and Canadian Basin deep waters and upper polar deep water (UPDW). The Eurasian deep water feeds the densest water of all Nordic seas: the Greenland Sea bottom water. The Canadian Basin deep water and the UPDW supply the Arctic intermediate water in the Greenland Sea, and the UPDW also includes products of the winter convection. The deep southward outflow from the North Atlantic in the deep western boundary current is fed by the cold and dense overflow waters. The deepest and densest is the Denmark Strait overflow water. This water mass originates in the Arctic intermediate water produced in the Greenland and Iceland seas by winter convection and mixing with surrounding water masses. The Denmark Strait overflow water sinks to the bottom as it passes over the Denmark Strait sill, vigorously entraining ambient water. Downstream, it is overlain by an intermediate water mass, that of Labrador Sea water, formed by deep winter convection in the Labrador Sea. The middle layer of the deep, cold-water export in the deep western boundary current is supplied by the Iceland–Scotland overflow water, originating in water masses formed in the Norwegian Sea (Arctic intermediate water and Norwegian Sea deep water). Passing through the Icelandic Basin, the Iceland–Scotland overflow water also entrains upper ocean water and Labrador Sea water. The deep Antarctic bottom water enters the North Atlantic on the western side, but its signature is present also in eastern Atlantic abyssal basins. At intermediate levels, Mediterranean water originates from vigorous mixing of Atlantic central waters and Mediterranean outflow waters at the Gulf of Cadiz. This water mass spreads in all directions at a depth of about 1000 m, with a main vein progressing northwards along the European margin. Around the Canaries, the Mediterranean water encounters the northern limit of Antarctic intermediate waters.

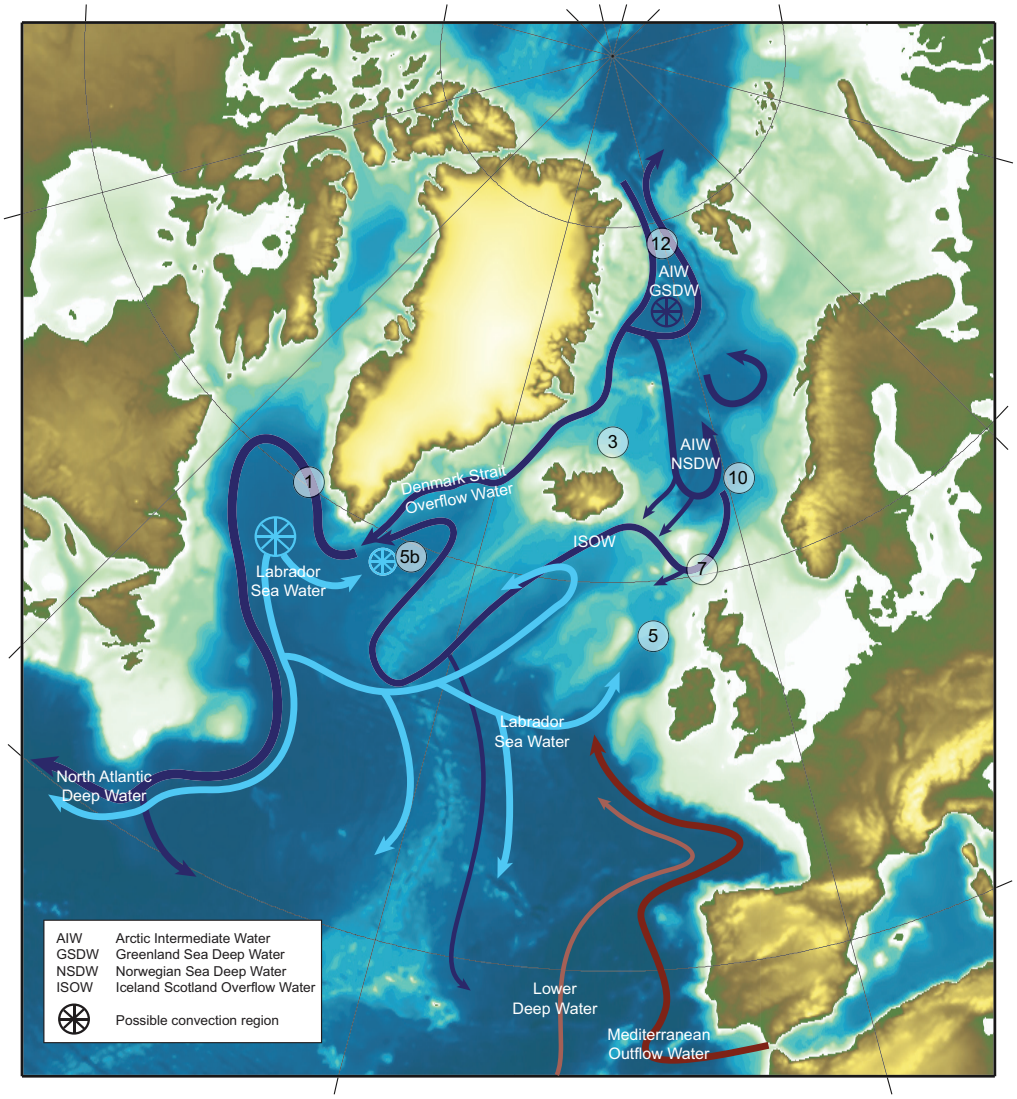

Figure 75.
Schematic circulation of the intermediate to deep waters in the Nordic seas and the North Atlantic.

5.2 Nordic seas deep waters

The deep waters of the Greenland, Iceland, and Norwegian seas are all warming. The source of the warming is the deep outflow from the Arctic Ocean, a southward flowing current of the Eurasian and Canadian Basin deep waters, and the upper polar deep water found on the western side of Fram Strait at a depth of around 2000 m. The Greenland Sea deep water (GSDW) is warming fastest owing to its direct contact with this Arctic outflow, whereas the Iceland and Norwegian seas are warming more slowly because they are products of the mixing of their own ambient waters with GSDW and Arctic outflow water.

Greenland Sea Basin

Continuous warming has been observed in the Greenland Sea deep layer at 3000 m (no data for 2011–2015), and the temperature increase between 2009 and 2010 was slightly lower (0.01°C) than the increase over the past five years (0.014°C). Warming in the Greenland Sea was accompanied by a year-to-year increase in salinity of 0.001. The long-term warming rate for the last decade is 0.134°C.

The doming structure in the Greenland Sea gyre is being replaced by a two-layered water mass arrangement, after a cessation of deep convection. Since measurements began in 1993, the winter convection depth has varied between 700 and 1600 m and has only been significantly deeper in small-scale convective eddies. In winter 2007/2008, the maximum convection depth was estimated to be 1700 m, deeper than the previous year (1200 m) and similar to the maxima observed during 2001/2002 and 2002/2003. The import of warm and saline Atlantic water (AW) to the Greenland Sea is currently not balanced by an import of cool and fresh polar water from the north. The AW, which dominates changes in the upper ocean, took over the role of former ice production as a source of salt and densification in the context of winter convection. The input of AW tends to prevent ice formation and to vertically homogenize the waters ventilated by convective processes. The GSDW formerly included a small admixture of surface freshwater through the convective process and, therefore, had a lower salinity than the Arctic outflow waters. The observed increase in GSDW salinity may be the result of an adjustment to the Arctic outflow in the continued absence of deep convection and an increased presence of AW in the upper layer.

In the Greenland Sea gyre in summer 2009, the usual relatively homogenous pool, mixed by previous winter convection, was replaced by a bipolar distribution of water masses with higher salinity in the western part of the gyre and fresher waters in its eastern part. This made it difficult to compose a reliable mean profile for the gyre centre and, consequently, because of the lack of a 2009 mean profile for comparison with the 2010 mean profile, it was not possible to provide an unambiguous estimate of the convection depth in winter 2009/2010. Therefore, two possible convection depths were obtained, depending on a choice of the 2009 mean profile. Since 2011 no measurements have been collected in the Greenland Sea deep water and development of the convection depth in the Greenland Sea gyre has not been updated.

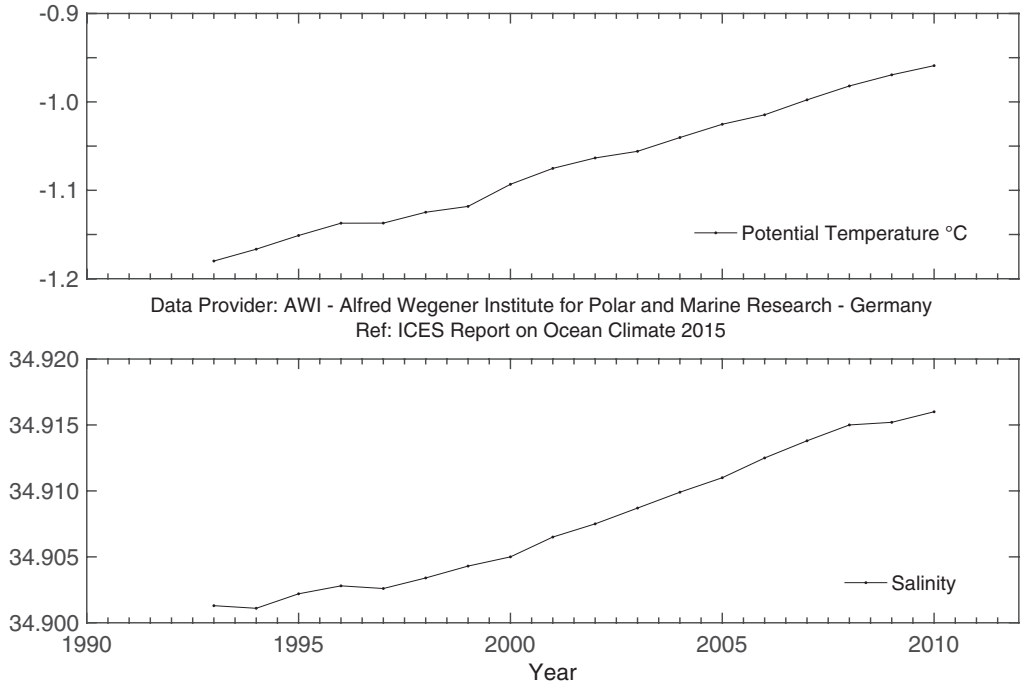

Figure 76.
Fram Strait. Temperature (upper panel) and salinity (lower panel) at 3000 m in the Greenland Sea Section at 75°N (data to 2010).

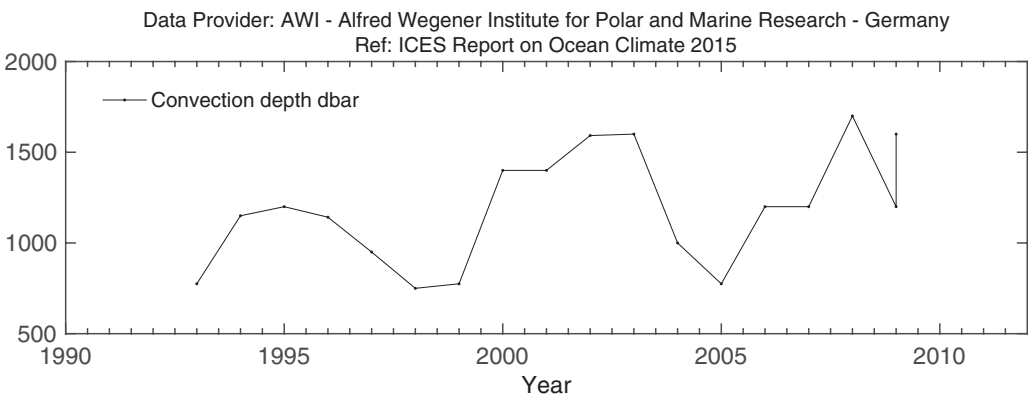

Figure 77.
Fram Strait. Winter convection depths in the Greenland Sea Section at 75°N (data to 2009; note that because of the ambiguous convection depth in winter 2009/2010, two values are provided for this period).

Norwegian Sea Basin

The longest time-series in the Nordic seas is from the Ocean Weather Ship "M" in the Norwegian Sea. It reveals warming from the mid-1980s; however, a slight decrease in temperature occurred in the period 2010–2011 and again in 2014. In 2015, the temperature increased slightly from 2014. The long-term warming rate for the last decade is 0.06°C, similar to that in the Iceland Sea, but lower than in the Greenland Sea.

It is unclear whether there has been any corresponding salinity trend in the Norwegian Sea deep waters in recent decades. After some decrease in the early 1990s, salinity in the Norwegian Sea deep basins has remained relatively stable over the 2000s and until 2015, but with a record-low value in 2012.

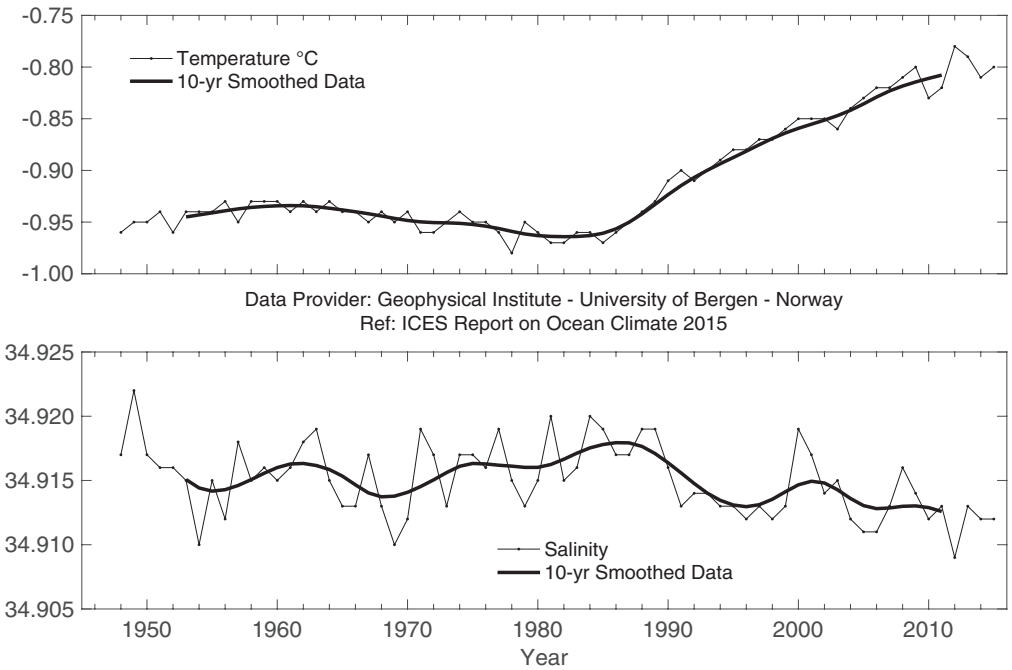

Figure 78.
Norwegian Sea. Temperature (upper panel) and salinity (lower panel) at 2000 m at Ocean Weather Station "M" (66°N 2°E).

Iceland Sea Basin

In the Iceland Basin, an increase in temperature in the depth range 1500–1800 m has been observed since the beginning of the time-series (early 1990s), and the temperature continued to rise slowly until the end of 2014. The long-term warming rate for the last decade is 0.064°C. Temperature lowered slightly in 2015 after continuous rising since 1998.

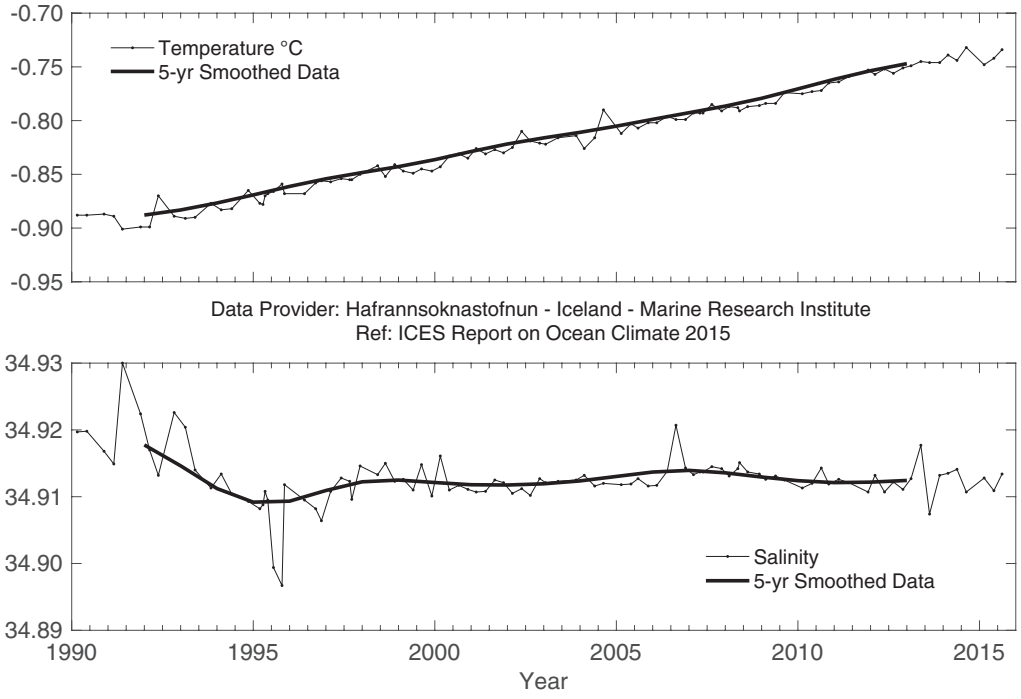

Figure 79.
Icelandic waters. Temperature (upper panel) and salinity (lower panel) at 1500–1800 m in the Iceland Sea (68°N 12.67°W).

Photo: Sarah Hughes, FRS, Aberdeen, UK.

5.3 North Atlantic deep waters

Greenland–Scotland Ridge overflow waters

In the deep layers of the Faroe–Shetland Channel, the properties at 800 m are the same as those of Norwegian Sea deep water as it passes through the Channel back into the North Atlantic.

Temperature at this depth has relatively strong variability, but the overall trend was of decreasing temperature from the 1950s to the 1990s. There has been an increasing trend in temperature since 1995, but it still remains lower than the highest values observed in the 1950s, 1960s, and early 1980s. Relatively stable salinity in the first period of measurements (1950 to mid-1970s) was followed by a slow decline. The lowest salinity values were observed in 1887; since then, there has been a slow, but gradual, increase in salinity.

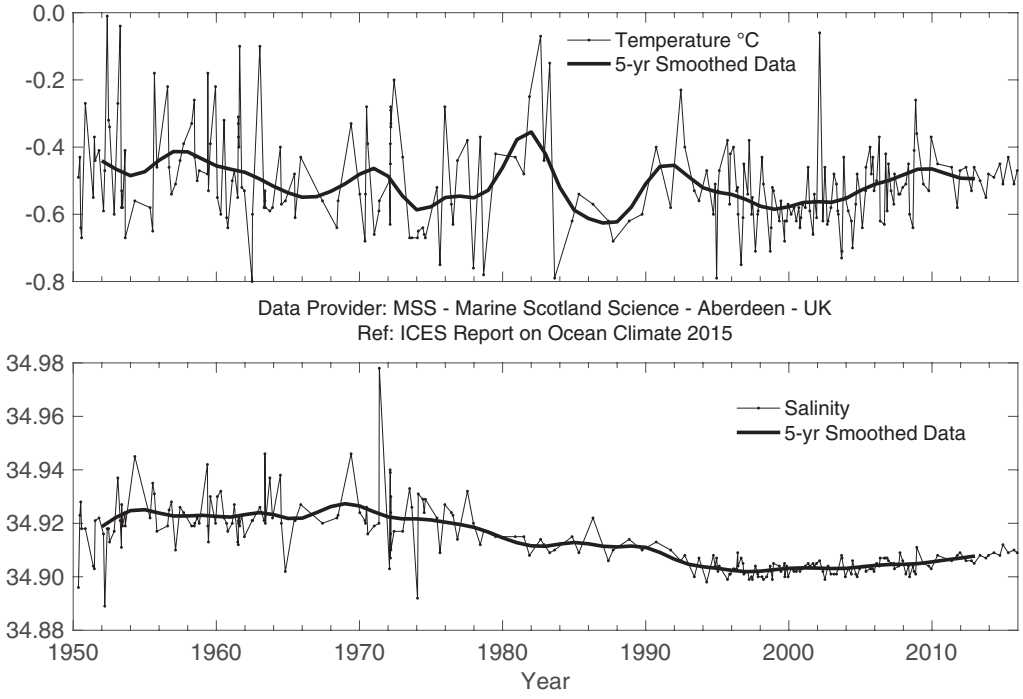

Figure 80.
Faroe–Shetland Channel. Temperature (upper panel) and salinity (lower panel) at 800 m.

Iceland Basin

After the Norwegian Sea deep water flows through the Faroe–Shetland Channel and Faroe Bank Channel and into the Iceland Basin, it becomes known as Iceland–Scotland overflow water (ISOW). The dense water, supplemented by a small amount of additional flow over the sill between Iceland and the Faroes, mixes rapidly with the upper ocean and intermediate water of the Iceland Basin, entraining the lighter water and increasing the volume of the overflow plume. The properties of the ISOW measured at 20°W in the Iceland Basin, therefore, become a product of the properties of the dense water at the sill and the entrained ambient water. The ISOW temperature and salinity vary rather closely with the Labrador Sea water and upper ocean water in the Iceland Basin; since 1996, the water has warmed and increased in salinity, though there has been a slight decrease in both since 2011.

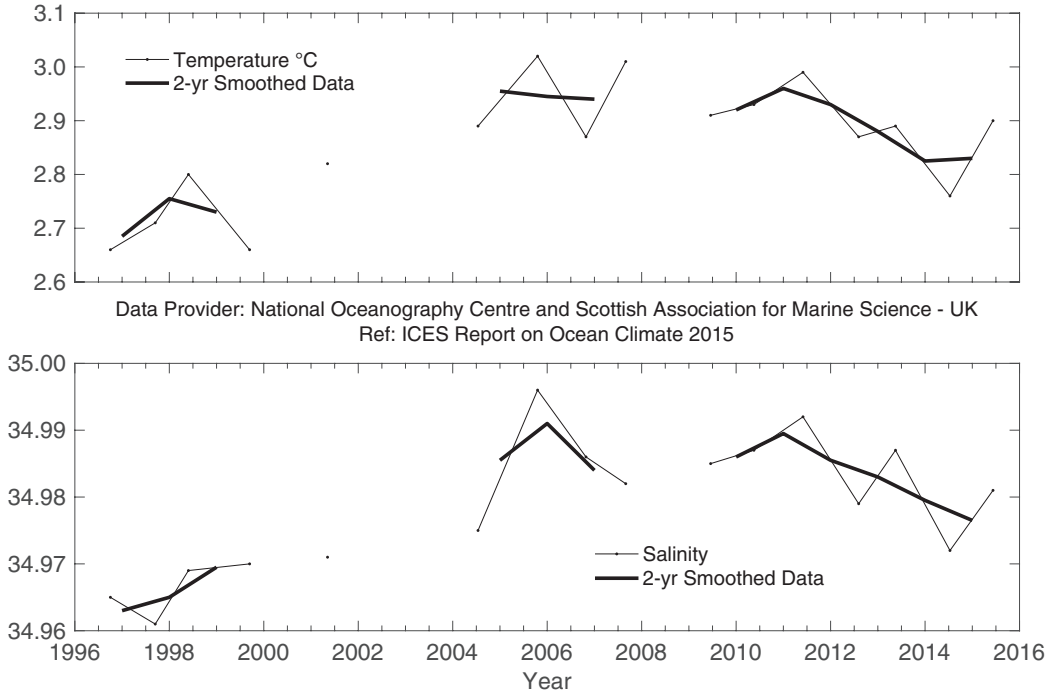

Figure 81.
Iceland Basin. Temperature (upper panel) and salinity (lower panel) of Iceland–Scotland overflow water (potential density >27.85 kg m^{-3}, ca. 2000–2600 m).

Irminger Basin

Salinity and potential temperature of the Denmark Strait overflow water (DSOW) near Cape Farewell exhibited correlated interannual variations between 1991 and 2007 (correlation = 0.75). However, since 2007, changes in temperature and salinity of the DSOW meant that the correlation was reduced to about 0.6. This implies that < 30% of the variance of the salinity can be explained by the variance of the temperature variability. Density of the DSOW hardly changes on long time-scales. Measurements with moored instrumentation have demonstrated that temperature and density mainly vary at an annual time-scale, possibly forced by wind-driven processes near Denmark Strait. In 2014 and 2015, temperature of the DSOW was 0.086°C and 0.153°C, respectively, above the long-term mean, and salinity values were 0.014 and 0.02 above average (Note: this includes a correction from the 2014 report).

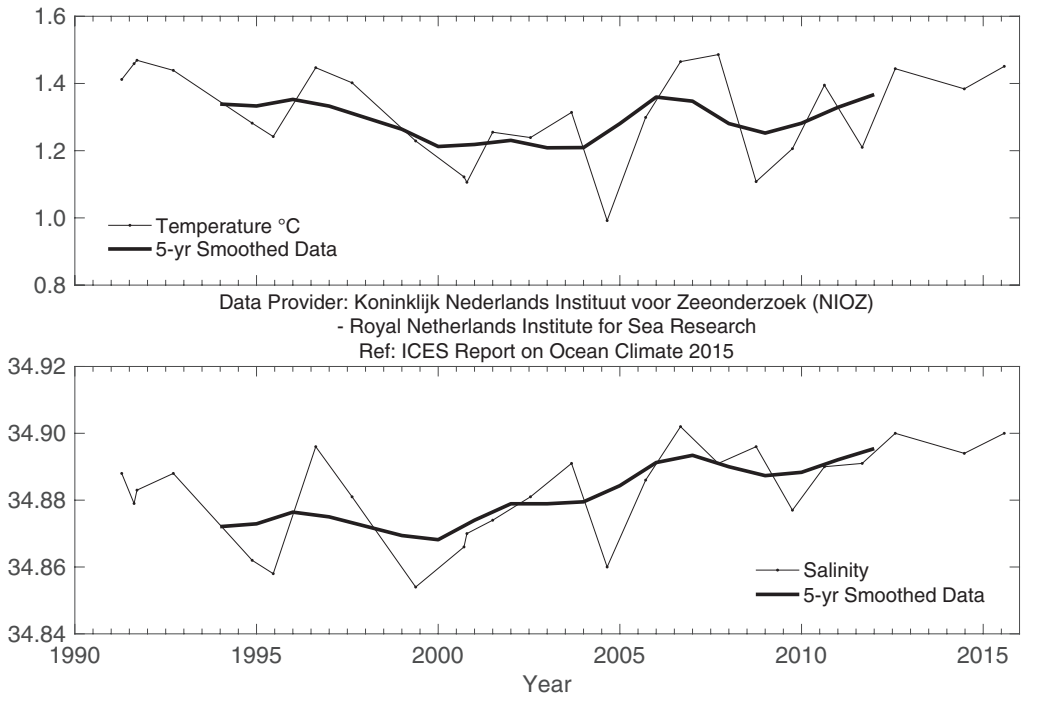

Figure 82.
Irminger Sea. Temperature (upper panel) and salinity (lower panel) in Denmark Strait overflow water on the East Greenland slope.

Labrador Basin

The properties of the North Atlantic deep water (NADW) in the deep boundary current west of Greenland are monitored at a depth of 2000 m at Cape Desolation Station 3. Temperature and salinity of this water mass underwent strong interannual variability during the 1980s. Since the beginning of the 1990s, both characteristics have decreased and reached their minimum values in 1998 and 1997, respectively. After that, the temperature of the NADW revealed a positive trend until 2014, whereas its salinity rather stagnated between 2007 and 2014. In 2015, temperature decreased and salinity increased to 0.02°C and 0.03, respectively, above the long-term mean.

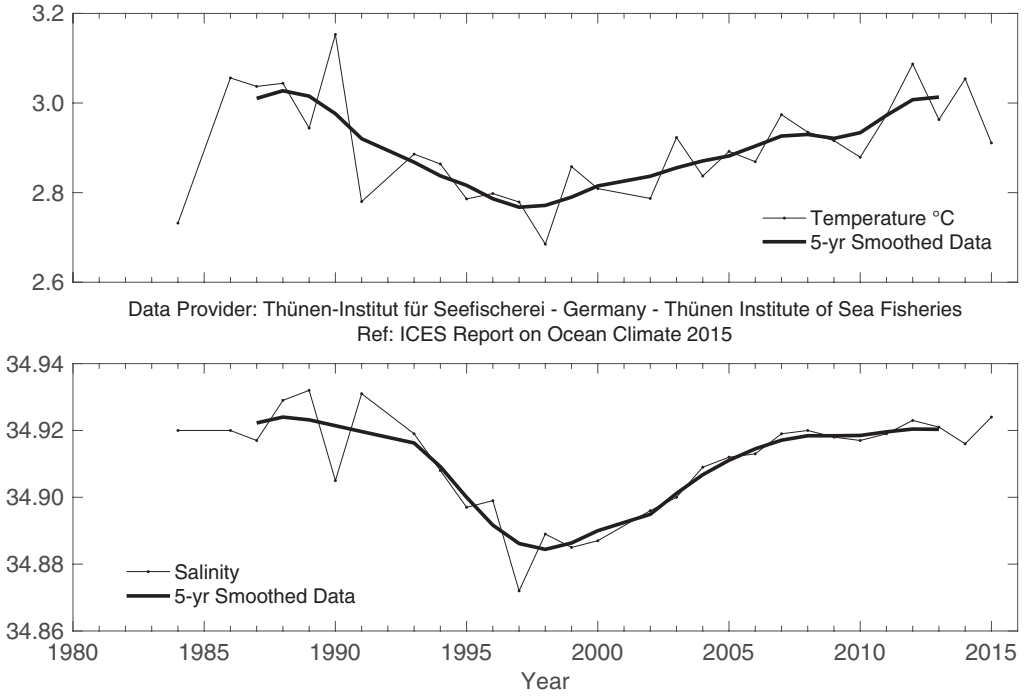

Figure 83.
West Greenland. Temperature (upper panel) and salinity (lower panel) at a depth of 2000 m at Cape Desolation Station 3 (60.47°N 50°W).

Western Iberian margin

Hydrography and biogeochemistry at western Iberia and the Bay of Biscay have been monitored for the entire water depth (>5500 m) since 2003 by a repeated section programme that supplements the monthly monitoring of the upper ocean in the area. Cruises were carried out semi-annually for the period 2003–2010 and annually after that. The Finisterre Section, ca. 400 km, starts west of the Iberian Peninsula (43°N 9.3°W) and reaches the centre of the Iberian abyssal plain (43°N 15°W).

The Finisterre Section provides information about upper, intermediate, and deep waters. A depth of 2000 m corresponds to the core of the LSW and the base of the permanent thermocline; therefore, this is considered the limit of intermediate waters. The abyssal waters in this basin are the NADW (consisting of a mixture of all Arctic water masses) and what is known as lower deep water that has a signature of water with Antarctic origin. Interannual variability of these abyssal waters within the monitored period has been weak, with interannual swings below 0.1°C and 0.01 in salinity. No trends have been observed. The 2015 values are equal to long-term average.

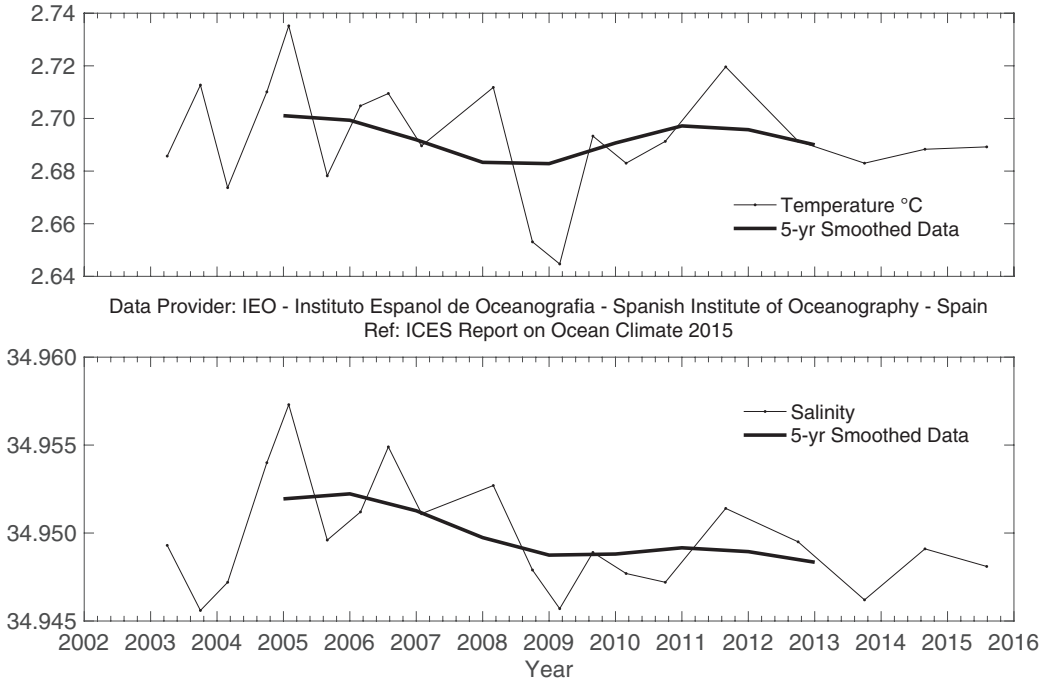

Figure 84.
Western Iberian margin. Potential temperature (upper panel) and salinity (lower panel) for the 2000–5500 m layer averaged across the Finisterre Section.

Canary Basin

The deepest levels in the Canary Basin are filled by the North Atlantic deep waters (NADW); waters deeper than 1600 m are taken as reference of NADW status.

In the layer corresponding to the upper NADW (1600–2600 m), there was a weak warming and increase in salinity, statistically not different from zero. However, in strata corresponding to the NADW (2600–3600 m), a marginally statistically significant cooling (–0.01 ± 0.01°C decade^{-1}) and freshening (–0.002 ± 0.002°C decade^{-1}) was observed in 2015.

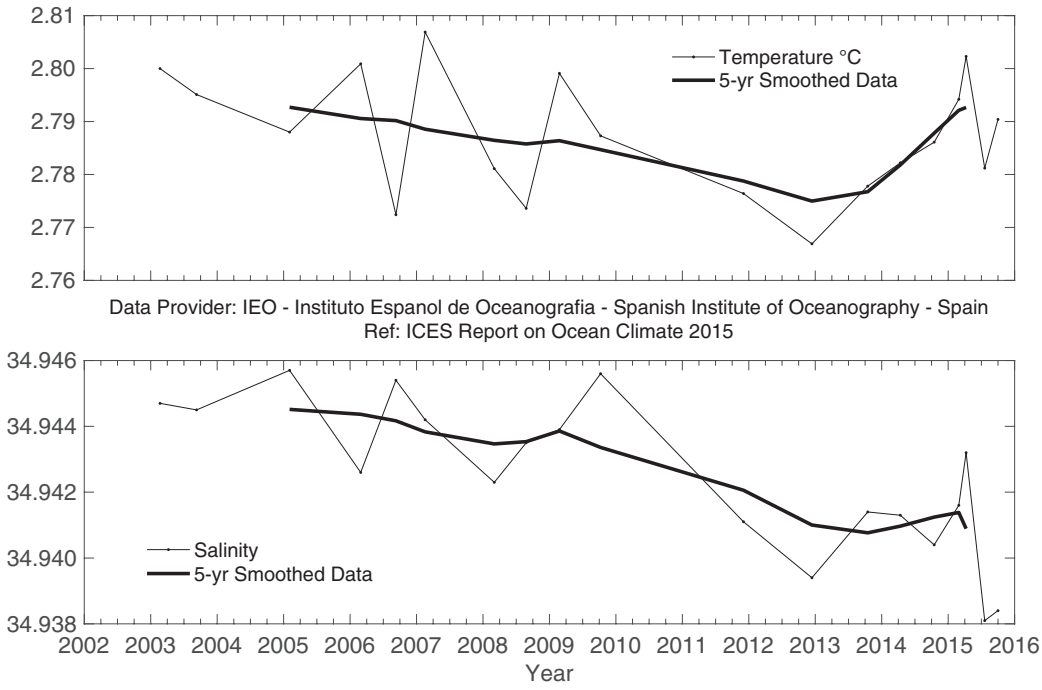

Figure 85.
Canary Basin. Potential temperature (upper panel) and salinity (lower panel) for the 2600–3600 m layer averaged across the Canaries Section.

5.4 North Atlantic intermediate waters

Iceland Basin

In the Iceland Basin, the dominant water mass below about 1000 m is Labrador Sea water (LSW), evident as a large recirculating body of relatively fresh and low stratified water whose core lies between 1700 and 2000 m. In 2015, the LSW was slightly warmer and more saline than in the previous year; temperature and salinity were both very close to their respective 1996–2010 means.

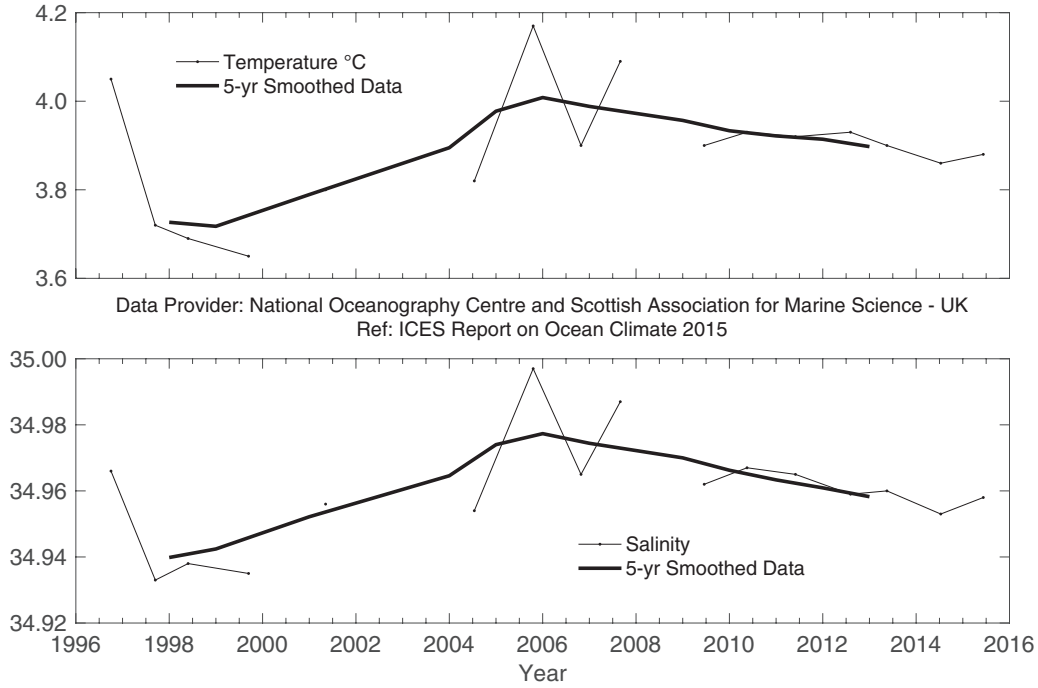

Figure 86.
Iceland Basin. Temperature (upper panel) and salinity (lower panel) of Labrador Sea water (potential density range: 27.70–27.85 kg m^{-3}, ca. 1200–2000 m).

Rockall Trough

In Rockall Trough, the dominant water mass below about 1500 m is Labrador Sea water (LSW), which usually has its maximum concentration between 1700 and 2000 m. East of the Anton Dohrn seamount, this peak tends to be characterized by a minimum in salinity and potential vorticity, although its patchy temporal distribution (possibly due to aliasing of mesoscale eddies) results in a noisy year-on-year signal. Over the length of the time-series, a trend of cooling and freshening can be detected. In 2015, the LSW potential temperature and salinity were cooler and fresher than the long-term means.

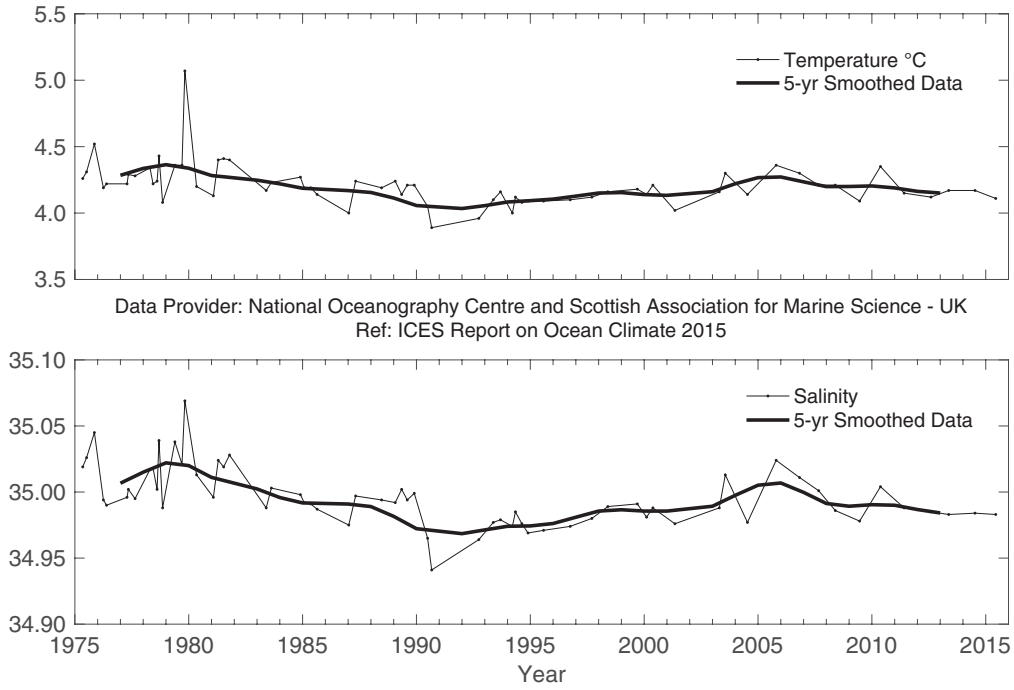

Figure 87.
Rockall Trough. Temperature (upper panel) and salinity (lower panel) of Labrador Sea water (potential density range: 27.70–27.85 kg m^{-3}, ca. 1500–2000 m).

Irminger Basin

A cold and low-salinity core was observed between 1600 and 2000 m in the central Irminger Sea during the early 1990s. This was the result of the presence of deep Labrador Sea water (LSW) formed in the period 1988–1995. Since summer 1996, this LSW core has generally been increasing in temperature and salinity as it mixes with surrounding water masses. In 2012, temperature and salinity were only slightly below the long-term maximum observed in 2011. In 2014, the temperature of LSW in the Irminger Sea continued to decline relative to 2011. Salinity, however, was higher in 2014 than in 2011 and actually achieved its highest value ever in the whole time-series since 1991. In 2015, salinity continued to increase and exceeded the 2014 value. The temperature in 2015 was only slightly higher than in 2014, but it did not exceed the 2011 maximum. Deep convection occurred in the Irminger Sea in the cold winter of 2014/2015 and produced a water mass with LSW properties down to 1400 m in the central Irminger Sea; however, this did not affect the properties of LSW at depths below 1400 m.

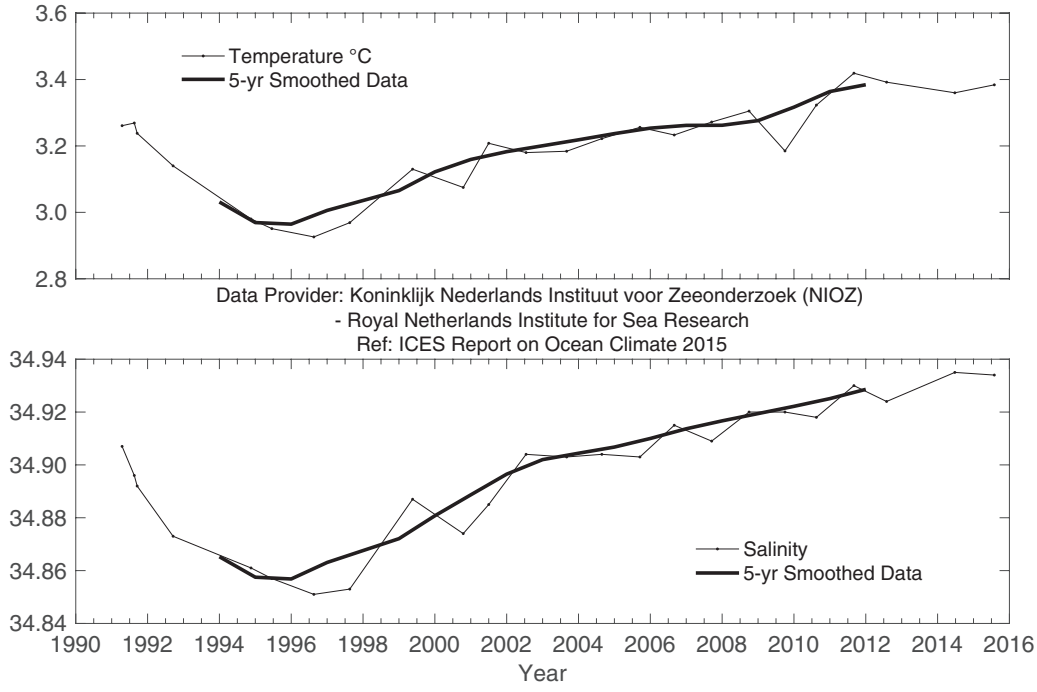

Figure 88.
Irminger Sea. Temperature (upper panel) and salinity (lower panel) of Labrador Sea water (averaged over 1600–2000 m).

Photo: Sarah Hughes, FRS, Aberdeen, UK.

Labrador Basin

In winter 2014/2015, the mid-high latitude North Atlantic experienced the most extreme heat loss in the region since 1979; this was primarily forced by strong westerly and northerly winds. This heat loss from the ocean to the atmosphere led to the most significant formation, in terms of volume, of Labrador Sea water (LSW) since 1994. The 2015 vintage of LSW is associated with low temperature (< 3.3°C) and salinity (< 34.85) below 1000 m. The winter convection of this year is arguably the deepest since the record of 2400 m in 1994, and the resulting volume of LSW is one of the largest ever observed outside of the early 1990s.

The deeper intermediate layer (1000–1600 m) became fresher in 2015 as a result of winter convective mixing that penetrated deeper than in previous years, interrupting the general warming trend that has persisted in the intermediate waters of the Labrador Sea since the mid-1990s. In contrast, the deeper part of the intermediate layer of the central Labrador Sea (1800–2500 m) residing below the reach of the recent convective mixing events has been gradually warming since the mid-1990s.

Interannual variability in Labrador Sea ocean heat content and cumulative surface heat loss during the cooling seasons indicates that the anomalously strong winter atmospheric cooling associated with the North Atlantic Oscillation is continuing to drive the recurrent convection. In turn, recurrent deep convection is contributing to decadal-scale variability in deep-water properties, to transport across and from the subpolar North Atlantic (by the ocean's western boundary and interior pathways), and potentially also to the Atlantic meridional overturning circulation.

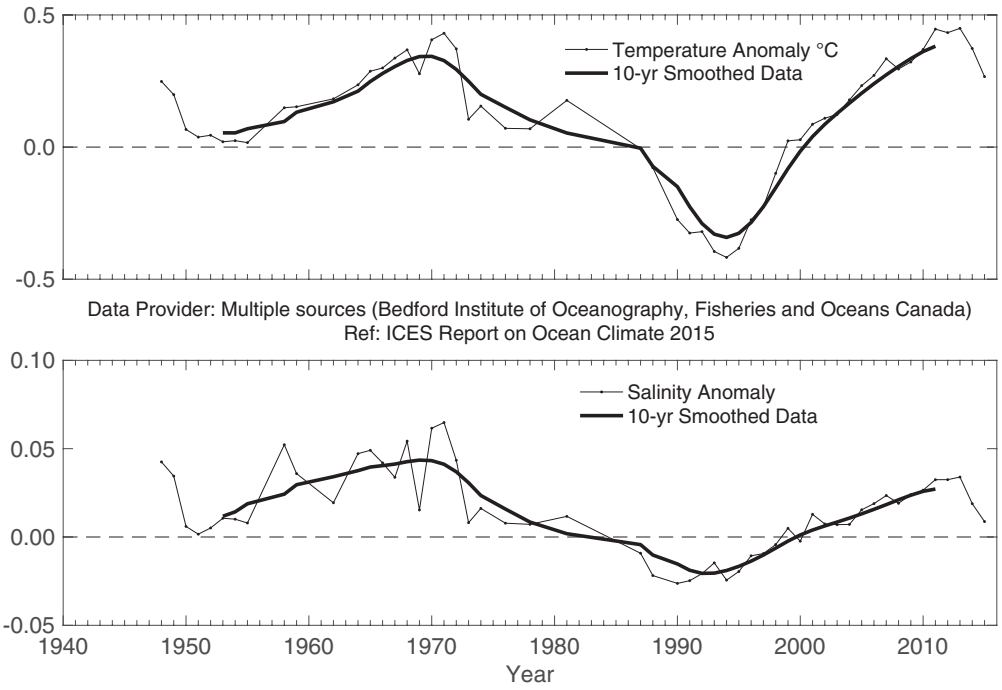

Figure 89.
Labrador Sea. Temperature (upper panel) and salinity (lower panel) anomalies of Labrador Sea water (averaged over 1000–1800 m).

Western Iberian margin

The external stations in Santander have been sampling the entire water column down to 1000 m [core of Mediterranean water (MW)] on a monthly basis since the early 1990s. Overall warming trends for the previous 20 years are evident at most layers, corresponding to the eastern North Atlantic central water (ENACW; 300–600 m) and upper MW (600–950 m). Salinity also exhibits a notable increase along the whole series, but less smooth than temperature. The evolution of the water masses is strongly influenced by a strong shift in salinity at lower ENACW water depths (~400 m) in 2005 after the occurrence of very strong winter mixing. In 2014, upper central waters underwent freshening for the first time in about a decade. In 2015, salinity values fell continuously during the year and were about 0.05 units lower by the end of 2015 than in mid-2014. In deeper waters, at the level of the MW, the water mass has remained fairly stable since the mid-2000s, being fresher at its core in 2015 after peaking around 2007–2009 and slightly colder.

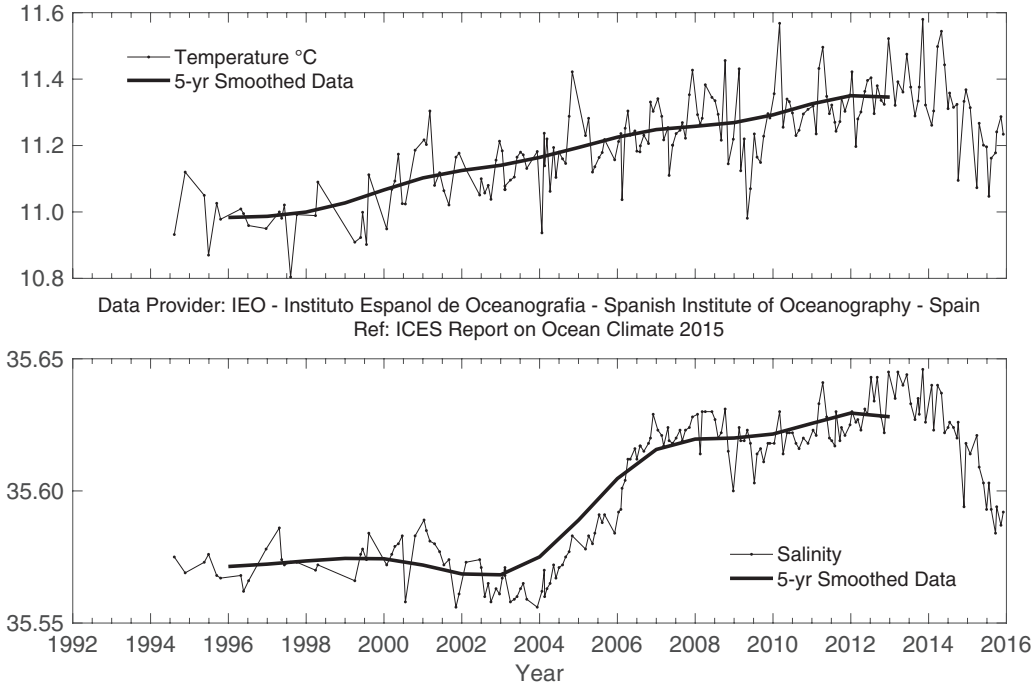

Figure 90.
Bay of Biscay. Potential temperature (upper panel) and salinity (lower panel) for the 200–600 m layer at Santander Station 7.

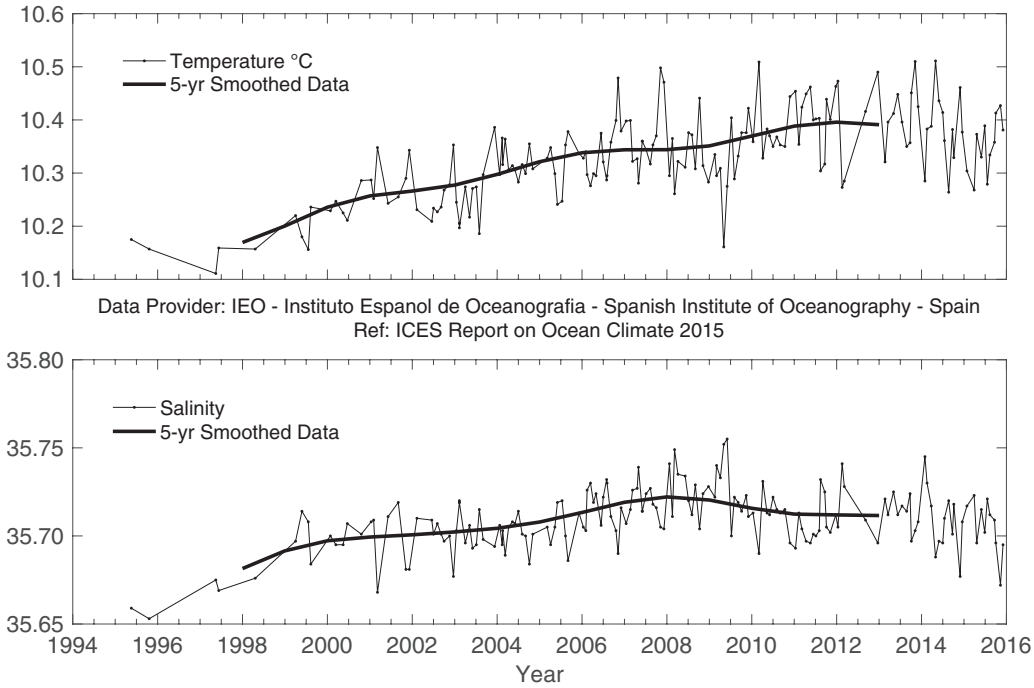

Figure 91.
Bay of Biscay. Potential temperature (upper panel) and salinity (lower panel) for the 600–950 m layer at Santander Station 7.

Deeper levels than 1000 m have been monitored in the region and at the western Iberian margin on a yearly/semi-yearly basis. From the core of MW to the core of LSW (ca. 1900 m), there is a strong gradient and some coherence in variability, indicating the influence of large-scale atmospheric patterns. The main highlight of the series is the passage of a cold and fresh anomaly from 2008 to 2010. The upward swing of temperature and salinity observed in these intermediate waters in 2014 continued in 2015.

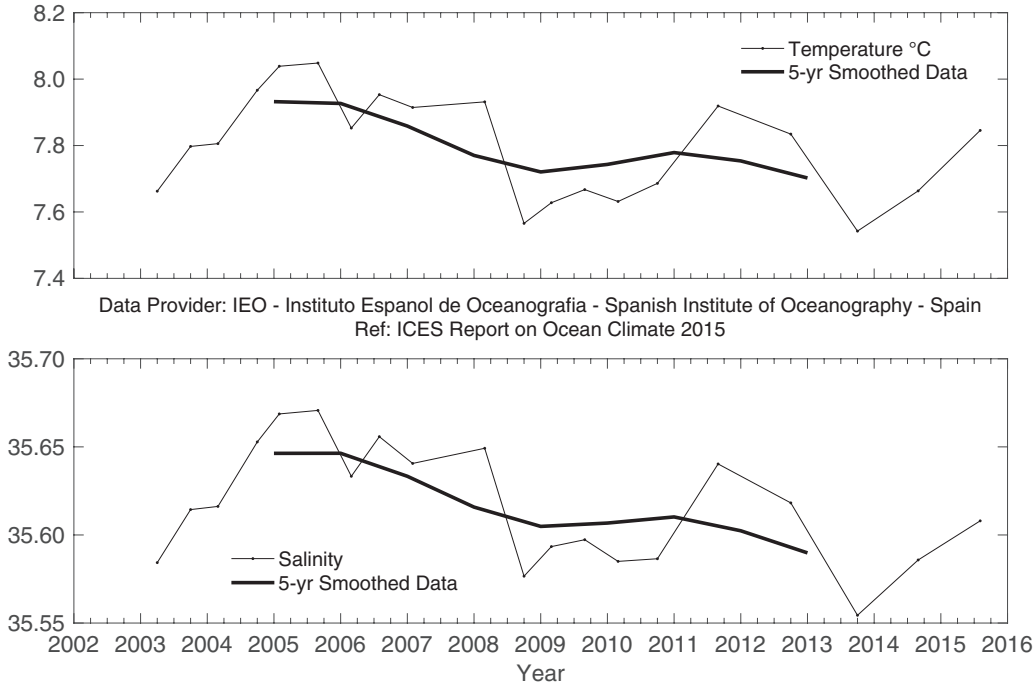

Figure 92.
Western Iberian margin. Potential temperature (upper panel) and salinity (lower panel) for the 800–2000 m layer averaged across the Finisterre Section.

THE DEEP AND INTENSE WINTER MIXING OF TWO CONSECUTIVE WINTERS OF 2013–2014 AND 2014–2015 INTERRUPTED THE GENERAL WARMING TREND THAT HAS PERSISTED IN THE INTERMEDIATE WATERS OF THE LABRADOR SEA SINCE THE MID-1990s.

Canary Basin

Since the early 2000s two areas in the Canary Islands archipelago region have been monitored by the Spanish Institute of Oceanography: the oceanic waters west of Lanzarote and the coastal transition zone (CTZ) of the upwelling region of the Canary Current Large Marine Ecosystem. The Canary Basin area is characterized by three water masses below the seasonal mixed-layer development: North Atlantic central waters (NACW), roughly between 200 m and 800 m; and intermediate waters, mainly the Mediterranean (MW) and Antarctic intermediate waters (AAIW), between 800 m and 1400 m.

The surface waters in the CTZ show a non-statistically significant cooling of –0.34 ± 0.57°C decade^{-1}, and a non-statistically significant decrease in salinity of –0.043 ± 0.115 decade^{-1}, both consistent with an increase in the upwelling in the Canary Current Large Marine Ecosystem. During 2015, there was a decrease in the cooling and a decrease in salinity relative to 2014, which was the coolest and freshest year on record for the upwelling-influenced surface waters.

In the depth stratum that characterizes the NACW waters (200–800 m), both the oceanic area and the CTZ area show a statistically significant warming trend: 0.25 ± 0.12°C decade^{-1} for the oceanic area and 0.05 ± 0.28°C decade^{-1} for the CTZ. Variability in the CTZ is higher because of the proximity of the upwelling region and the frequent intrusions of upwelling filaments; therefore, uncertainty is higher in the trend estimations. In this stratum, there is an increase in salinity of 0.04 ± 0.020 decade^{-1} for the oceanic area and 0.006 ± 0.045 decade^{-1} for the CTZ. The increase in temperature and salinity almost compensates in density, confirming that the observed trends are due to a deepening of the isoneutral surfaces rather than changes along the isoneutrals. During 2015, there was a decrease in warming and an increase in salinity relative to 2014, which was the saltiest and warmest year on record for the NACW waters.

In the intermediate waters, the trends for temperature and salinity were not statistically significant, neither in the oceanic region nor in the CTZ. Both time-series exhibit high variability because of the two very different intermediate water masses converging in the region.

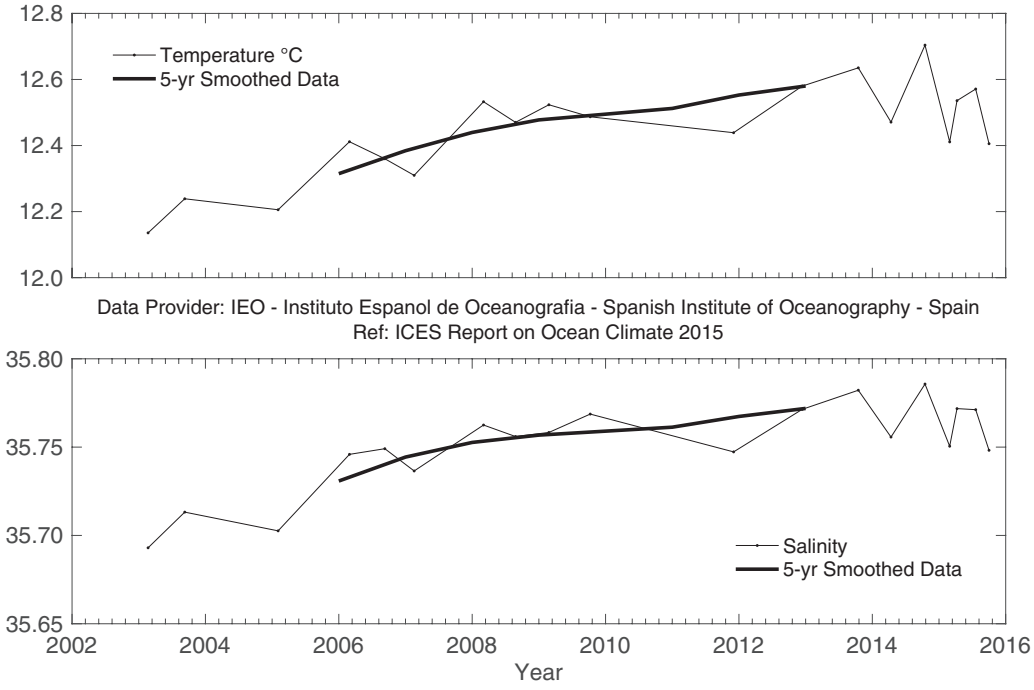

Figure 93.
Canary Basin. Potential temperature (upper panel) and salinity (lower panel) for the 200–800 m layer.

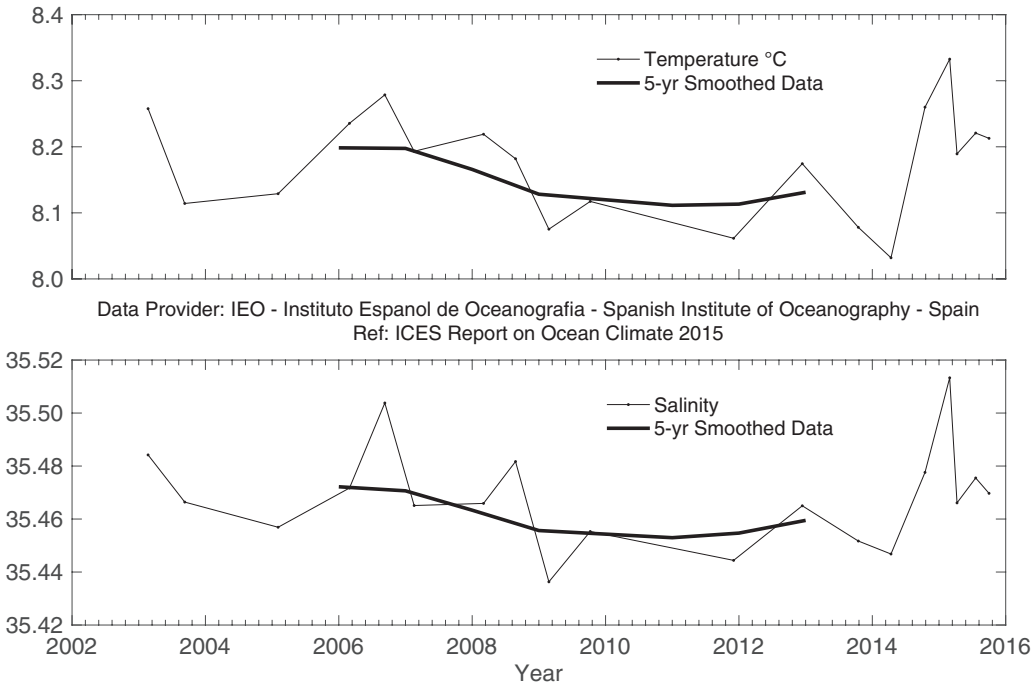

Figure 94.
Canary Basin. Potential temperature (upper panel) and salinity (lower panel) for the 800–1400 m layer.

CONTACT INFORMATION

Area	Area name	Figures	Time-series	Contact	Institute
1	West Greenland	15	Nuuk – air temperature	Boris Cisewski (boris.cisewski@thuenen.de)	Danish Meteorological Institute, Copenhagen, Denmark
1	West Greenland	16, 17, 83	Fylla and Cape Desolation sections	Boris Cisewski (boris.cisewski@thuenen.de)	Thünen-Institut für Seefischerei (Thünen Institute of Sea Fisheries), Germany
2	Northwest Atlantic	22, 23, 24	Sable Island air temperature, Cabot Strait sea ice, Misaine Bank, Emerald Bank	David Hebert (David.Hebert@dfo-mpo.gc.ca)	BIO (Bedford Institute of Oceanography), Department of Fisheries and Oceans, Canada
2	Northwest Atlantic	20, 21	Newfoundland and Labrador sea ice, Cartwright air temperature, Station 27 CIL	Eugene Colbourne (eugene.colbourne@dfo-mpo.gc.ca)	Northwest Atlantic Fisheries Centre, Canada
2b	Labrador Sea	18, 19, 89	Section AR7W	Igor Yashayaev (Igor.Yashayaev@dfo-mpo.gc.ca)	BIO (Bedford Institute of Oceanography), Department of Fisheries and Oceans, Canada
2c	Mid-Atlantic Bight	25, 26, 27, 28, 29, 30, 31	Central MAB and Gulf of Maine, Georges Bank	Paula Fratantoni (paula.fratantoni@noaa.gov)	NOAA Fisheries, NEFSC, Oceanography Branch, USA
3	Icelandic waters	32, 33, 34, 35, 36, 50, 79, 81	Reykjavik and Akureyri air temperature, Siglunes stations 2–4, Selvogsbanki Station 5, Langanes stations 2–6, Faxafloi Station 9, Icelandic deep water (1800 m)	Hedinn Valdimarsson (hv@hafro.is)	Hafrannsoknastofnun (Marine Research Institute), Iceland
4	Canary Basin	85, 93, 94	Canary Basin oceanic waters section	Pedro Vélez-Belchi (pedro.velez@ca.ieo.es)	Instituto Español de Oceanografía (IEO, Spanish Institute of Oceanography), Spain
4	Bay of Biscay	37	San Sebastian air and water temperature	Victor Valencia (vvalencia@azti.es)	AZTI, Aquarium of San Sebastian (SOG) and Igeldo Meteorological Observatory (INM) in San Sebastian, Spain
4	Bay of Biscay and Western Iberian Margin	38, 39, 84, 90, 91, 92	Santander and Finisterre sections	Cesar Pola (cesar.pola@gi.ieo.es)	Instituto Español de Oceanografía (IEO, Spanish Institute of Oceanography), Spain
4b	NW European Continental Shelf	40, 41	Astan Section, Point 33	Pascal Morin (pmorin@sb-roscoff.fr)	CNRS, Observatoire Oceanologique de Roscoff and IFREMER, France
4b	NW European Continental Shelf	42, 43	Western Channel Observatory, Station E1	Tim J. Smyth (tjsm@pml.ac.uk)	Marine Biological Association and Plymouth Marine Laboratory, UK
4b	Rockall Trough	44, 45	Malin Head Weather Station, M3 Weather Buoy	Caroline Cusack (Caroline.Cusack@Marine.ie)	National Oceanography Centre Southampton and Scottish Association for Marine Science, UK
5	Irminger Sea	46, 47, 48, 86, 87	Ellett Line	N. Penny Holliday (nph@noc.soton.ac.uk)	Koninklijk Nederlands Instituut voor Zeeonderzoek (NIOZ, Royal Netherlands Institute for Sea Research), Netherlands
5b	Faroese waters	49, 82, 88	Central Irminger Sea, East Greenland Slope	Laura de Steur (Laura.de.Steur@nioz.nl)	Koninklijk Nederlands Instituut voor Zeeonderzoek (NIOZ, Royal Netherlands Institute for Sea Research), Netherlands
6	Faroe–Shetland Channel	51, 52, 53	Faroe Bank Channel, Faroe Current, Faroe Shelf	Karin Margretha H. Larsen (KarinL@hav.fo)	Havstovan (Faroe Marine Research Institute), Faroe Islands
7	North Sea	54, 55, 80	Faroe–Shetland Channel – Faroe Shelf and Shetland Shelf, deep waters (800 m)	Sarah Hughes (s.hughes@marlab.ac.uk)	Fisheries Research Services (FRS, Aberdeen), UK

Area	Area name	Figures	Time-series	Contact	Institute
8&9	North Sea	56	North Sea Utsira, modelled North Sea Inflow	Jon Albretsen (jon.albretsen@imr.no) Solfrid Hjollo (solfrids@imr.no)	Institute of Marine Research (IMR), Norway
8&9	North Sea	57	Fair Isle Current water	Sarah Hughes (s.hughes@marlab.ac.uk)	Fisheries Research Services (FRS, Aberdeen), UK
8&9	North Sea	58, 59	Helgoland Roads – coastal waters – German Bight, North Sea	Karen Wiltshire (Karen.Wiltshire@awi.de)	Alfred Wegener Institute for Polar and Marine Research (AWI)/Biologische Anstalt Helgoland (BAH), Germany
8&9	North Sea	60	Felixstowe–Rotterdam Section average (52°N)	Stephen Dye (stephen.dye@cefas.co.uk)	Centre for Environment, Fisheries and Aquaculture Science (CEFAS), UK
9b	Baltic Sea	61, 62, 65	Station BY15, Baltic Proper, east of Gotland, and observed ice extent	Karin Borenas (karin.borenas@smhi.se)	Swedish Meteorological and Hydrological Institute (SMHI), Sweden
9b	Baltic Sea	63, 64	Stations LL7 and SR5	Pekka Alenius (pekka.alenius@fimr.fi)	Finnish Institute of Marine Research (FIMR), Finland
10	Norwegian Sea	66, 68, 69	Svinøy, Gimsøy, and Sørkapp sections	Kjell Arne Mork (kjell.arne.mork@imr.no)	Institute of Marine Research (IMR), Norway
10	Norwegian Sea	67, 78	Ocean Weather Station Mike	Svein Østerhus (Svein.Osterhus@gfi.uib.no)	Geophysical Institute, University of Bergen, Norway
11	Barents Sea	70	Fugløya – Bear Island Section, western Barents Sea	Randi Ingvaldsen (randi.ingvaldsen@imr.no)	Institute of Marine Research (IMR), Norway
11	Barents Sea	71	Kola Section, eastern Barents Sea	Oleg V. Titov (titov@pinro.ru)	Knipovich Polar Research Institute of Marine Fisheries and Oceanography (PINRO), Russia
12	Greenland Sea and Fram Strait	72, 73, 74	Greenland Sea Section N, west of Spitsbergen (76.5°N)	Waldemar Walczowski (walczows@iopan.gda.pl)	Institute of Oceanology, Polish Academy of Sciences (IOPAN), Poland
12	Greenland Sea and Fram Strait	72, 76, 77	Greenland Sea Section 75°N, Greenland Gyre convection depth and deep waters (3000 m)	Gereon Budeus (Gereon.Budeus@awi.de)	Alfred Wegener Institute, Helmholtz Centre for Polar and Marine Research (AWI), Germany
12	Greenland Sea and Fram Strait	74	Fram Strait (78.83°N): West Spitsbergen Current, and East Greenland Current	Wilken-Jon von Appen (Wilken-Jon.von.Appen@awi.de)	Alfred Wegener Institute, Helmholtz Centre for Polar and Marine Research (AWI), Germany
12	Greenland Sea and Fram Strait	74	Fram Strait (78.83°N): West Spitsbergen Current, and East Greenland Current	Paul Dodd (paul.dodd@npolar.no)	Norwegian Polar Institute, Norway

Photo: Cornelius Hammer, Thünen-Institut, Germany.

REFERENCES

Antonov, J. I., Locarnini, R. A., Boyer, T. P., Mishonov, A. V., and Garcia, H. E. 2006. World Ocean Atlas 2005, Volume 2: Salinity. S. Levitus (Ed.) NOAA Atlas NESDIS 62, US Government Printing Office, Washington, DC. 182 pp.

Cappelen, J. (Ed). 2013. The Greenland – DMI Historical Climate Data Collection 1873–2012 – with Danish abstracts. DMI Technical Report 13-04. Copenhagen.

Gaillard, F. 2015. ISAS-13 temperature and salinity gridded fields. Pôle Océan. http://doi.org/z77.

Hurrell, J.W., Kushnir, Y., and Ottersen, G. 2003. An overview of the North Atlantic Oscillation. *In* The North Atlantic Oscillation: Climatic Significance and Environmental Impact. Ed. by J. W. Hurrell, Y. Kushnir, G. Ottersen, and M. Visbeck. Geophysical Monograph Series, 134: 1–35.

Hurrell, J., and National Center for Atmospheric Research Staff (Eds). 2016. The Climate Data Guide: Hurrell North Atlantic Oscillation (NAO) Index (station-based). Webpage, last modified 02 March 2016. Accessed 21/07/2016 at https://climatedataguide.ucar.edu/climate-data/hurrell-north-atlantic-oscillation-nao-index-station-based.

Kalnay, E., Kanamitsu, M., Kistler, R., Collins, W., Deaven, D., Gandin, L., *et al.* 1996. The NCEP/NCAR reanalysis 40-year project. Bulletin of the American Meteorological Society, 77(3): 437–471. doi: 10.1175/1520-0477(1996)077<0437:TNYRP>2.0.CO;2.

Larsen, K. M. H., Gonzalez-Pola, C., Fratantoni, P., Beszczynska-Möller, A., and Hughes, S. L. (Eds.) 2016. ICES Report on Ocean Climate 2014. ICES Cooperative Research Report No. 329. 139 pp.

Locarnini, R. A., Mishonov, A. V., Antonov, J. I., Boyer, T. P., and Garcia, H. E. 2006. World Ocean Atlas 2005, Volume 1: Temperature. S. Levitus (Ed.) NOAA Atlas NESDIS 61, US Government Printing Office, Washington, DC. 182 pp.

Rudels, B., Björk, G., Nilsson, J., Winsor, P., Lake, I., and Nohr, C. 2005. The interaction between waters from the Arctic Ocean and the Nordic Seas north of Fram Strait and along the East Greenland Current: Results from the Arctic Ocean-02 Oden expedition. Journal of Marine Systems, 55: 1–30.

Photo: Simon Cooper, ICES.

ABBREVIATIONS AND ACRONYMS

AAIW	Antarctic intermediate waters
AAW	Arctic Atlantic water
AW	Atlantic water
AZOMP	Atlantic Zone Off-Shelf Monitoring Program
CIL	cold intermediate layer
CTD	conductivity, temperature, and depth profiles
CTZ	coastal transition zone
DJF	December, January, and February
DSOW	Denmark Strait overflow water
EGC	East Greenland Current
ENAC	Weastern North Atlantic central water
GSDW	Greenland Sea deep water
ISOW	Iceland–Scotland overflow water
JJA	June, July, and August
LME	large marine ecosystem
LSW	Labrador sea water
MAM	March, April, and May
MNAW	modified North Atlantic water
MW	Mediterranean water
NAC	North Atlantic Current
NACW	North Atlantic central waters
NADW	North Atlantic deep water
NAO	North Atlantic Oscillation
NL	Newfoundland–Labrador
RAC	Return Atlantic Current
RAW	return Atlantic water
RP	reference period
SON	September, October, and November
SPMW	subpolar-mode water
SST	sea surface temperature
UPDW	upper polar deep water
WGC	West Greenland Current
WSC	West Spitsbergen Current